National Library of Canada
Acquisitions and Bibliographic Services Branch
395 Wellington Street
Ottawa, Ontario
K1A 0N4

Bibliothèque nationale du Canada
Direction des acquisitions et des services bibliographiques
395, rue Wellington
Ottawa (Ontario)
K1A 0N4

Your file Votre référence

Our file Notre référence

NOTICE

The quality of this microform is heavily dependent upon the quality of the original thesis submitted for microfilming. Every effort has been made to ensure the highest quality of reproduction possible.

If pages are missing, contact the university which granted the degree.

Some pages may have indistinct print especially if the original pages were typed with a poor typewriter ribbon or if the university sent us an inferior photocopy.

Reproduction in full or in part of this microform is governed by the Canadian Copyright Act, R.S.C. 1970, c. C-30, and subsequent amendments.

AVIS

La qualité de cette microforme dépend grandement de la qualité de la thèse soumise au microfilmage. Nous avons tout fait pour assurer une qualité supérieure de reproduction.

S'il manque des pages, veuillez communiquer avec l'université qui a conféré le grade.

La qualité d'impression de certaines pages peut laisser à désirer, surtout si les pages originales ont été dactylographiées à l'aide d'un ruban usé ou si l'université nous a fait parvenir une photocopie de qualité inférieure.

La reproduction, même partielle, de cette microforme est soumise à la Loi canadienne sur le droit d'auteur, SRC 1970, c. C-30, et ses amendements subséquents.

Canada

Adaptive Signal Processing in Subbands Using Sigma-Delta Modulation Technique

by

Lu Lin

A thesis submitted to the School of Graduate Studies and Research

in partial fulfilment of the requirements for the

Degree of Master of Applied Science

in Electrical Engineering

Ottawa-Carleton Institute for Electrical Engineering

Department of Electrical Engineering

University of Ottawa

Ottawa, Ontario

Canada

August 1993

ISBN 0-315-95935-5

Canada

UNIVERSITÉ D'OTTAWA
UNIVERSITY OF OTTAWA

I hereby declare that I am the sole author of this document. I authorize the University of Ottawa to lend this document to other institutions or individuals for the purpose of scholarly research.

Lu Lin

I further authorize the University of Ottawa to reproduce this document by photocopying or by other means, in total or in part, at the request of other institutions or individuals for the purpose of scholarly research.

Lu Lin

Abstract

In this thesis, the use of subbanding and sigma-delta modulation in interference/noise cancellation is intensively studied and a sigma-delta modulated subbanded adaptive interference/noise cancellation system is proposed. The filter bank is fully sigma-delta modulated. The output signal from the filter bank is then used to produce the input to the adaptive filter. The adaptive filter is partially sigma-delta modulated. The output is demodulated at the final stage.

Maintaining the sigma-delta modulated signal representation throughout the system results in considerable savings in complexity. The performance of the proposed system is studied and compared to the regular non sigma-delta modulated case regarding complexity, convergence speed and steady state error. The effect of the oversampling rate used in the sigma-delta modulation as well as the quality of the demodulator is also considered. It is shown that in the case of interference cancellation a comb filter is sufficient, while in the case of noise canceller a good quality demodulator is essential.

The thesis concludes by highlighting the tradeoffs between the hardware complexity reduction and the overall system performance.

Acknowledgements

I would like to thank deeply my supervisor, Dr. Tyseer Aboulnasr, for her invaluable guidance and encouragement throughout my graduate studies.

I would also like to thank my family for their special support.

Table of Contents

List of Figures

List of Tables

List of Symbols

x(n)	reference input
y(n)	adaptive filter output
d(n)	primary input
ds(n)	primary signal input
dn(n)	primary noise input
e(n)	system output
a(n)	adaptive filter impulse response
K	adaptive filter length
h(n)	lower band filter impulse response
f(n)	upper band filter impulse response
$J_{ex}(\infty)$	steady state excess error
J_{min}	minimum mean-square error
$J(\infty)$	steady state mean-square error
λ	eigenvalues of the input autocorrelation matrix
μ	step size
f_N	Nyquist frequency
f_s	oversampling frequency
f_B	baseband frequency
f_c	cutoff frequency
R	oversampling ratio
N_B	baseband quantization power
σ_e^2	quantization noise power

1 Introduction

1.1 Why Adaptive Signal Processing

Adaptive signal processing is successfully applied in such diverse fields as communications, control, radar, sonar, seismology and biomedical engineering. It provides expanded signal processing capabilities, owing to the adaptive feature of its system. Adaptive filters, as opposed to fixed filters whose design is based on prior knowledge of both signal and channel, have the ability to adjust their own parameters automatically, and their design generally requires little or no prior knowledge of signal or channel characteristics. Therefore, the use of adaptive filters offers an attractive solution to the problem of processing signals that result from an unknown environment.

[S. Haykin 1991] depicted the functions of the four basic classes of adaptive filtering applications, and listed some applications, totaling twelve, that are illustrative of those four basic classes, such as system identification, adaptive equalization, linear predictive coding, signal detection, adaptive noise cancelling, echo cancellation and adaptive beamforming. Although these applications seem to be different in nature, they all have common features, and can be viewed as variations of one another.

The type of application studied in this thesis is the adaptive noise cancellation (ANC) as shown in Fig.1.1 and its variant adaptive interference cancellation (AIC). This system makes use of a reference input derived from one or more sensors located at points in the noise field where the desired signal is weak or undetectable. Then the

reference input is processed by an adaptive filter whose impulse response can be automatically adjusted. The adjustment is accomplished through an algorithm that responds to an error signal dependent, among other things, on the filter's output. Thus the filter can readjust itself continuously to minimize the error signal.

This noise cancellation system is used in personal vehicular cellular phones, communication services in military vehicles and other high noise environment, such as in some industries, where the filter can optimally adapt for a particular situation and follow the changes in noise characteristics that a fixed filter cannot achieve.

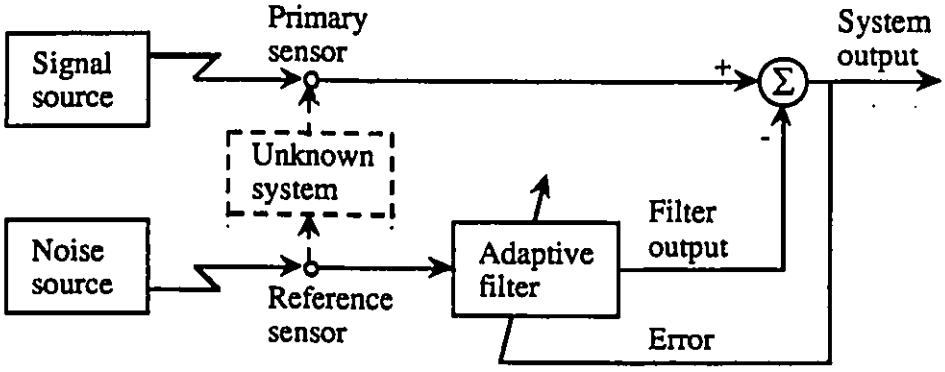

Figure 1.1 Adaptive noise cancellation.

Because of their particular applications, cases where the reference signal (noise source) is a sinusoidal function or a limited combination of sinusoidal functions will be referred to as adaptive interference cancellation throughout this thesis to adhere to the accepted terminology. In treating periodic interference, the adaptive noise canceller acts as a notch filter with narrow bandwidth, infinite null, and the capability of tracking the exact frequency of the interference. This type of system merits separate treatment because it offers effective solutions to a variety of practical applications, which includes the cancelling of periodic interference in electrocardiograph, acoustic adaptive line enhancement and military radio frequency scrambler.

Among the adaptive signal processing algorithms, the least-mean-square (LMS) algorithm is the most popular. This is due to its relatively simple implementation and when applied to adapting the coefficients of a FIR filter, its guaranteed stability. In this thesis, we will be considering both ANC and AIC where the LMS algorithm is used to update tne coefficients.

1.2 Why Adaptive Filtering in Subbands

Although it has been successfully applied to solve many problems, the LMS algorithm has certain limitations. The most troublesome is the dependence of performance on the input signal characteristics and adaptive filter length. The LMS algorithm converges slowly for input signals with non-flat power spectra and for cases where long FIR filters are being adapted. The concept of adaptive filtering in subbands was introduced with the double purpose of reducing the computational complexity and of improving the convergence speed of LMS algorithm.

The structure of adaptive filtering in subbands shown in Fig.1.2 was proposed by [W. Kellerman 1985 1988] for cancelling acoustic echoes in hands-free telephones.

In this structure, the primary input d(n) and reference input x(n) are split into K adjacent frequency subbands by an analysis filter bank (AFB). The subbanded error signals are recombined by a synthesis filter bank (SFB) to form the fullband output. The back-to-back analysis/synthesis system is designed to give distortion-free reconstruction of the input signal in the absence of the adaptive filters (AF) in subbands.

The implementation of adaptive filter in subbands proposed in [W. Kellerman 1988] is based on polyphase DFT filter banks. The subbanded signals are decimated by an integer factor D, where D is chosen less than K to reduce the aliasing effect.

While the adaptive filter in each band operates at the reduced sampling rate, this system provides faster convergence than the conventional fullband LMS adaptive filter, since the adaptive filter in each subband is now shorter and the input signal is flatter. The step size can be adjusted to match the signal energy in the individual bands. Thus, adaptive filtering in subbands, that is adapting several short filters in parallel on downsampled frequency subbands, is an attractive alternative to implementing long adaptive FIR filter from both computational efficiency and fast convergence perspectives.

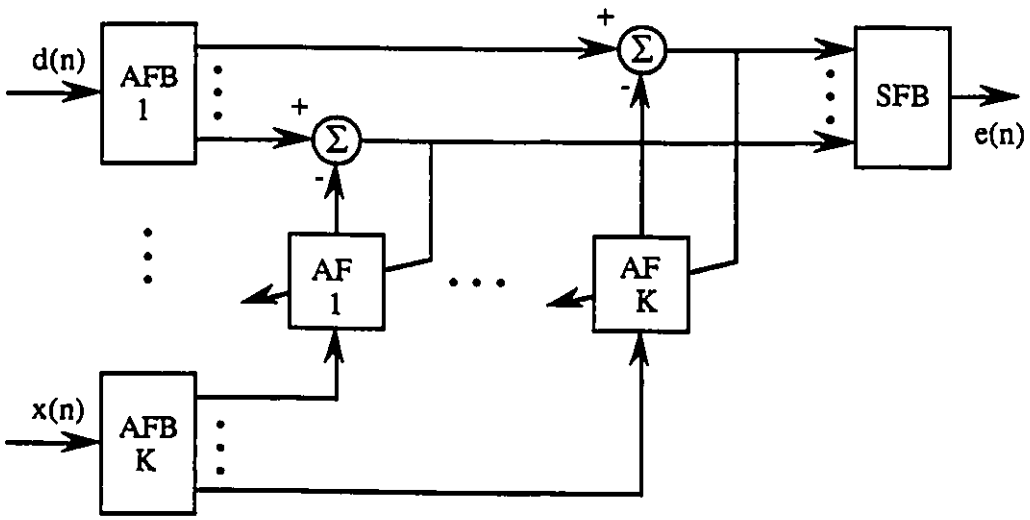

Figure 1.2 Subbanded adaptive filter structure.

By applying the theory of adaptive filtering in subbands, several authors successfully solved some problems encountered in mobile communication. To cancel the background acoustic noise in mobile telephones, a two-microphone system was used: a primary microphone measuring the speech signal and a reference one measuring the noise source. Simulations of fullband adaptive noise cancellation systems showed an overall noise reduction. But this noise power reduction was confined only to low frequencies where the input signal power was the largest. At

higher frequencies, undesired noise enhancements were observed [R. A. Goubran 1986] [M. M. Goulding 1990].

It was suggested in [R. A. Goubran 1986] that noise cancellation process should be performed only in low frequency band by bandlimiting the primary and reference filter inputs. The theory of adaptive filtering in subbands was extended in [R. Hebert 1990] and [R. B. Wallace 1992] to cover the entire frequency range by using multiband systems. After passing through individual LMS adaptive filters in subbands, signals were combined by SFB and a fullband output was produced. Based on the same reasoning, adaptive filtering in subbands can also be very successful in eliminating the interference of several sinusoidal signals by using a filter bank to isolate signals of different frequencies before they are cancelled individually by adaptive filters in subbands.

However, [A. Gilloire 1992] raised an interesting issue. Through experimental results with application to acoustic echo cancellation, it was found out that with the white noise as input the convergence performance of the subbanded adaptive filter is degraded in comparison with the full-band case, because the aliased components in the output error are not cancelled. So it was suggested adaptive cross-filters between the subbands be used. Since the focus of this thesis is not on the performance of the subbanded structure, but on how to implement the subbanded adaptive filter in an efficient fashion, we thus apply the non-compensated filter bank (without adding the cross-filters) to both the AIC and ANC cases.

1.3 Why Sigma-delta Modulation

Due to the advances in digital techniques in recent years, digital processing has been applied more and more to analog signals. By using an analog-to-digital

(A/D) converter, the analog input in Fig.1.3 is converted to its pulse code modulation (PCM) representation, and then the resulting digital signal is processed by a digital filter.

The lowpass filter at the input to the conventional A/D converter, i.e. the anti-aliasing filter, which attenuates high frequency noise and out-of-band components of the signal to minimize aliasing when the signal is sampled at the Nyquist rate. At the output stage another lowpass filter (reconstruction filter) is used to smooth the sampled output of the D/A converter.

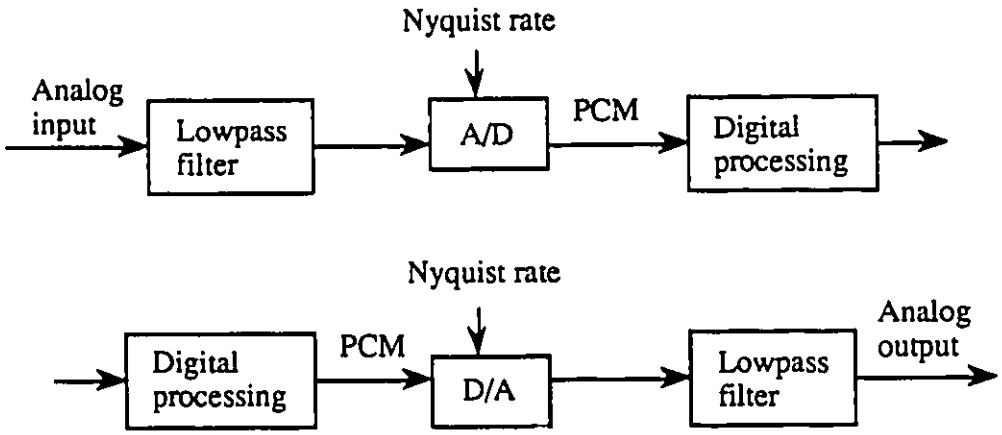

Figure 1.3 Conventional pulse code modulation.

This standard approach has several disadvantages. First, the accuracy of the output of a digital system is limited by the resolution of the A/D converter. The circuits of these conventional converters require high accuracy analog components in order to achieve high overall resolution. Second, during digital processing the conventional digital filter with input signal in PCM representation requires multibit multipliers and adders. The hardware complexity, i.e. the cost for these components can be very high in some applications [P. W. Wong 1990-1].

Recently, high-precision high-speed A/D converters were proposed based on sigma-delta modulation [Motorola]. The sigma-delta modulation system shown in

Fig.1.4 is a differential coding scheme which encodes a given signal into binary values. Processing these signals does not require multibit multipliers, and hence the system hardware complexity can be kept low.

The sigma-delta modulated converters operate in an oversampled mode, i.e. at a frequency much higher than the Nyquist rate with only single-bit words. The design of the modulator can trade resolution in time for resolution in amplitude. The use of oversampled modulation and demodulation can eliminate the need for abrupt cutoffs in the analog anti-aliasing filters at the input to the A/D converter, as well as in the filters that smooth the analog output of the D/A converter.

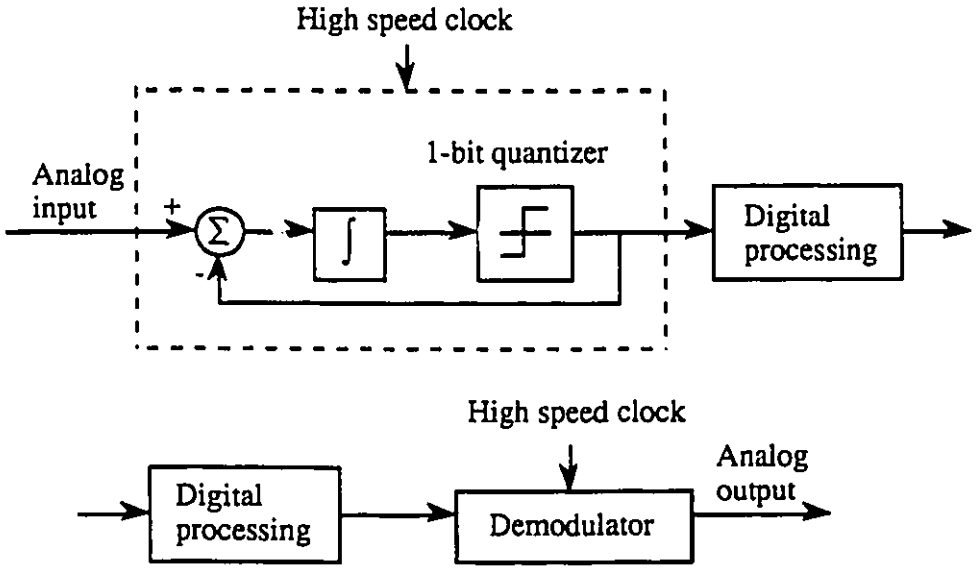

Figure 1.4 Block diagram of sigma-delta modulation.

Even though sigma-delta modulation was used to implement the A/D converters, it was assumed that the signal will be "demodulated" back to its PCM format before further processing. Recently, there have been several proposals for maintaining the signal in its sigma-delta modulated format during the subsequent

processing. This allows for taking full advantage of the low accuracy of the signal in reducing the system complexity.

Moreover, in building a digital filter, be it a fixed filter or an adaptive filter, besides using the sigma-delta modulated signal directly as an input, it was shown in [P. W. Wong 1990-1] that it is also possible to code the filter coefficients in the same way to further increase the reduction in complexity.

1.4 Thesis Motivation and Organization

This thesis examines the use of adaptive filtering in subbands as a means to overcome some of the limitations of regular LMS adaptive filters. The main focus is on digital signal processing (DSP) implementations of adaptive interference (sinusoidal signal) cancellation and adaptive noise (white noise) cancellation in Fig.1.5 using sigma-delta modulated signals and filters.

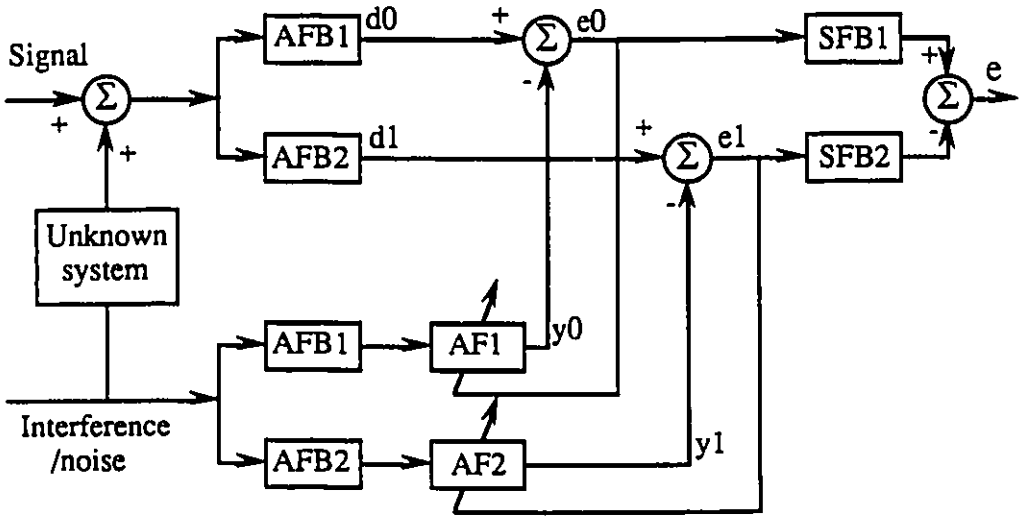

Figure 1.5 Subbanded adaptive interference/noise canceller.

After the sinusoidal interference passing through any unknown system, the output is still a sinusoidal signal with the same frequency, but might have an arbitrary phase shift. So for the AIC case, it is reasonable to use a phase shifter to model the unknown system. For the ANC case, the unknown system which distorts the white noise, is assumed to be an arbitrary multiband filter.

So the sigma-delta modulated subbanded adaptive interference and noise cancellers are proposed, where the above structure is implemented using sigma-delta modulation technique. The filter bank is fully sigma-delta modulated. The output signal from each filter bank is then used to produce the sigma-delta modulated input to the adaptive filter. The output of the partially modulated adaptive filter is demodulated at the final stage.

The performance of the proposed system will be studied compared to regular non sigma-delta modulated case regarding complexity, convergence speed and steady state error. The effect of the oversampling ratio used in the modulation as well as the quality of the demodulator will also be considered.

The thesis is organized as follows. Chapter 2 provides a review of the relevant background materials on the subbanded structures, the adaptive signal processing algorithm to be used here, and sigma-delta modulation theory. Chapter 3 presents some theoretical analysis of FIR filter banks and adaptive filtering operation implemented either partially or fully using sigma-delta modulation. Chapters 4 and 5 provide a performance analysis of the proposed structure compared to the conventional structure based on the simulation results for adaptive interference cancellation and adaptive noise cancellation, respectively. The main conclusion derived from the work of this thesis and suggestions for further research are discussed in Chapter 6.

2 Overview of Subbanded Adaptive Systems and Sigma-Delta Modulation Theory

This chapter provides the background material needed for this thesis. We start by reviewing the fundamentals of filter bank design as applied in our work. Then, the LMS algorithm, as it applies to interference and noise cancellers, is briefly summarized. This chapter ends by presenting the principles of sigma-delta modulation/demodulation and the study of the noise introduced in the process.

2.1 Subbanded Signal Processing

Subbanded structure contains two types of filter banks—analysis filter bank (AFB) and synthesis filter bank (SFB). From the structural point of view, a filter bank is a collection of filters which cover different frequency bands depending on the application. The input signal is decomposed in frequency into subbands by analysis filter bank, and after being processed, it is reconstructed from the elementary signal components by synthesis filter bank.

There are several important characteristics that distinguish different classes of filter banks [P. P. Vaidyanathan 1993] [R. E. Crochiere 1983]. Filter banks can be classified based on the manner in which the spacing and width of the frequency bands are chosen. Uniform filter banks have channels with the same bandwidths. Theoretically, for the N-band uniform bank system, the sampling rate of each of the

channel signals can be reduced by a factor N. The filter banks are then referred to as critically-sampled filter banks, and otherwise as oversampled filter banks.

Since the signals in the specific subbands are effectively oversampled, they are decimated following the analysis filter bank. They are later interpolated before the synthesis bank. Decimation can cause aliasing and interpolation can cause imaging [R. E. Crochiere 1983]. The aliasing and imaging make the design and realization of exact reconstruction analysis/synthesis bank systems a challenging task. However, several successful techniques have been developed to solve the problem based on the fact that information about the aliased signal in one channel is available in the other channels. An N-channel uniform filter bank is illustrated in Fig.2.1.1.

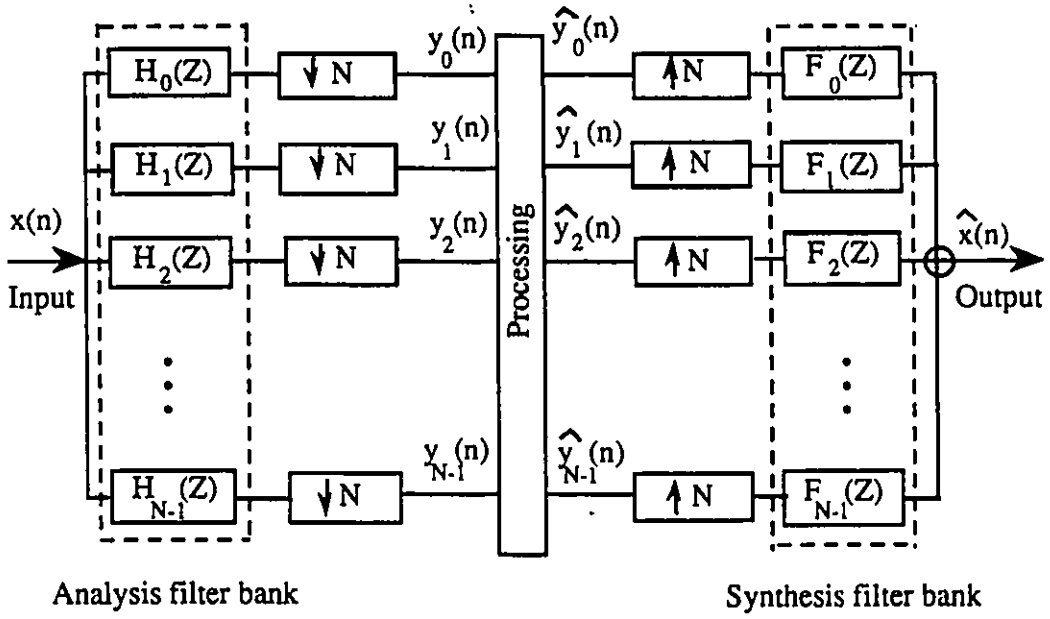

Figure 2.1.1 An N-channel analysis/synthesis uniform filter bank.

2.1.1 Perfect Reconstruction Requirements for QMF Filter Banks

Fig.2.1.2 shows a special case with only two bands. This filter bank was first introduced by [A. Croisier 1976], initiating a lot of research in this area. This type of filter bank is referred to as the quadrature mirror filter (QMF) filter bank.

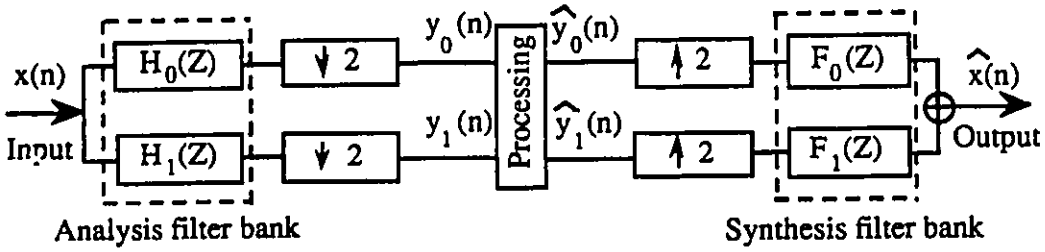

Figure 2.1.2 Quadrature mirror filter (QMF) filter bank.

The analysis part of the two-channel system in Fig.2.1.2 consists of a lowpass filter $h_0(n)$ and a highpass filter $h_1(n)$ followed by a 2-to-1 downsampler. Similarly, the filters $f_0(n)$ and $f_1(n)$ after the 1-to-2 upsampler represent the respective lowpass and highpass synthesis filters. Quadrature mirror filter banks were proposed in [R. E. Crochiere 1983] to ensure perfect reconstruction (PR). The QMF has the advantage of using the mutual information between the channel signals to cancel aliasing and imaging distortion. Given that $X(e^{j\omega})$, $Y_0(e^{j\omega})$, $Y_1(e^{j\omega})$, $H_0(e^{j\omega})$, $H_1(e^{j\omega})$ are the Fourier transforms of $x(n)$, $y_0(n)$, $y_1(n)$, $h_0(n)$ and $h_1(n)$ respectively, we get the analysis relation

$$Y_0(e^{j\omega})=X(e^{j\omega/2})H_0(e^{j\omega/2})+X(e^{j(\omega+2\pi)/2})H_0(e^{j(\omega+2\pi)/2}) \qquad (2.1.1)$$

and

$$Y_1(e^{j\omega})=X(e^{j\omega/2})H_1(e^{j\omega/2})+X(e^{j(\omega+2\pi)/2})H_1(e^{j(\omega+2\pi)/2}) \qquad (2.1.2)$$

Similarly, assuming $\hat{X}(e^{j\omega})$, $\hat{Y}_0(e^{j\omega})$, $\hat{Y}_1(e^{j\omega})$, $F_0(e^{j\omega})$, $F_1(e^{j\omega})$ be the transform of $\hat{x}(n)$, $\hat{y}_0(n)$, $\hat{y}_1(n)$, $f_0(n)$ and $f_1(n)$ respectively, we get the synthesis relation

$$\hat{X}(e^{j\omega})=\hat{Y}_0(e^{j2\omega})F_0(e^{j\omega})+\hat{Y}_1(e^{j2\omega})F_1(e^{j\omega}) \qquad (2.1.3)$$

In the absence of any processing, i.e. $Y_0(e^{j\omega})=\hat{Y}_0(e^{j\omega})$ and $Y_1(e^{j\omega})=\hat{Y}_1(e^{j\omega})$, by combing the three equations (2.1.1), (2.1.2) and (2.1.3), we get the input-to-output frequency domain relationship of the filter bank in the form

$$\hat{X}(e^{j\omega})=[H_0(e^{j\omega})F_0(e^{j\omega})+H_1(e^{j\omega})F_1(e^{j\omega})]X(e^{j\omega})$$

$$+[H_0(e^{j(\omega+\pi)})F_0(e^{j\omega})+H_1(e^{j(\omega+\pi)})F_1(e^{j\omega})]X(e^{j(\omega+\pi)}) \quad (2.1.4)$$

The first term in this equation represents the desired signal translation from $\hat{X}(e^{j\omega})$ to $X(e^{j\omega})$, whereas the second term represents the undesired frequency domain aliasing components. To eliminate these aliasing components, the second term must be canceled, i.e.

$$H_0(e^{j(\omega+\pi)})F_0(e^{j\omega})+H_1(e^{j(\omega+\pi)})F_1(e^{j\omega})=0 \quad (2.1.5)$$

This results in the input-to-output relation of the filter bank in the form

$$\hat{X}(e^{j\omega})=[H_0(e^{j\omega})F_0(e^{j\omega})+H_1(e^{j\omega})F_1(e^{j\omega})]X(e^{j\omega}) \quad (2.1.6)$$

From (2.1.6), it is known that the filter bank system becomes a unity gain system if

$$|H_0(e^{j\omega})F_0(e^{j\omega})+H_1(e^{j\omega})F_1(e^{j\omega})|=1 \quad (2.1.7)$$

which represents a perfect reconstruction operation under the condition that the delay is constant.

The analysis and synthsis filter would have to be designed to ensure (2.1.5) and (2.1.7) are satisfied. It can be shown that this is achieved for

$$F_0(e^{j\omega})=H_1(-e^{j\omega}) \quad (2.1.8)$$

$$F_1(e^{j\omega})=-H_0(-e^{j\omega}) \quad (2.1.9)$$

$$|H_0(e^{j\omega})H_1(-e^{j\omega})-H_1(e^{j\omega})H_0(-e^{j\omega})|=1 \quad (2.1.10)$$

Since the QMFs are defined to be frequency shifted versions of one another, i.e.

$$H_1(e^{j\omega})=H_0(e^{j(\omega+\pi)})=H_0(-e^{j\omega}) \quad (2.1.11)$$

i.e.

$$h_1(n)=(-1)^n h_0(n) \quad (2.1.12)$$

in time domain.

This condition implies that the filters $H_0(e^{j\omega})$ and $H_1(e^{j\omega})$ have mirror-image symmetry around half of the sampling frequency. Taking this into consideration, (2.1.10) will be simplified as

$$|H_0^2(e^{j\omega}) -H_1^2(e^{j\omega})|=1 \quad (2.1.13)$$

In conclusion, QMF will provide a perfect reconstruction if the delay is constant and following three equations are satisfied:

$$|H_0^2(e^{j\omega}) - H_1^2(e^{j\omega})|=1 \quad (2.1.14)$$

$$F_0(e^{j\omega})=H_0(e^{j\omega}) \quad (2.1.15)$$

$$F_1(e^{j\omega})=-H_1(e^{j\omega}) \quad (2.1.16)$$

2.1.2 PR Requirements for QMF Filter Banks Using Symmetric FIR Filters

Several approaches have been suggested for this design, including symmetric finite impulse response (FIR) filters [A. Croisier 1976], infinite impulse response (IIR) filters [T. P. Barnwell 1981], and variation of half-band filters [D. Esteban 1981]. Among them, the particular class of design based on symmetric FIR filter is the most useful, since they have the advantage of linear phase response (i.e. flat group delay) [R. E. Crochiere 1983].

Assume that $h_0(n)$ is a symmetric FIR filter with N taps, denoted specially by h(n), h(n)=h(N-1-n), n=0,1,...,N-1. The Fourier transform of h(n) has the form

$$H(e^{j\omega})=H_r(e^{j\omega})e^{-j\omega(N-1)/2} \quad (2.1.17)$$

where $e^{-j\omega(N-1)/2}$ is the linear phase term and $H_r(e^{j\omega})$ is a real function such that

$$H_r^2(e^{j\omega})=|H(e^{j\omega})|^2 \quad (2.1.18)$$

Applying (2.1.15), (2.1.16), (2.1.17) and (2.1.18) to (2.1.6) gives the input-to-output frequency response of the filter bank in the form

$$\hat{X}(e^{j\omega})=[|H(e^{j\omega})|^2 - |H(e^{j(\omega+\pi)})|^2 e^{-j(\omega+\pi)(N-1)}]X(e^{j\omega})$$

$$=[|H(e^{j\omega})|^2 - (-1)^{(N-1)}|H(e^{j(\omega+\pi)})|^2]e^{-j\omega(N-1)}X(e^{j\omega}) \quad (2.1.19)$$

Ignoring the $e^{-j\omega(N-1)}$ term since it does not affect the magnitude, the overall magnitude response should approximate a unity gain to reconstruct x(n). From (2.1.19), it is obvious that N being even or odd strongly affects the ability to reconstruct $X(e^{j\omega})$. If N is even, the equation above has the form

$$\hat{X}(e^{j\omega})=[|H(e^{j\omega})|^2+|H(e^{j(\omega+\pi)})|^2]e^{-j\omega(N-1)}\,X(e^{j\omega}) \qquad (2.1.20)$$

and of N is odd it has the form

$$\hat{X}(e^{j\omega})=[|H(e^{j\omega})|^2-|H(e^{j(\omega+\pi)})|^2]e^{-j\omega(N-1)}\,X(e^{j\omega}) \qquad (2.1.21)$$

In the latter case it is seen that at $\omega=\pi/2$, the overall magnitude response of the filter is zero due to the fact that $|H(e^{j\pi/2})|=|H(e^{j3\pi/2})|$. Thus, only designs for N even are useful, i.e.

$$|H(e^{j\omega})|^2+|H(e^{j(\omega+\pi)})|^2=1 \quad \text{for all } \omega \qquad (2.1.22)$$

is the PR requirement for symmetric FIR QMF filter banks, while N-1 is the delay.

For the special case of oversampled QMF filter banks, i.e. the sampling rate of two channel signals is kept unchanged, as opposed to being reduced by 2, the overall frequency response is

$$\hat{X}(e^{j\omega})=[H_0(e^{j\omega})F_0(e^{j\omega})+H_1(e^{j\omega})F_1(e^{j\omega})]X(e^{j\omega}) \qquad (2.1.23)$$

If $F_0(e^{j\omega})=H_0(e^{j\omega})$ and $F_1(e^{j\omega})=-H_1(e^{j\omega})$ hold, the PR will be

$$|\,H_0^2(e^{j\omega})\,-H_1^2(e^{j\omega})\,|^2=1 \qquad (2.1.24)$$

When it is a symmetric FIR filter implementation, this leads

$$|H_0(e^{j\omega})|^2+|H_1(e^{j\omega})|^2=1 \qquad (2.1.25)$$

if and only if N is even. If $F_0(e^{j\omega})=H_0(e^{j\omega})$ and $F_1(e^{j\omega})=H_1(e^{j\omega})$ hold, the PR will be

$$|H_0(e^{j\omega})|^2+|H_1(e^{j\omega})|^2=1 \qquad (2.1.26)$$

if and only if N is odd.

2.1.3 Designs for QMF Filter Bank Using Symmetric FIR Filters

A Hanning window design is chosen, because of its nearly flat frequency response in the passband. The filter length is 64 and the cutoff frequency is 0.5π corresponding one half of the magnitude response. The QMFs' frequency responses are shown in Fig.2.1.3(a) with the overall response shown in Fig.2.1.3(b). Notice that the reconstruction error ripple dipped down to -6dB at $\omega=0.5\pi$, because $|H_0(e^{j\omega})|^2+|H_1(e^{j\omega})|^2=(1/2)^2+(1/2)^2=1/2$, i.e. -6dB at $\omega=0.5\pi$. To keep the

reconstruction error minimal, we slightly shift the point of symmetry from 0.5π to 0.5127π. The QMFs' frequency responses are shown in Fig.2.1.4(a) with the overall response shown in Fig.2.1.4(b). Now the reconstruction error is within $\pm$0.2dB, which is quite acceptable for many applications. These two filters will be used as the QMF filter bank for all the simulations in this thesis.

QMF designs with better lowpass characteristics and smaller reconstruction error for a given filter length N can be achieved by using a nonlinear computer aided optimization technique [J. D. Johnston 1980] [V. K. Jain 1983]. The optimization program is applied to systematically search for the coefficients that minimize the error function defined as a weighted sum of two terms

$$E=E_r+\alpha E_s(\omega_s) \tag{2.1.27}$$

where

$$E_s(\omega_s)=\int_{\omega=\omega s}^{\pi}|H(e^{j\omega})|^2 d\omega \tag{2.1.28}$$

describes the energy in the stopband region of the frequency response $H(e^{j\omega})$ with cutoff frequency $\omega_s>0.5\pi$. And

$$E_r=\int_{\omega=0}^{\pi}[|H_0(e^{j\omega})|^2+|H_1(e^{j\omega})|^2-1]d\omega \tag{2.1.29}$$

represents the error in approximating (2.1.23). And α is a weighting factor.

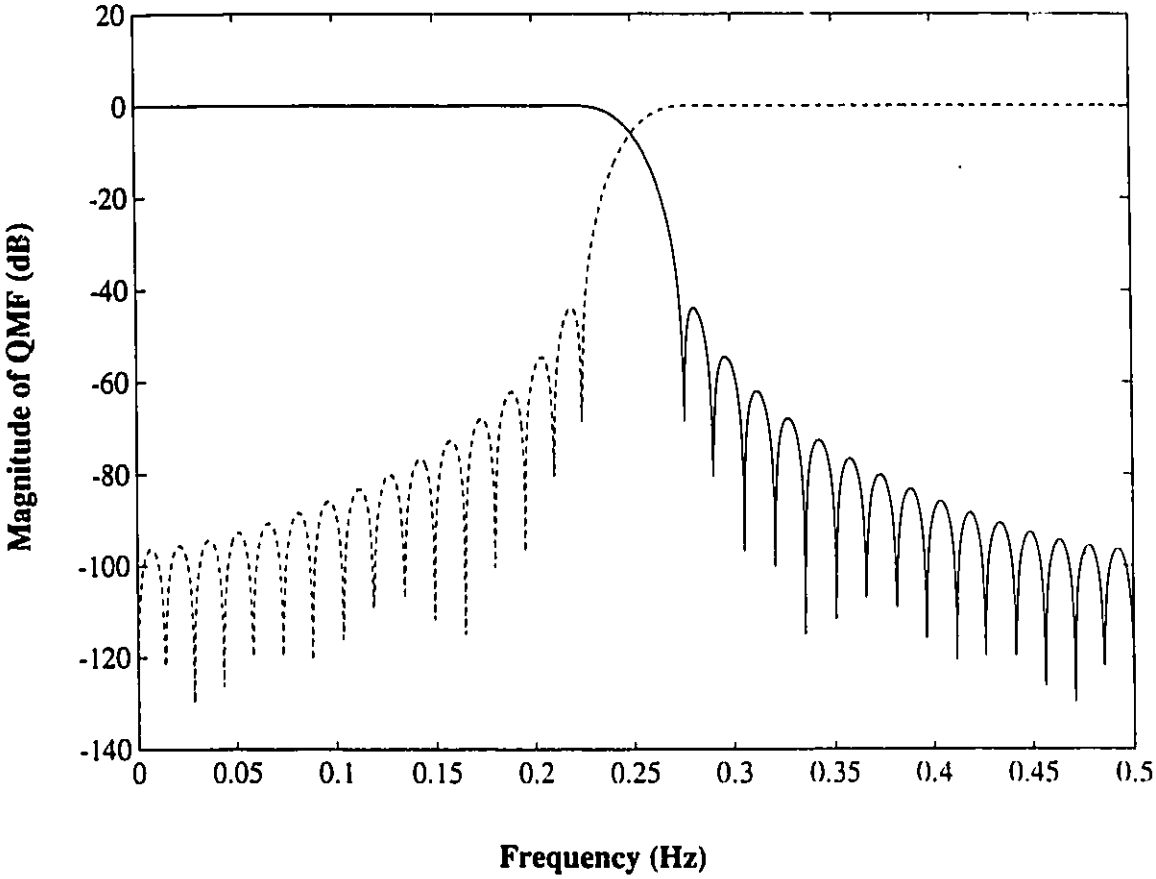

Figure 2.1.3 QMF with $f_c=0.5\pi$: (a) filters' frequency responses.

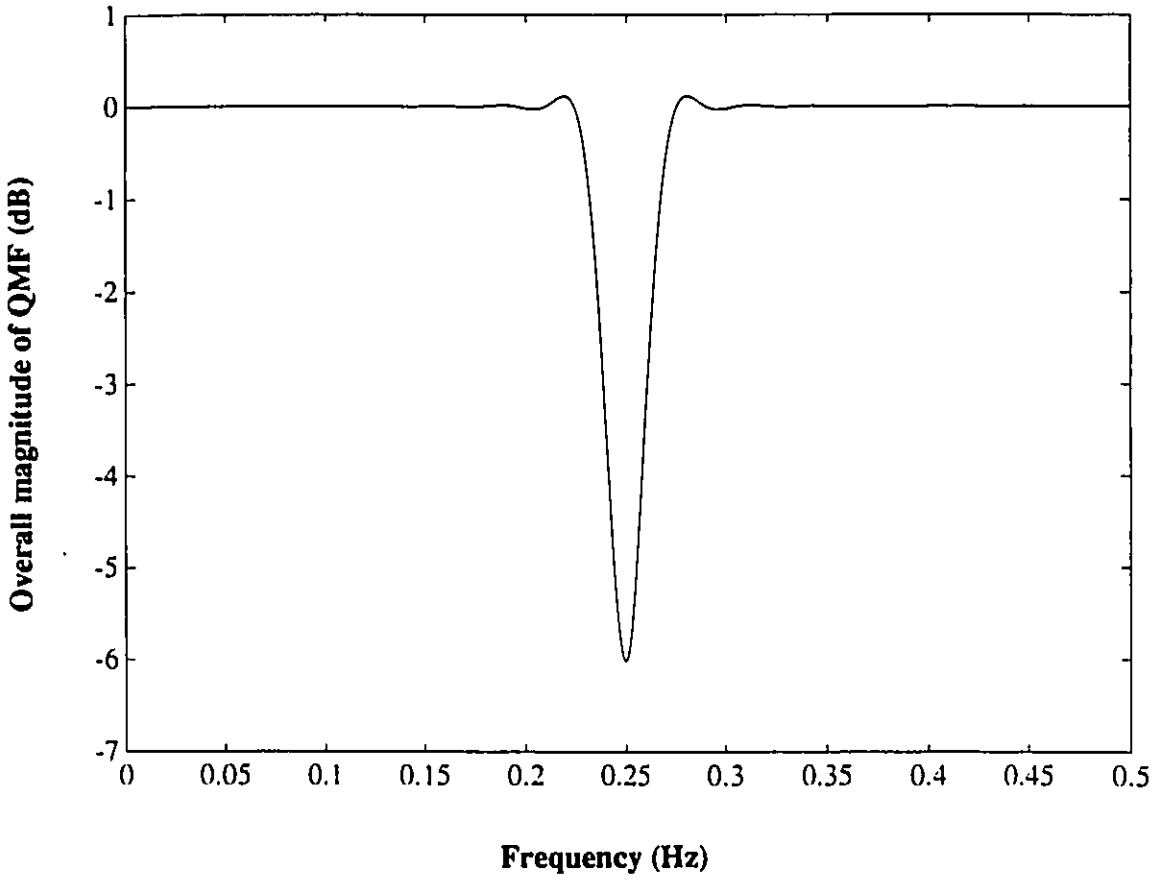

Figure 2.1.3 QMF with $f_c=0.5\pi$: (b) overall frequency response.

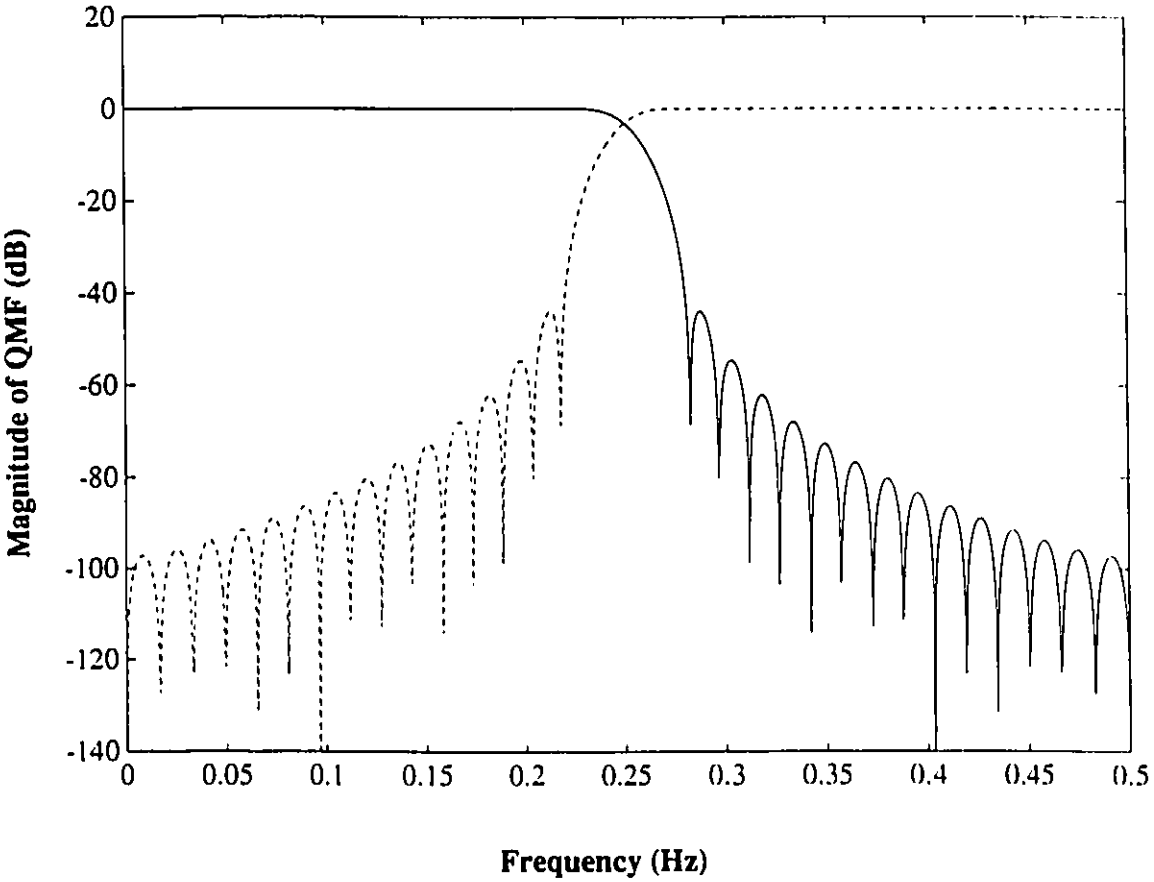

Figure 2.1.4 QMF with f_c=0.5127π: (a) filters' frequency responses.

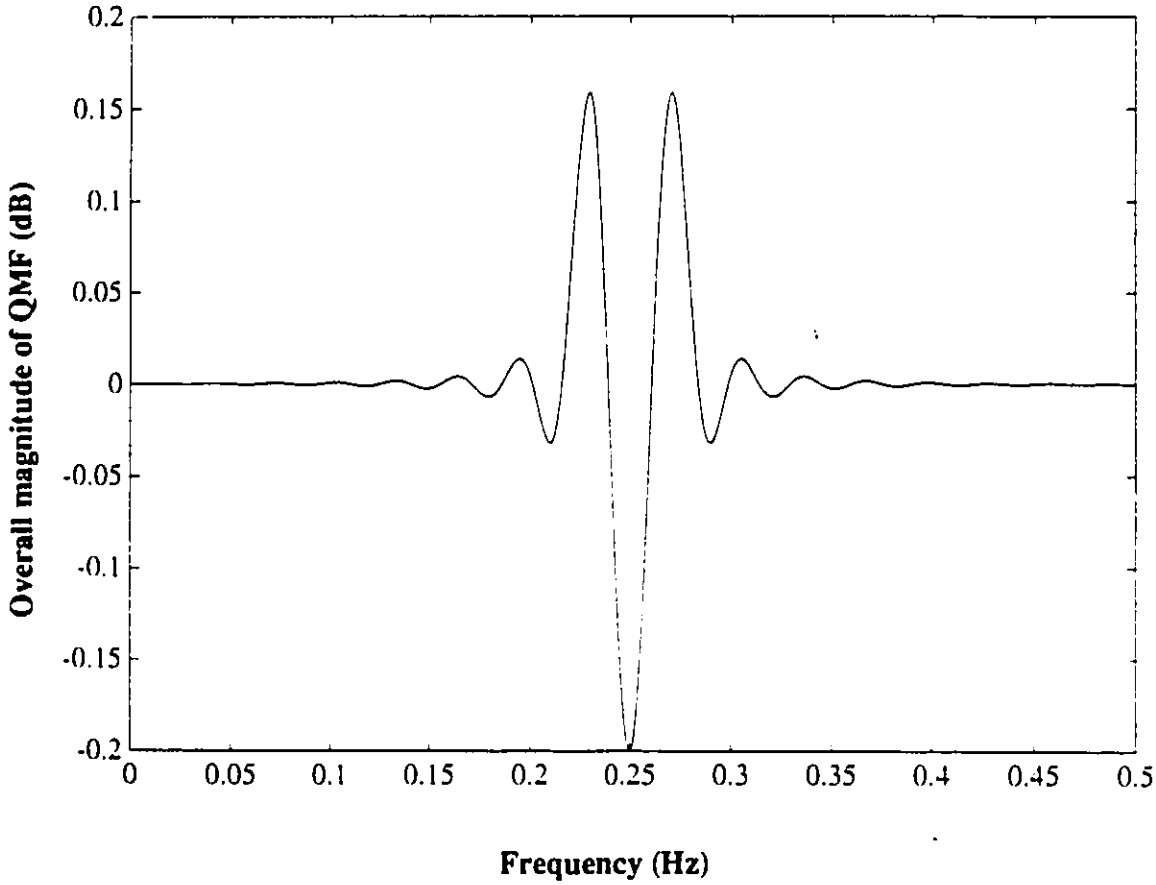

Figure 2.1.4 QMF with f_c=0.5127π: (b) overall frequency response.

2.2 Adaptive Signal Processing

2.2.1 Least-mean-square Adaptive Algorithm

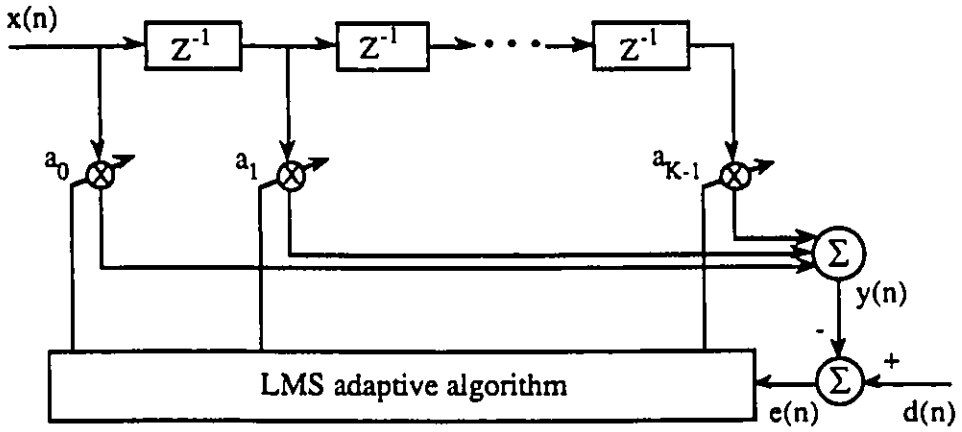

Figure 2.2.1 Least-mean-square (LMS) algorithm.

Fig.2.2.1 shows the basic structure for an adaptive FIR filter being updated by least-mean-square (LMS) algorithm. The overall system operation can be divided into:

1. Filtering operation

This is simply processing the output y(n) corresponding to the weighted sum of delayed input with the weights being the adaptive filter coefficients at that instant:

$$y(n)=\sum_{r=0}^{K-1} a_r(n)x(n-r) \qquad (2.2.1)$$

where $a_r(n)$ is the rth coefficient of the adaptive filter.

2. Error generation

An error function is generated as the difference between the actual output of the adaptive filter, y(n), and the desired output d(n):

$$e(n)=d(n)-y(n) \qquad (2.2.2)$$

3. Coefficient update

Based on the value of e(n), the coefficients are updated so as to minimize the instantaneous squared error. The update equation is give by:

$$a_r(n)=a_r(n-1)+2\mu e(n-1)x(n-r-1) \qquad (2.2.3)$$

where is μ the step size.

The LMS algorithm defined by (2.2.1), (2.2.2) and (2.2.3) aims at minimizing the instantaneous squared value of the error signal e(n) at steady state. The final error consists of two components: the theoretical minimum mean squared error J_{min} produced by the adaptive filter with optimum coefficients, and the excess mean squared error $J_{ex}(\infty)$ produced by the operation of the algorithm itself [S. Haykin 1991].

The minimum mean-square error J_{min} is determined by the characteristics of the desired signal and by the ability of the number of coefficients to model the unknown system. The steady state excess error $J_{ex}(\infty)$ is determined by the selection of the step size value and is given in [S. Haykin 1991] as

$$J_{ex}(\infty)= J_{min} \frac{\mu \sum_{i=0}^{K-1} \frac{\lambda_i}{2-\mu\lambda_i}}{1-\mu \sum_{i=0}^{K-1} \frac{\lambda_i}{2-\mu\lambda_i}} \qquad (2.2.4)$$

where λ_i's are the eigenvalues of the autocorrelation matrix of the input vector. The total steady state mean-square error $J(\infty)$ is the sum of J_{min} and $J_{ex}(\infty)$, which is

$$J(\infty)= J_{min}+J_{ex}(\infty)= \frac{J_{min}}{1-\mu \sum_{i=0}^{K-1} \frac{\lambda_i}{2-\mu\lambda_i}} \qquad (2.2.5)$$

From this result, it can be seen that three principal factors affect the performance of the LMS algorithm: the step size parameter μ, the number of taps K, and the eigenvalues of the correlation matrix of the input vector. When the latter two factors are fixed, the value of the step size has a predominant influence on the behavior of the algorithm. A small value for μ produces a small $J(\infty)$, but results in a slow adaptation of coefficients and thus slow convergence. On the other hand, a large

value for μ results in a fast adaptation, but at the expense of an increase in $J(\infty)$. This trade-off should be considered throughout every related performance simulation.

2.2.2 Adaptive Interference Cancellation

The traditional method of suppressing a sinusoidal interference corrupting an information-bearing signal is to use a fixed notch filter tuned to the frequency of the interference. To design the filter, we naturally need to know the precise frequency of the interference. But if the notch is required to be very sharp and the interfering sinusoid is known to drift slowly, we have to find an adaptive solution provided by the use of adaptive interference cancellation illustrated in Fig.2.2.2.

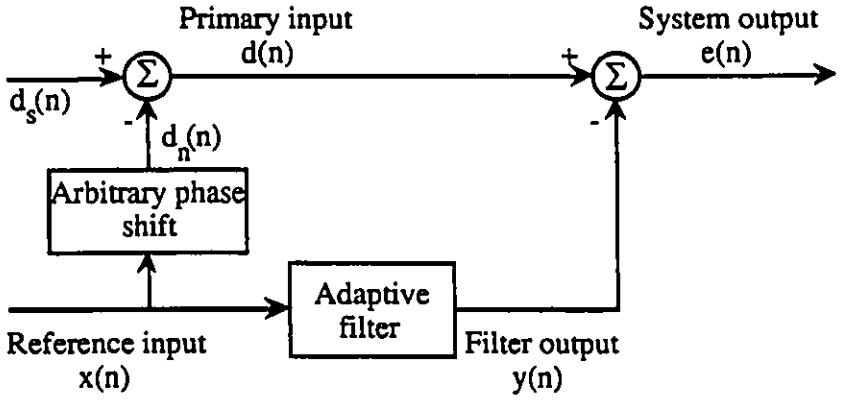

Figure 2.2.2 Adaptive interference cancellation.

In the examples considered in this thesis, the input/output data are assumed to be real valued when using the real LMS algorithm:

1. Primary input:

$$d(n)=d_s(n)+A_0\cos(2\pi f_0 n+\phi_0) \qquad (2.2.6)$$

where A_0 is the amplitude of the sinusoidal interference, f_0 is the frequency, ϕ_0 is the phase, and $d_s(n)$ is an information-bearing signal simulated using a white noise signal in this thesis.

2. Reference input:

$$x(n)=A\cos(2\pi f_0 n+\phi) \tag{2.2.7}$$

where the frequency f_0 is the same, but the phase ϕ is different from ϕ_0, and A could be different from A_0.

3. System error output:

$$e(n)=d(n)-y(n) \tag{2.2.8}$$

where the filter output y(n) is as close as a replica as possible of the periodic interference, and e(n) is expected to be interference free after the algorithm converges, i.e. $e(n)\approx d_s(n)$.

2.2.3 Adaptive Noise Cancellation

The adaptive noise cancellation system is shown in Fig.2.2.3.

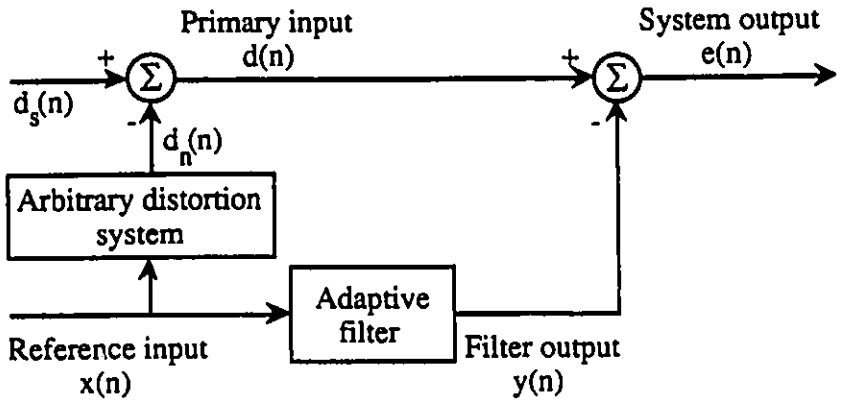

Figure 2.2.3 Adaptive noise cancellation.

This is basically identical to interference cancellation except for the difference in the nature of inputs.

1. A signal $d_s(n)$ is transmitted over a channel corrupted by a noise $d_n(n)$ which is uncorrelated with $d_s(n)$. The combined signal and noise form the primary input to the canceller

$$d(n)=d_s(n)+d_n(n) \tag{2.2.9}$$

2. A second noise x(n) uncorrelated with the signal $d_s(n)$, but correlated in some unknown way with the noise $d_n(n)$, provides the reference input to the canceller.

3. The noise x(n) is processed by the adaptive filter to produce an output y(n) that is as close a replica of $d_n(n)$ as possible. This output is subtracted from the primary input d(n) to produce the system error output

$$e(n)=d_s(n)+d_n(n)-y(n) \tag{2.2.10}$$

For ANC case in this thesis, $d_s(n)$ is assumed to be zero so that the error e(n) should go close to zero at steady state.

2.3 Sigma-Delta Modulation Technique

With the developments in digital VLSI technologies, sigma-delta (Σ–Δ) modulation has been receiving increased popularity as a cost effective alternative to conventional high-resolution A/D converters. It uses oversampling and one-bit quantization to achieve high-resolution A/D conversion at a low rate. The reason for its suitability for VLSI implementation is a result of the fact that circuit precision requirements can be significantly reduced when using oversampled input signals, coarse quantization, followed by digital decoding [R. M. Gray 1987] [S. H. Ardalan 1987] [J. C. Candy 1986].

Conventional high-resolution A/D converters operate at the Nyquist rate, defined as the sampling frequency approximately twice the maximum frequency of the input signal. This does not make full use of the exceptionally high speeds achievable with the VLSI technologies. Besides, for this type of converters, the analog anti-aliasing lowpass filter is generally fairly expensive. Conversely, the oversampled sigma-delta A/D converters operate at a sampling rate which is much higher than the Nyquist rate. They use a one-bit quantizer as a low resolution A/D converter, noise shaping technique and a decimation process to gain high-resolution normal-rate digital signal. In many applications, in order to relax the brick-wall requirement on the anti-aliasing filter, a rate slightly higher than the Nyquist frequency is used.

Several advantages of Σ–Δ converters have been verified [Motorola]: the implementation is simple and robust against circuit imperfections; the oversampling method eases the requirements on the sample-and-hold function as well as on the anti-aliasing and reconstruction filters; the one-bit quantizer eliminates the need for precise component matching; and most part of the circuit is digital and is suitable for the implementation of complex monolithic systems using VLSI technologies .

Oversampled Σ–Δ converters have found use in such applications as digital audio, digital telephone and instrumentation. The related treatments can be found in [K. Hamashita 1989] [R. W. Adams 1986] [P. Defraeye 1985] [T. Misawa 1981] [K. Matsumoto 1988] [V. Friedman 1989] [B. H. Leung 1988] [J. W. Scott 1986].

Since the oversampling rate usually needs to be several times higher than the Nyquist rate, this oversampling method is most suitable for relatively low frequency signals. Applications in high frequency range as video or radar system will be available as the technology develops [J. C. Candy 1991].

In this chapter, through structure derivation and noise analysis, we will show the advantages of oversampled Σ–Δ A/D converters over both conventional A/D converters and oversampled A/D converters without Σ–Δ modulation.

2.3.1 Conventional A/D Converters and Noise Analysis

Most A/D converters can be classified into two groups according to the sampling rate criterion: conventional Nyquist-rate converters and oversampled converters. Conventional converters sample analog signal with a maximum frequency f_B at the Nyquist frequency f_N, which is $f_N \approx f_B * 2$. Meanwhile, oversampled converters perform the sampling process at a much higher rate, $f_s >> f_N$, where f_s denotes the input sampling rate.

Fig. 2.3.1 illustrates the conventional A/D converter that transforms an analog input signal into a sequence of digital codes at a sampling rate of $f_N = 1/T$, where T denotes the sampling interval.

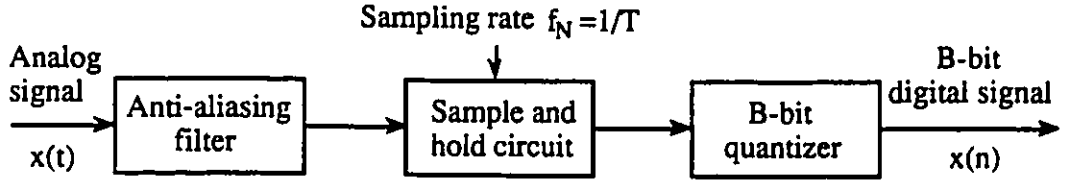

Figure 2.3.1 Conventional analog-to-digital converter.

The analog anti-aliasing filter at the input attenuates high-frequency noise and out-of-band components of the signal that alias into the signal when sampled at Nyquist rate. This lowpass filter must have flat response over the frequency band of interest, i.e. baseband, and have enough attenuation outside this band. In many applications, in order to relax the requirements on the anti-aliasing brick-wall filter, a rate slightly higher than the Nyquist frequency is used.

With a proper anti-aliasing filter, periodic sampling at the Nyquist rate does not introduce distortion in the sense that the sampled sequence can be used to reconstruct the original analog signal. However, the sample-and-hold and quantization processes can introduce significant distortion, and the main objective in designing a converter is to limit this distortion [J. C. Candy 1991]. Assume q is the interval between two successive reference levels in the quantizer, and the quantization error e is treated as white noise with equal probability in the interval (-q/2, q/2), then the noise power, i.e. variance σ_e^2, can be found as

$$\sigma_e^2 = E(e^2) = \frac{1}{q}\int_{-q/2}^{q/2} e^2 de = \frac{q^2}{12} \qquad (2.3.1)$$

Fig.2.3.2 shows the spectrum of the quantization noise. Since the noise power is spread over the entire positive frequency range equally, the level of the noise power spectral density is

$$N(f) = \frac{q^2}{12*2f_B} = \frac{\sigma_e^2}{2f_B} = \frac{\sigma_e^2}{f_N} \qquad (2.3.2)$$

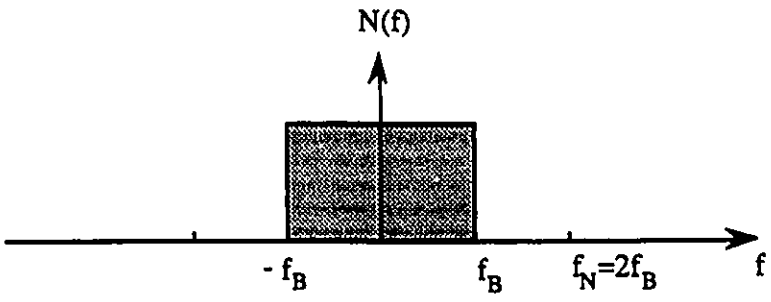

Figure 2.3.2 Quantization noise spectrum of conventional Nyquist converter.

It is obvious that the resolution of such converters is predetermined by the number and spacing of the quantization levels. For standard 16-bit A/D converters which have 2^{16}-1 different levels, the requirement on the accuracy of the converters is very strict [Motorola].

2.3.2 Oversampled A/D Converters and Noise Analysis

Fig.2.3.3 shows the immediate advantage of using oversampling method in relaxing the requirement on the anti-aliasing filter. The filter requirement for Nyquist rate A/D converter is shown in Fig.2.3.3(a), while the requirement for the R times oversampling (f_s=Rf_N) PCM A/D converter is shown in Fig.2.3.3(b).

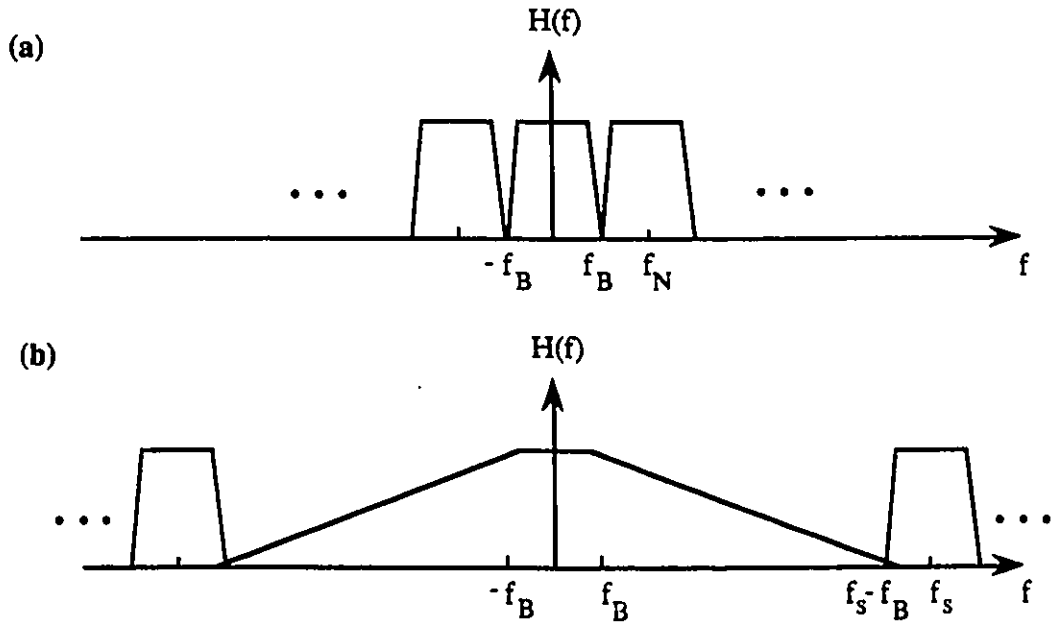

Figure 2.3.3 Frequency response of analog anti-aliasing filters. (a) for Nyquist-rate A/D converter, (b) for oversampled A/D converter.

In order to provide adequate aliasing protection without affecting the information-bearing signal within bandwidth f_B, the Nyquist rate A/D converter requires the anti-aliasing filter to have a very narrow transition band. On the other

hand, the transition bandwidth for the oversampled case can be significantly increased, from f_B up to about f_s-f_B as shown in Fig.2.3.3(b). Since the complexity of the filter is a strong function of the ratio of the transition bandwidth to the signal bandwidth f_B, oversampled A/D converters need simpler, easier-to-build analog anti-aliasing filters compared to conventional converters while providing similar performance.

Assuming that the baseband input to an oversampled converter is PCM encoded using the same number of quantization level spacing q as the conventional converter, then the total noise power will be the same. However, the noise spectral density is different

$$N(f)= \frac{q^2}{12f_s} = \frac{\sigma_e^2}{f_s} \tag{2.3.3}$$

This leaves the baseband noise power N_B as

$$N_B= \int_{-f_B}^{f_B} N(f)\, df = \frac{2f_B}{f_s}\,\frac{q^2}{12} = \frac{\sigma_e^2}{R} \tag{2.3.4}$$

where R is the oversampling ratio defined as $f_s/(2f_B)=f_s/f_N$. This results in a 3dB in-band noise decrease with each doubling of the oversampling frequency [J. C. Candy 1991]. Fig.2.3.4 shows the spectrum of overall quantization noise level (in shaded area) and baseband noise level for an oversampled converter (in double shaded area).

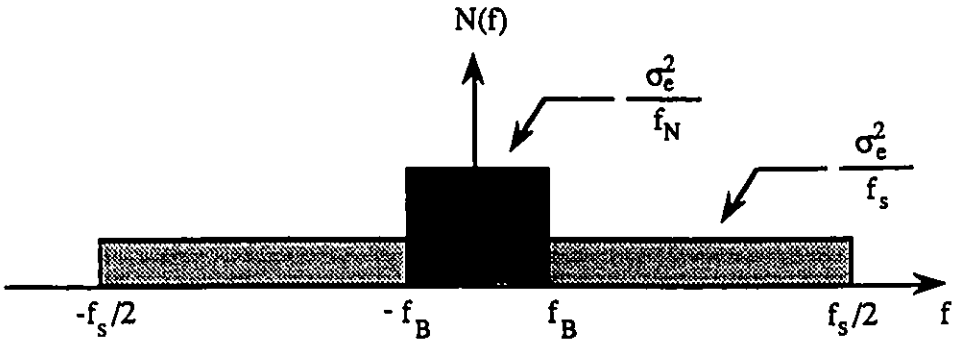

Figure 2.3.4 Quantization noise spectrum of oversampled A/D converter.

Regardless of the advantage of a simpler anti-aliasing filter, oversampled A/D converters are highly desirable since they can make use of a coarse quantization with proper quantization noise reshaping to reach high precision requirement, while a Nyquist-rate one can only use fine quantizer with a large number of levels to achieve the same goal [Motorola]. This feature paves the way for oversampled Σ–Δ A/D converter. Since the final sampling rate should be brought back to Nyquist rate, a decimation filter is required. However, because this decimator is implemented with digital circuitry, as opposed to anti-aliasing filters which are implemented with analog circuitry, it is more economical and can be implemented in fairly efficient ways.

2.3.3 Oversampled Sigma-Delta A/D Converters and Noise Analysis

The oversampled sigma-delta modulated A/D converter is shown in Fig.2.3.5. The input to the circuit is processed by the quantizer via an integrator, and the quantized output is fed back to the input through a recursive loop.

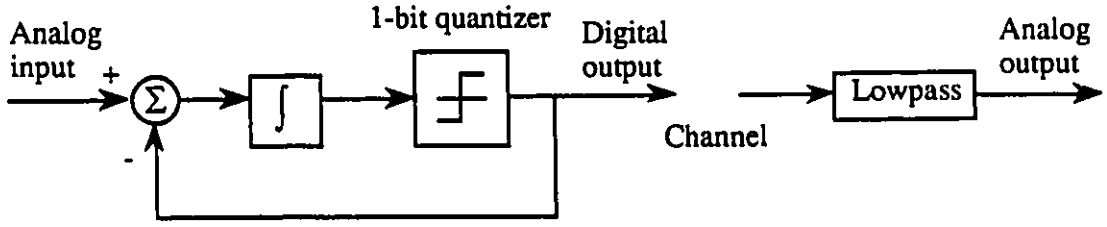

Figure 2.3.5 Block diagram for sigma-delta modulation.

The sigma-delta modulator's equivalent circuit is shown in Fig. 2.3.6(a). The corresponding S domain and Z domain models are shown in Fig.2.3.6(b) and (c). From Fig.2.3.6(b), we get

Integrator transfer function: $I(S)=\frac{1}{S}$ (2.3.5)

Signal transfer function: $Y(S) = [X(S)-Y(S)]I(S)$ (2.3.6)

(when N(S)=0) $\frac{Y(S)}{X(S)} = \frac{I(S)}{1+I(S)} = \frac{1}{S+1}$:is a lowpass filter

Noise transfer function: $Y(S) = [N(S)-Y(S)]I(S)$ (2.3.7)

(when X(S)=0) $\frac{Y(S)}{N(S)} = \frac{1}{1+I(S)} = \frac{S}{S+1}$:is a highpass filter

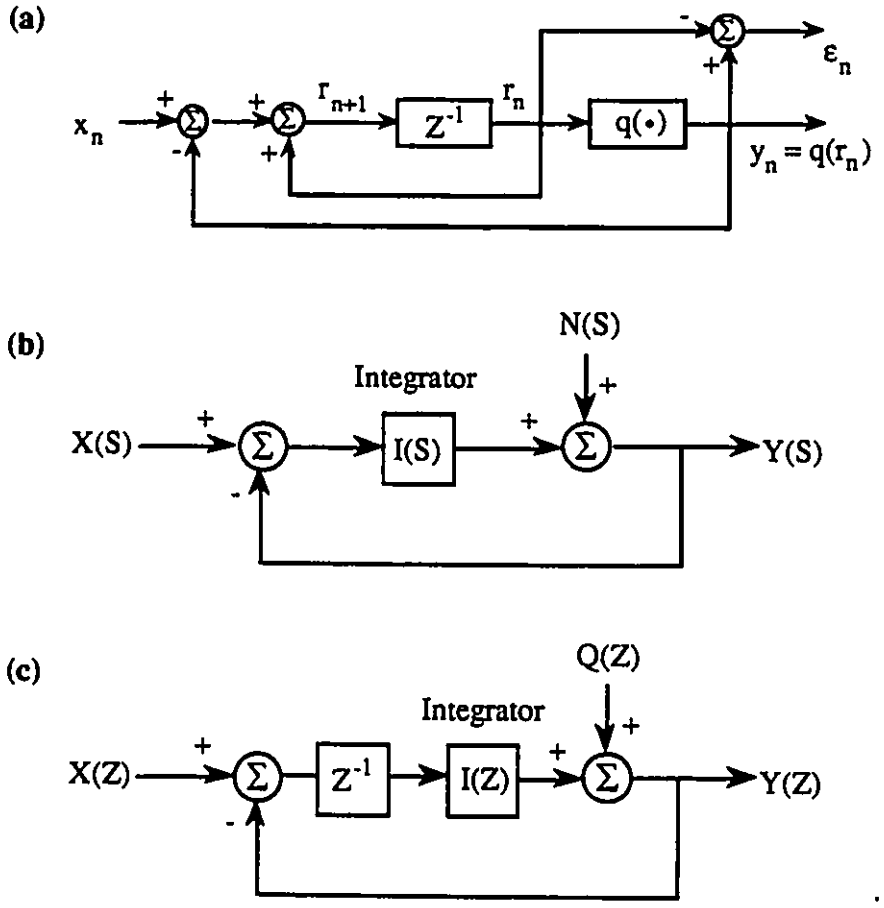

Figure 2.3.6 Sigma-delta modulator model.
(a) in time domain, (b) in S domain, (c) in Z domain.

This implies that the loop has a noise-shaping function which low-pass filters the signal and high-pass filters the noise, as it integrates the error between the quantized signal and the actual input. In other words, the signal in baseband is left unchanged, but the Σ–Δ recursive loop shapes the noise into a higher frequency band.

Recall that with a larger oversampling ratio the quantization noise is spread over a wider bandwidth and the noise density in the bandwidth of interest is greatly decreased. The noise shaping provided by the sigma-delta modulator does not reduce this overall noise power but minimizes its in-band component.

Z-domain analysis of Σ–Δ modulator is illustrated in Fig.2.3.6(c). The transfer function of an integrator is denoted by I(Z) as

$$I(Z)= \frac{1}{1-Z^{-1}} \tag{2.3.8}$$

and the 1-bit quantizer is modeled as an additive noise source Q. This gives

$$Y(Z)=Q(Z)+I(Z)Z^{-1}[X(Z)-Y(Z)] \tag{2.3.9}$$

i.e.

$$Y(Z)=Z^{-1}X(Z)\,\frac{I(Z)}{1+I(Z)Z^{-1}} + Q(Z)\,\frac{1}{1+I(Z)Z^{-1}} \tag{2.3.10}$$

and Y(Z) can be simplified to

$$Y(Z)=Z^{-1}X(Z)+(1-Z^{-1})Q(Z) \tag{2.3.11}$$

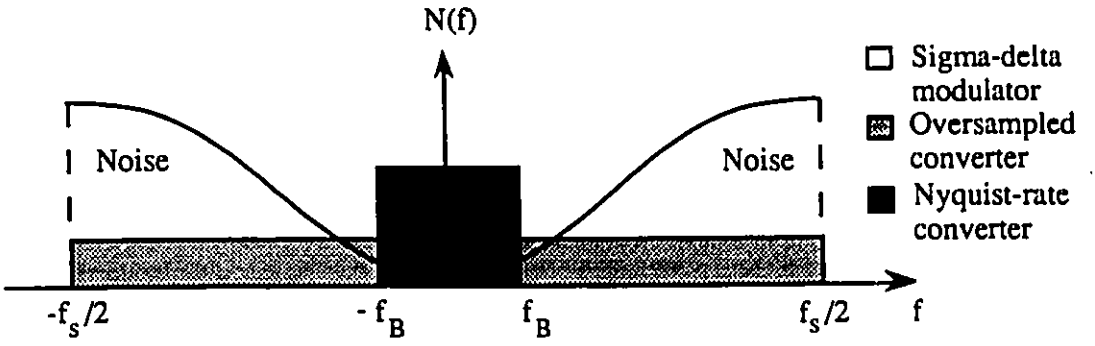

Figure 2.3.7 Comparison of noise spectrums for Nyquist-rate, oversampled and sigma-delta modulated A/D converters.

Again, this implies that the differentiator $1-Z^{-1}$ pushes the noise towards the high frequency band while leaving the desired signal unaffected. The high frequency quantization noise can be eventually removed by a digital lowpass filter without affecting the input signal characteristics residing in baseband. This is shown in

Fig.2.3.7. It is obvious that if only two-level coarse quantizer is used, at every sampling instance, the quantization errors are large for both oversampling PCM converter and oversampling sigma-delta modulator. However, the difference between them is that the quantization error for the modulator is summed up in the integrator before being quantized. The one-bit output sequence can be later averaged over several input sample periods by decimation filter to produce a very accurate result.

Referring to Fig.2.3.6(a), we can write the quantization error as

$$\varepsilon_n = q(r_n) - r_n \tag{2.3.12}$$

The output of the modulator is

$$y_n = q(r_n) = x_{n-1} + \varepsilon_n - \varepsilon_{n-1} \tag{2.3.13}$$

Assume the modulation error can be treated as white noise uncorrelated with the signal, the spectral density of the modulation noise

$$n_n = \varepsilon_n - \varepsilon_{n-1} \tag{2.3.14}$$

may then be expressed as

$$N(f) = \frac{\sigma_e^2}{f_s} |1 - e^{-j\omega T}|^2 = T\sigma_e^2 |2e^{-j\omega T/2}(e^{j\omega T/2} - e^{-j\omega T/2})/2|^2$$

$$= T\sigma_e^2 (2\sin(\frac{\omega T}{2}))^2 \tag{2.3.15}$$

where $T = \frac{1}{f_s}$, $\omega = 2\pi f$ and $e_{rms}^2 = \frac{q^2}{12} = \sigma_e^2$. The noise power in the signal band is thus given by

$$N_B = \int_{-f_B}^{f_B} N(f)\, df = \int_{-f_B}^{f_B} T\sigma_e^2 (2\sin(\frac{2\pi f T}{2}))^2\, df$$

$$= \sigma_e^2 \frac{\pi^2}{3}(2f_B T)^3 = \sigma_e^2 \frac{\pi^2}{3}(\frac{1}{R})^3, \qquad f_s^2 >> f_B^2 \tag{2.3.16}$$

Each doubling of the oversampling ratio thus reduces this noise by 9dB [J. C. Candy 1991] compared to the 3dB reduction achievable by oversampling only.

During the implementation, the equation (2.3.12) and (2.2.13) are used to encode the input x_n into the 1-bit sequence v_n which is the output of the modulator, assuming that r_n has an initial value of zero.

2.3.4 Decimating the Sigma-Delta Modulated Signal

The digital output of the modulator shown in Fig.2.3.5 contains the information-bearing input signal together with its significant out-of-band component: the modulation noise. A digital lowpass filter is then used to attenuate all of the out-of-band energy of this signal so that it may be decimated down to the Nyquist rate without incurring significant noise penalty due to aliasing.

In the time domain, this is effectively equivalent to transforming the 1-bit data stream at a high sampling rate into a high-resolution data stream at a low sampling rate. Essentially, decimation is both an averaging filter function and a rate reduction function performed simultaneously.

An ideal decimator is a perfect brick-wall lowpass filter. The simplest and most economical decimation filter to reduce the input sampling rate is a comb filter:

$$h(n)=1 \quad 0 \le n \le K-1;$$

$$h(n)=0 \quad \text{otherwise.} \qquad (2.3.17)$$

Such a filter does not require any multipliers. However, the comb filter is not always very effective in removing the out-of-band quantization noise depending on the signal bandwidth and the decimation factor. For those applications which can not tolerate this distortion, a better quality lowpass filter should be designed.

Efficient designs for good quality decimators have been studied extensively in [J. C. Candy 1986] [E. Dijkstra 1987 1988] [T. Saramaki 1988] [D. J. Goodman 1977]. Some filter design approaches and relevant considerations are reviewed here.

1. Multistage design

Multistage implementation has been shown to be particularly efficient when the decimation factor R is large. The strategy is based on using a wider transition band in the lowpass filters operating at the higher rates, thereby reducing the length of the required impulse responses in those stages. As decimation occurs, the sampling frequency is reduced and we can progressively reduce the widths of the transition

bands of the required filters while maintaining reasonable filter orders. In this manner, the overall number of computations required to implement the decimator may be reduced significantly [A. V. Oppenheim 1989][R. E. Crochiere 1983].

This approach was applied in [J. C. Candy 1986] to obtain the decoder in Fig.2.3.8. It has been pointed out that a cascade of comb filters is a good decimator for decimating a sigma-delta modulated signal down to $4f_N$, i.e. for a downsampling ratio of R/4. To decimate signal from $4f_N$ to the Nyquist frequency f_N, it is necessary to use a baseband filter with flat passband and sharp rolloff characteristics. Though this filter has to have sharp cutoff, it is not very complex since it operates at a much lower rate.

Exploiting the merits of a multistage implementation, [T. Saramaki 1988 1990] introduced a class of decimators which are much more efficient. Again a cascade of comb filters is used at the earlier stages. The following baseband filter is composed of three stages of low-order FIR filters where all the coefficients can be represented by sums or differences of powers of two, resulting in the overall filter requiring no general multipliers.

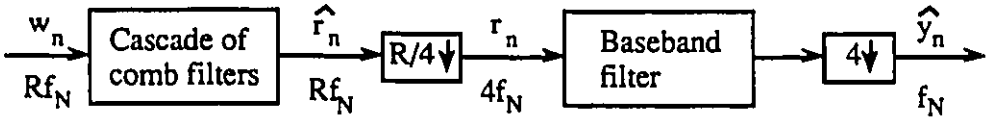

Figure 2.3.8 Decoder for sigma-delta modulated signals.

2. Design based on half-band filters

If R is chosen as a power of two, we can simplify the decimator by using a cascade of half-band filters. A half-band filter has the property that

$$H(e^{j\omega})=1-H(e^{j(\pi-\omega)}) \qquad (2.3.18)$$

i.e. the frequency response of the filter is anti-symmetric around $\omega=\pi/2$, and at $\omega=\pi/2$ the response value is one half of the unity

$$|H(e^{j\pi/2})|=0.5 \qquad (2.3.19)$$

A half-band filter based on symmetrical FIR filter specifications will result in a filter having every other filter coefficient equal to zero except for k=0, i.e.

$$h(k)=0, \quad k \text{ even}, k\neq 0 \qquad (2.3.20)$$

for a zero phase case. Hence, the number of required multiplications in implementing such filters is only one fourth of what is needed for arbitrary FIR filter designs [R. E. Crochiere 1983].

3. Considerations about structure implementation

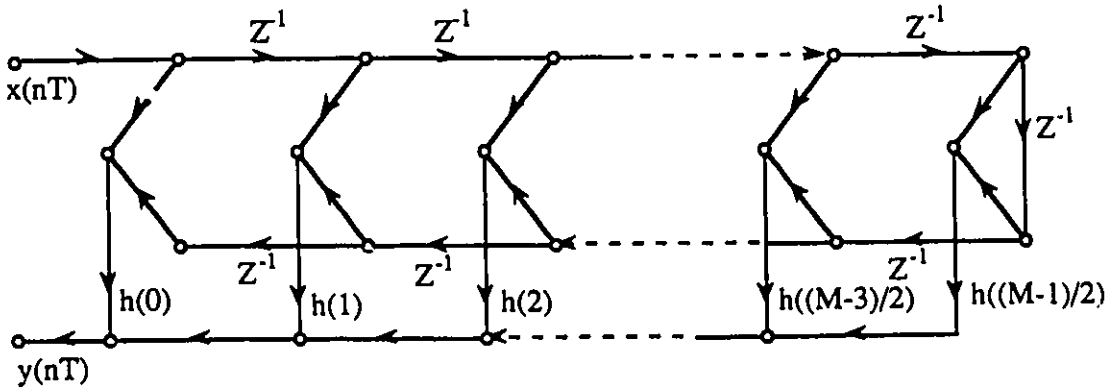

Figure 2.3.9 Direct form structure for an FIR filter.

Fig.2.3.9 is a direct form structure for an FIR linear phase system H(Z) when filter length M is an odd integer. The number of coefficients multipliers is essentially halved. If this filter is used as a decimator, and it will be followed by an R downsampler as depicted in Fig.2.3.10, then only one out of every R outputs from the lowpass will be kept while the remaining R-1 are simply not used. Logically, the outputs that will not be used need not be computed. This is easily achieved by moving the downsampler to precede the multiplications as shown in Fig.2.3.11.

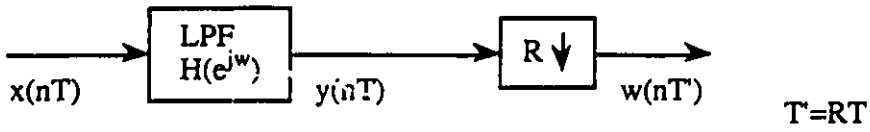

Figure 2.3.10 General diagram of a decimator.

This means instead of using multipliers which produce one output every T seconds, we can replace them with R times slower multipliers which produce one output every RT seconds, resulting in significantly reduced complexity.

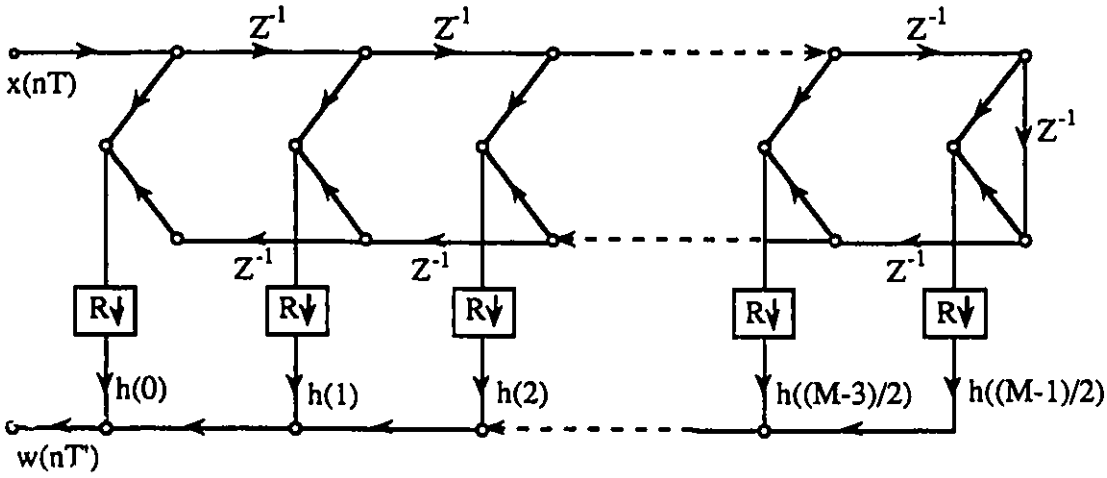

Figure 2.3.11 Efficient direct form structure for an FIR decimator.

Other structures providing further efficiencies in the implementation are given in [R. E. Crochiere 1983].

3 Analysis of Sigma-Delta Modulated Implementation of Fixed and Adaptive FIR Filters

The subbanded adaptive structure in Fig.1.2 is based on two main operations: fixed FIR filtering and adaptive FIR filtering. The objective of this thesis is to study the implementation of such a structure using signals and/or systems in the sigma-delta modulated format. In this chapter, we will study the sigma-delta implementation of fixed as well as adaptive FIR filters that form the basic blocks of Fig.1.2. Simulation results verifying the performance of these individual blocks are provided.

3.1 Sigma-Delta Modulated Fixed FIR Filtering

The function of an FIR filter is basically to perform a convolution between the digital signal input and the filter impulse response, i.e.

$$y_n = \sum_{i=0}^{K-1} a_i x_{n-i} \qquad (3.1.1)$$

where x_n is the input signal, y_n is the output signal, and $\{a_n;\ n=0, 1,...,K-1\}$ are the filter coefficients. The filter can be implemented using input signal x_n and coefficients a_n in PCM format. Alternatively, x_n and/or a_n can be represented by a sigma-delta modulated code. This principle can be explained as follows [P. W. Pong 1992]: let C, D, and F denote the encoding, decoding, and filtering operations respectively. Since the decoder for a sigma-delta modulated signal is a regular FIR filter, the decoding

operation D can be considered as a linear operation. So is the filtering operation F. We can thus exchange the order of two linear operations D and F:

$$\begin{aligned} D(F(C(x_n)))&=F(D(C(x_n)))\\ &=F(x_n+N_n)=F(x_n)+F(N_n)\\ &=y_n+F(N_n) \end{aligned} \qquad (3.1.2)$$

where N_n is the error due to the encoding-decoding process. N_n can be made very small if oversampling ratio R is large enough and the decoder is of good quality. This shows that the desired filter output y_n can be obtained by performing the filtering operation F on the coded single-bit sequence $C(x_n)$, after which the filtered multibit sequence $F(C(x_n))$ is decoded into full-precision $D(F(C(x_n)))$. This approach takes full advantage of the coded single-bit sequence in such a way that in computing the convolution sum, only the addition operation is performed on full-precision operands compared to both full-precision addition and multiplication for the convolution of PCM signals. This results in considerable reduction in system complexity.

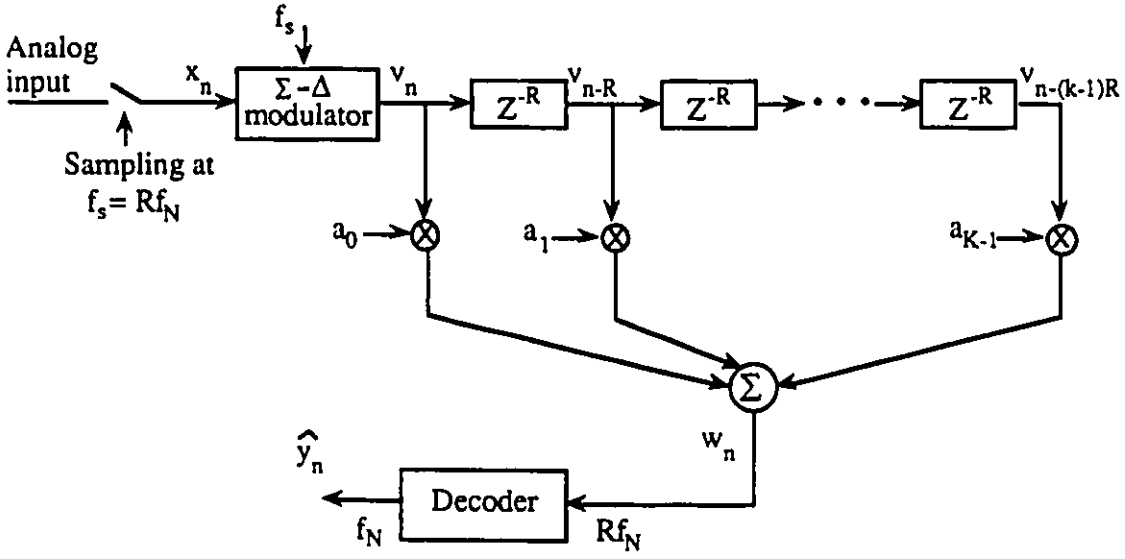

Figure 3.1.1 FIR filter implementation using modulated input.

Fig.3.1.1 illustrates an FIR filter implemented using sigma-delta modulated input signal and the full-precision PCM filter coefficients. The discrete-time analog input signal is accepted directly at the oversampling frequency f_s to generate x_n before being encoded into the sigma-delta modulated binary sequence. As was explained in chapter 2, the sigma-delta modulator is operated at a sampling frequency f_s substantially higher than the Nyquist frequency f_N with an oversampling ratio $R=f_s/f_N$. v_n is the oversampled modulated input available as the output of sigma-delta A/D converter before decimation. The filtered signal w_n is given by

$$w_n=\sum_{i=0}^{K-1} a_i v_{n-iR} \tag{3.1.3}$$

Since v_n is single-bit, each multiplier can be implemented using a switch to select either the stored coefficients a_n or $-a_n$, depending on the value of v_n. The final full-precision Nyquist-rate output is obtained by decimating w_n.

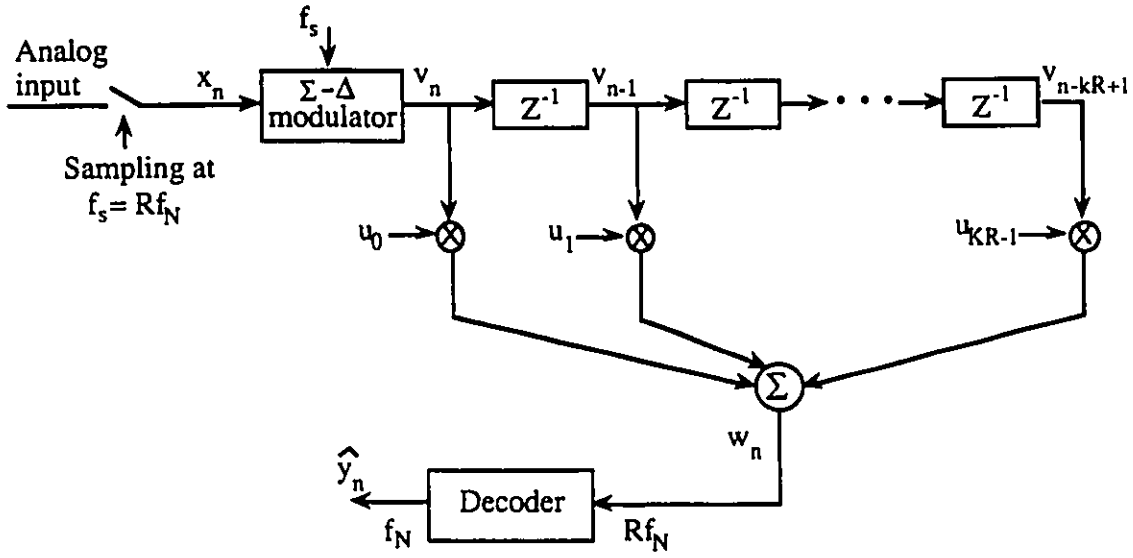

Figure 3.1.2 FIR filter implementation using modulated input and coefficients.

From an analysis point of view, we can assume that the decoder is an ideal lowpass filter working at the oversampling frequency with cutoff at one half of the

Nyquist frequency. However, we should note that multipliers involved in the decimation can be totally eliminated by proper implementation as suggested in [T. Saramaki 1988 1990].

Since the convolution operation is symmetric with respect to x_n and a_n, we can encode x_n using sigma-delta modulation and leave a_n in full precision, or as shown in Fig.3.1.2, encode both x_n and a_n to further simplify the full-precision addition required in the convolution into single-bit logic circuit [P. W. Wong 1990 1992]. The analog input signal is sampled at R times the Nyquist frequency to produce an analog sequence x_n, which is encoded by sigma-delta modulator into v_n. The impulse response a_n is upsampled by R times and encoded into u_n. The binary-valued signals v_n and u_n are convoluted to give the multibit output

$$w_n = \sum_{i=0}^{KR-1} u_i v_{n-i} \tag{3.1.4}$$

without the requirement of any multipliers. The high-rate w_n is then decoded to reconstruct the desired filter output at Nyquist rate.

In this thesis, we implement the fixed filter bank blocks in Fig.1.2 by encoding both input and coefficients into sigma-delta modulated format as shown in Fig.3.1.2.

3.2 Sigma-Delta Modulated Adaptive FIR Filtering

Conventional adaptive filter of length K requires 2K full precision multipliers for both FIR filtering and coefficients update, defined by

$$y(n) = \sum_{r=0}^{k-1} a_r(n) x(n-r) \tag{3.2.1}$$

$$a_r(n) = a_r(n-1) + 2\mu e(n-1) x(n-r-1) \tag{3.2.2}$$

where $a_r(n)$ and $a_r(n-1)$ are the coefficients of rth tap at time n and n-1 respectively. By exploiting the sigma-delta modulation technique, the multipliers can be eliminated if this structure is implemented as in Figure 3.2.1. In this realization, the sigma-delta modulator is used for analog-to-digital conversion at the input. Thus in (3.2.1) the signal passing through the adaptive filter is only one-bit stream w_n. And in (3.2.2), since the filter coefficients will have to be updated during each iteration, they are kept in PCM representation rather than sigma-delta modulated codes, in order to reduce the possibility of instability and added noise. But signal x_n will be replaced by w_n, so that even when the error e(n) still in full precision, no multiplication is needed in the coefficients update equation. The Z-domain modulator output is rewritten here as

$$W(Z)=Z^{-1}X(Z)+(1-Z^{-1})E(Z) \tag{3.2.3}$$

corresponding to the time domain

$$w_n=x_{n-1}+\varepsilon_n-\varepsilon_{n-1} \tag{3.2.4}$$

where ε_n is the noise introduced by the sigma-delta modulation coding and E(Z) is its Z-transform.

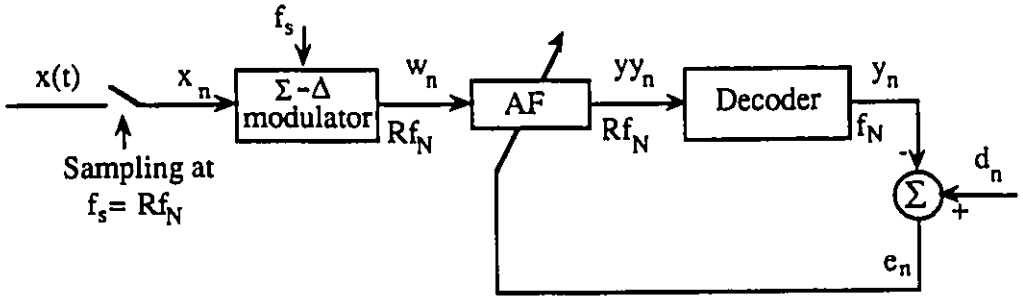

Figure 3.2.1 Adaptive filter implementation using modulated input.

3.2.1 Modulated Adaptive Interference Cancellation

A much more simplified and efficient approach based on Fig.3.2.1 is given in [C. Wei 1988] for sinusoidal interference cancellation case. The modulator is simply a sign identifier (neglecting the additive quantization noise E in (3.2.3)):

$$w(n)=sgn[x(n-1)] \tag{3.2.5}$$

Following the adaptive filter, the high-rate sequence is decoded using a comb filter

$$y(n)=\frac{1}{R}\sum_{i=0}^{R-1} yy(n-i) \tag{3.2.6}$$

The transversal filter is shown in Fig.3.2.2. The LMS algorithm is given as

$$yy(n-i)=\sum_{r=0}^{K-1} a_r(n-i)w(n-i-rR) \qquad i=0,1,...,R-1. \tag{3.2.7}$$

$$a_r(n-i)=a_r(n-i-1)+2\mu e(n-i)w(n-rR-i) \tag{3.2.8}$$

$$e(n)=d(n)-y(n) \tag{3.2.9}$$

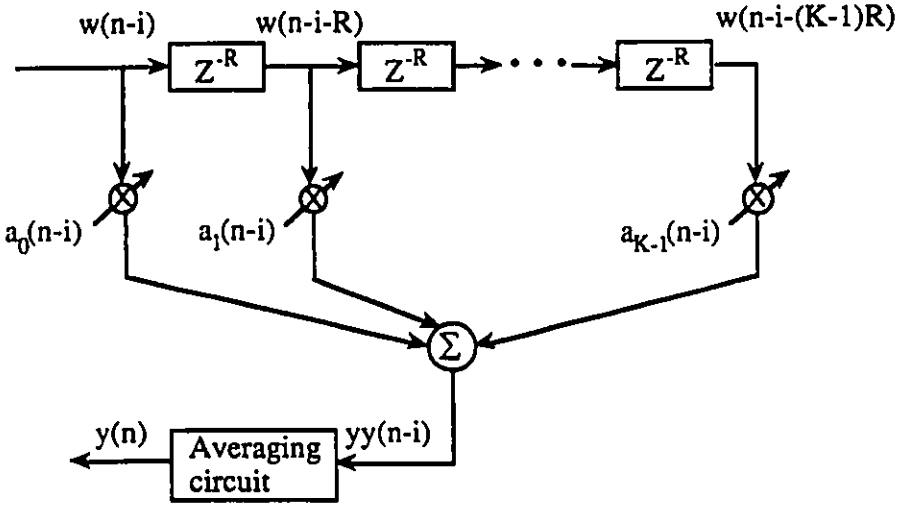

Figure 3.2.2 Simplified filter implementation for modulated interference cancellation.

To verify the performance of this adaptive sigma-delta modulated interference canceller, the example in [C. Wei 1988] is reproduced here.

The primary input is a combination of a 1kHz sinusoidal interference and a bandlimited (up to 3.2kHz) white noise with zero mean and standard deviation 0.25. The power of the bandlimited white noise is 26dB lower than sinusoidal signal, resulting in this sinusoidal signal having an amplitude of 7.054:

$$\text{Interference-to-noise ratio}=10\log_{10}\frac{(1/2)(7.054)^2}{(0.25)^2}\approx 26\text{dB} \tag{3.9.10}$$

The Nyquist sampling frequency f_N=8kHz. The oversampling ratio is R=4, and the length of the adaptive filter is K=32. The adaptation converges in about 1000 iterations. Fig.3.2.3 shows the convergence of the squared error. It is obtained by taking the average over an ensemble of 10 simulations, each starting with the zero coefficients with different noise inputs. Fig.3.2.4 and Fig.3.2.5 illustrate the spectrum of the primary input and output of the system respectively, showing more than 40dB sinusoidal interference reduction.

3.2.2 Modulated Adaptive Noise Cancellation

Based on the results reported in [C. Wei 1988] and verified in section 3.2.1, the next obvious step is to use the same simplified structure in section 3.2.1 for adaptive noise cancellation. In this section we will show that the performance of this simplified system is totally unacceptable for the noise cancellation case.

It was shown in [J. C. Candy 1976] that a typical oversampling ratio R ranges from 64 to 1024. However, for the interference cancellation we are able to achieve good results with R as low as 4 and the decimator being a simple comb-filter. This is possible since the interference is sinusoidal and the adaptive filter is a simple compensator for the phase shift.

In order to understand the effect of the oversampling ratio R and the quality of the decimator for the noise cancellation case, several simulations have been run. To simplify the system, the adaptive filter coefficients are fixed at their optimum values. The total system simulated is that in Fig.3.2.1 with the input sigma-delta modulated. Results for interference cancellation are also reported for comparison.

From Fig.3.2.6 we can see that the output of the adaptive interference canceller with R=4 is fairly close to the primary input d. Excluding the transients from the measurement, SNR is calculated to be 20dB.

Fig.3.2.7 shows that there is a big discrepancy between the output of the adaptive filter and the primary signal for the adaptive noise cancellation case, with SNR only 7dB even when R has been already increased up to 100, while still using a comb filter as decimator. Based on this, we conclude that the overall performance in the noise cancellation case is limited by the quality of the decimator used. Increasing the oversampling ratio can only improve the results to a certain limit.

Fig.3.2.8 shows the result when a good quality lowpass FIR filter replaced the comb filter. Now, the SNR can be increased to 14dB for R equal to 8.

The typical oversampling ratio is from 64 to 1024 to achieve acceptable SNR. Fig.3.2.9 shows the case for R=64 resulting in SNR of 25dB. The decimation filter's specification is shown in the appendix.

These results show that for sigma-delta modulated AIC, a comb filter and low oversampling ratio are sufficient to provide good performance. However, for ANC case a higher oversampling ratio and a good quality decimator are essential. A comb filter is definitely not capable of removing the quantization noise.

Thus, we conclude that the comb filter in the AIC structure in Fig.3.2.2 has to be replaced by a better quality FIR decimator for adaptive noise cancellation in future implementations and the oversampling ratio has to be increased significantly.

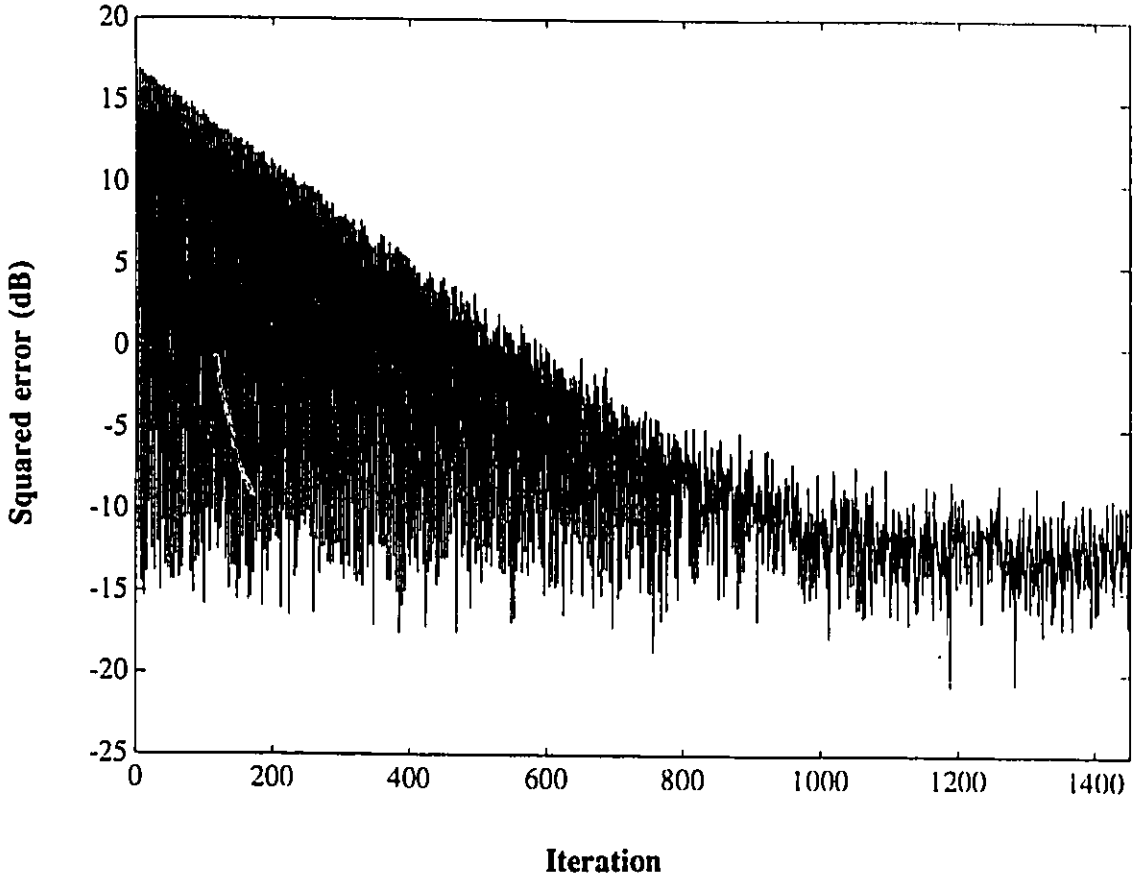

Figure 3.2.3 Time evolution of squared error signal of the modulated AIC (R=4). This is a reproduction of the example in [C. Wei 1988].

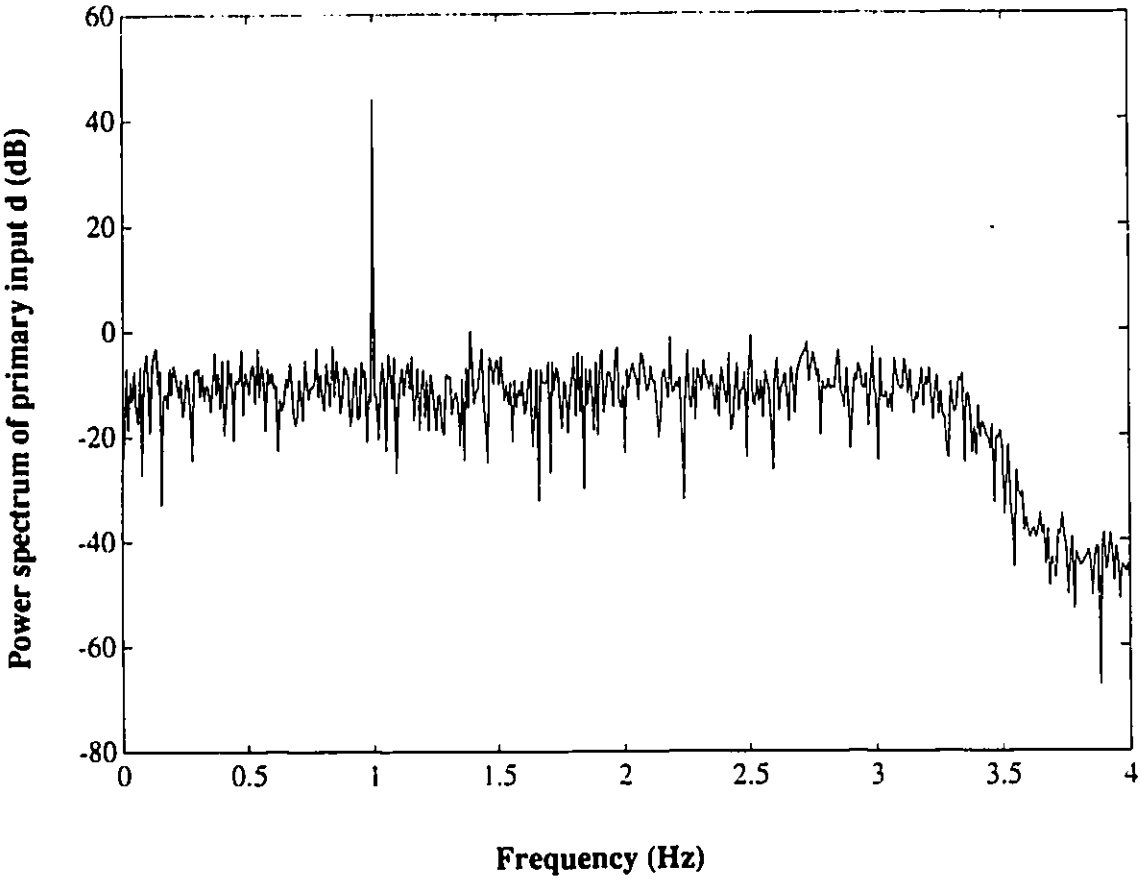

Figure 3.2.4 Power spectrum of primary input of the modulated AIC (R=4) consisting of 1KHz sine wave and bandlimited Gaussian white noise.

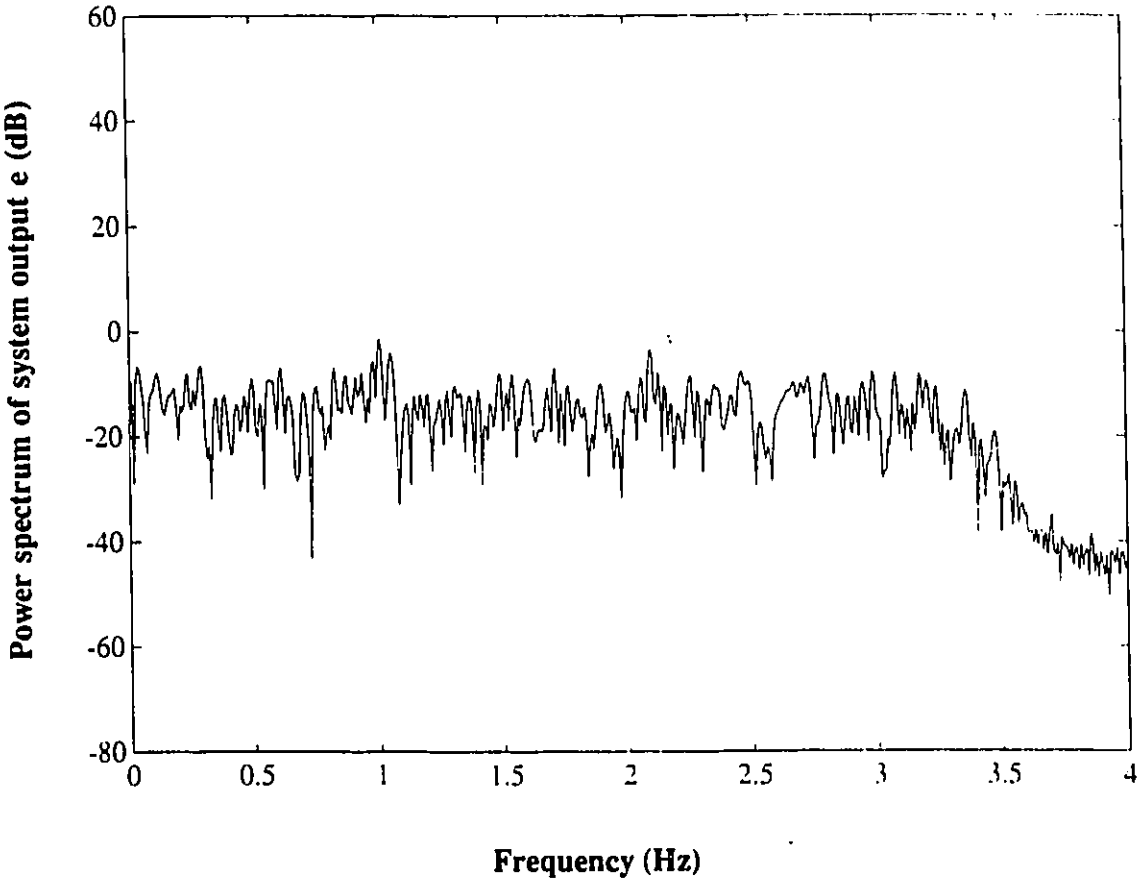

Figure 3.2.5 Power spectrum of the system output of the modulated AIC (R=4). The 1KHz sinusoidal interference is suppressed down by more than 40dB.

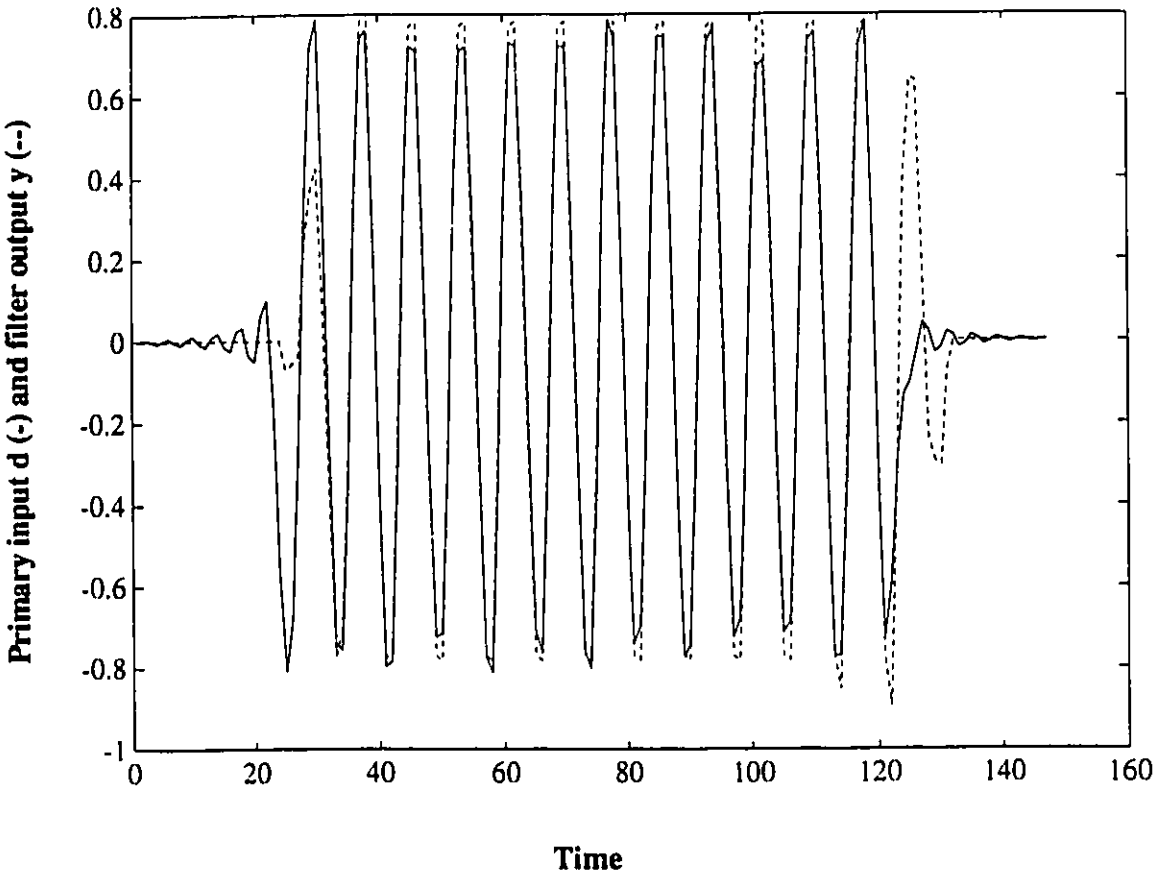

Figure 3.2.6 Primary input d and filter output y (dashed line) of the modulated AIC with coefficients fixed at optimum values. Interference is a sinusoidal signal. Decimator is a comb filter. R=4. SNR=20dB.

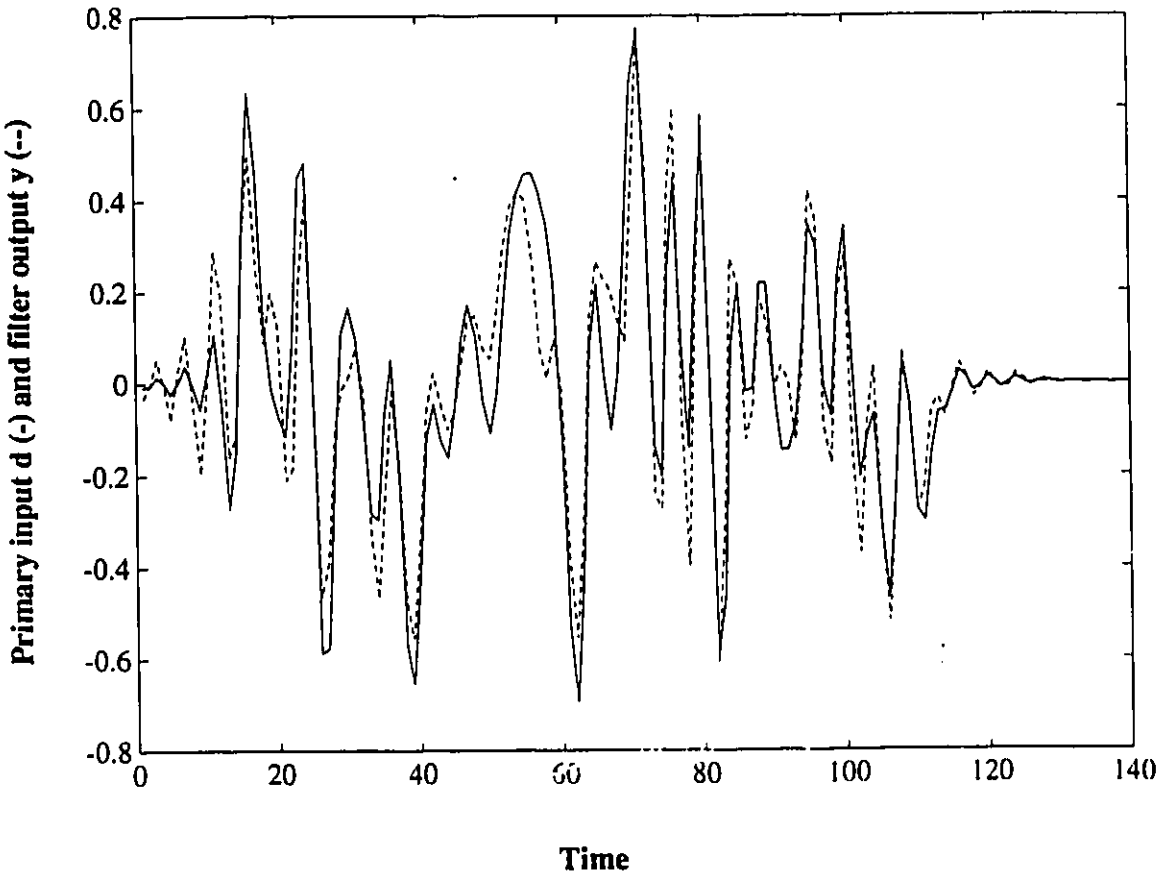

Figure 3.2.7 Primary input d and filter output y (dashed line) of the modulated ANC with coefficients fixed at optimum values. Noise is Gaussian white noise. Decimator is a comb filter. R=100. SNR=7dB.

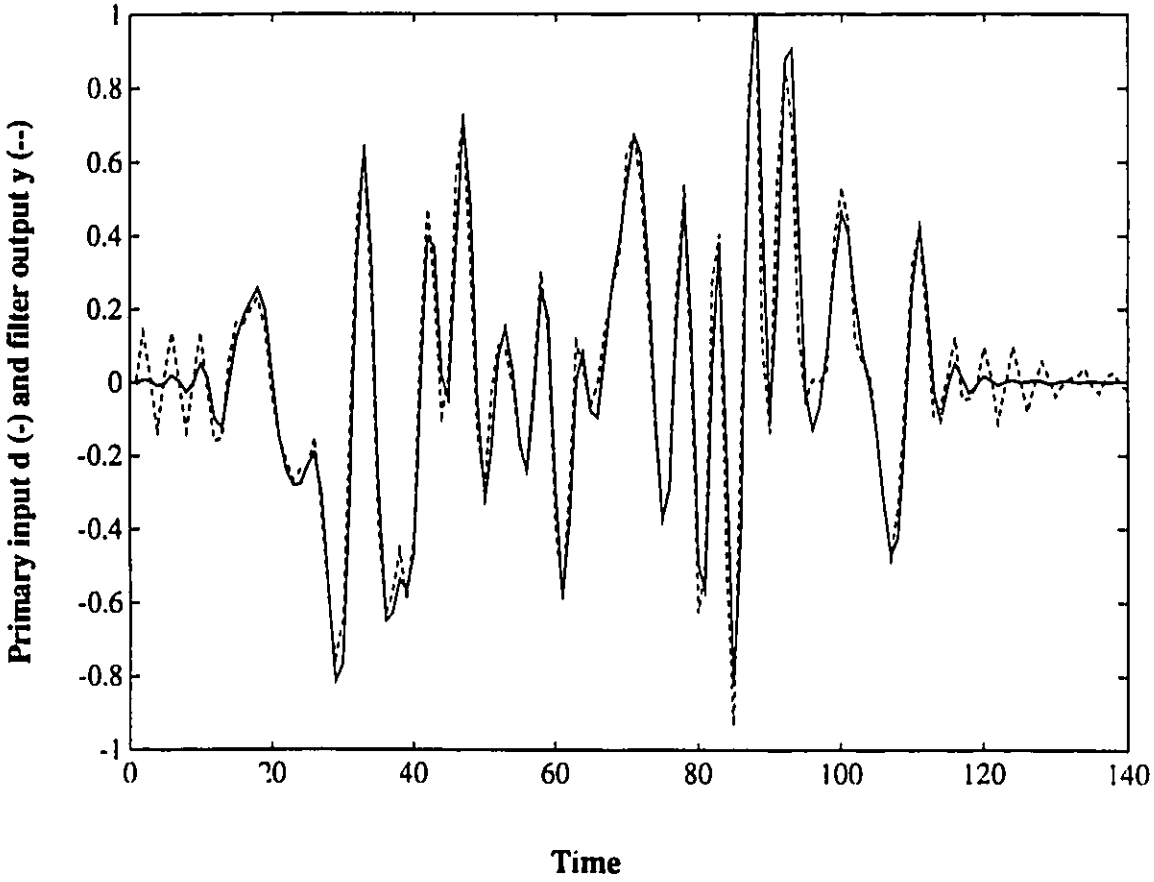

Figure 3.2.8 Primary input d and filter output y (dashed line) of the modulated ANC with coefficients fixed at optimum values. Noise is Gaussian white noise. Decimator is a regular FIR filter. R=8. SNR=14dB.

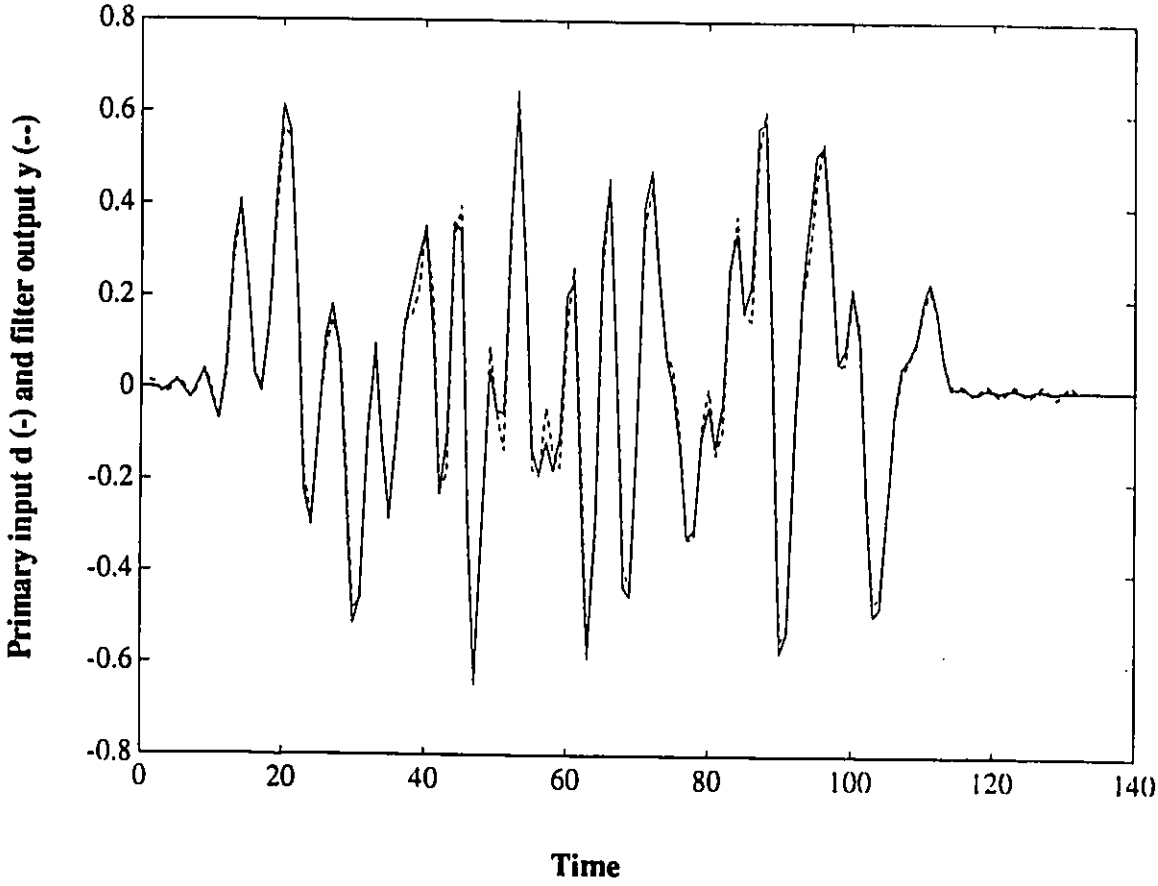

Figure 3.2.9 Primary input d and filter output y (dashed line) of the modulated ANC with coefficients fixed at optimum values. Noise is Gaussian white noise. Decimator is a regular FIR filter. R=64. SNR=25dB.

3.3 Sigma-Delta Modulated Subbanded Adaptive System

As stated in chapter 1, the main goal of this thesis is to implement the subbanded adaptive filter structure in Fig.1.5 using sigma-delta modulation technique to implement the filter bank as well as the adaptive filters for both interference and noise cancellation. The aim is to get similar performance compared to the conventional implementation, but at a significantly reduced cost, since considerably fewer full-precision multipliers will be required.

Fig.3.3.1 shows the detailed block diagram for sigma-delta modulated AIC implementation. Not much difference can be shown in this diagram for ANC case, except that the primary signal d(n) is a filtered version of the reference signal x(n).

In this structure, the sigma-delta modulated input x(n) (with oversampling ratio R_1) passes through the analysis filter bank whose coefficients are also implemented into sigma-delta modulated codes (with oversampling ratio R_1). The outputs from the filter bank are demodulated (decimator1) and then modulated again at a different rate (with oversampling ratio R_2) to create the adaptive filter input. The outputs from the decimation process (decimator2) during the adaptive filtering stage, go through the synthesis filter bank to produce the final output. This stage has the same implementation as the analysis filter bank part. Basically, the overall system is the combination of the sigma-delta modulated FIR proposed in [P. W. Pong 1992] for the filter bank implementation and the adaptive FIR in [C. Wei 1988] for the adaptive filter implementation.

In the diagram, R_1 and R_2 denote the oversampling ratios of the sigma-delta modulators for FIR filtering and adaptive filtering respectively. They can be the same value or different. It is reasonable to argue that there is no advantage in choosing R_1

to be small and R_2 much larger than R1, as we would be allowing large errors in the filter bank stage, then expecting the adaptive filter stage to compensate for it. In our simulations R_2 is chosen much smaller than R_1 for AIC and the same as R1 for ANC.

The output of the filter bank is a high-rate multibit signal. Decimator 1 is used to bring this signal down from the $R_1 f_N$ sampling rate to the Nyquist rate f_N. The signal is next upsampled by R_2 times and modulated into high-rate 1-bit stream to provide the input of the adaptive filter. Decimator 2 brings down the rate from $R_2 f_N$ to f_N. Here one question arises: Could we simplify the shaded block by combining the R_1 downsampler in decimator 1 and the subsequent R_2 upsampler?

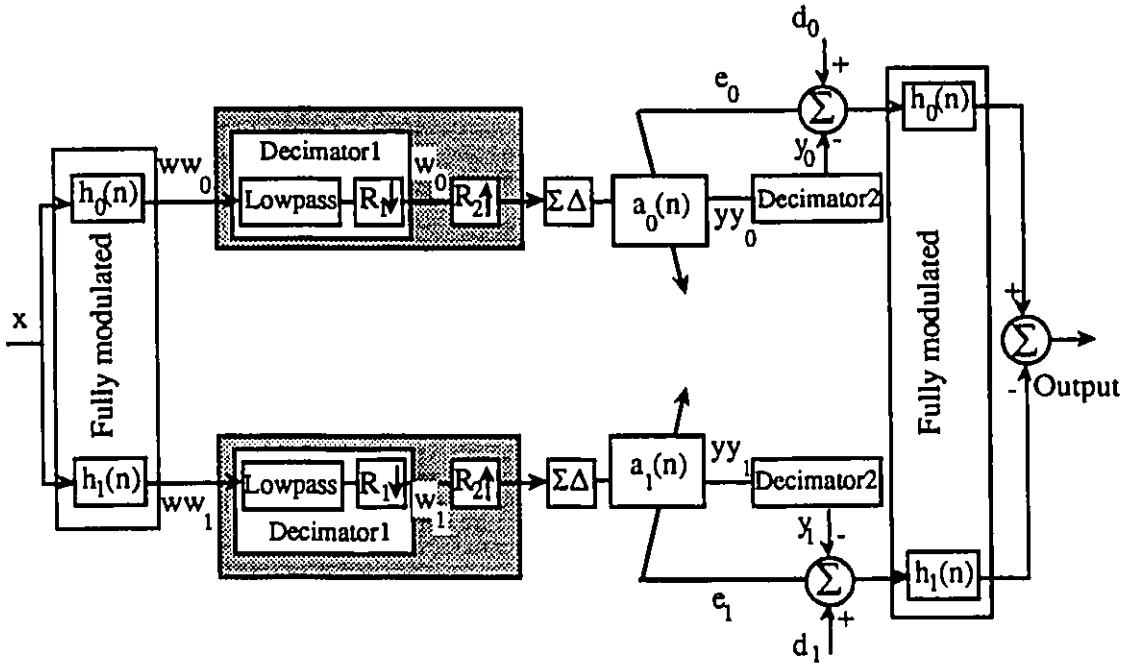

Figure 3.3.1 Block diagram for modulated subbanded AIC.

To answer this question we consider two separate cases:

Case 1: $R_1=R_2=R$

This is the case for ANC when R_1 has to be as high as R_2. The shaded block can be totally removed since basically no rate change in required at this stage. Following the modulated FIR filtering, the multibit sequence ww_n is directly decoded into 1-bit input of the adaptive filter. The sequence ww_n contains original signal part which remains unchanged in baseband 0--f_B, and highpass shaped noise. This noise dominating the high-frequency band will be eventually filtered out by decimator 2 when demodulating the output signal yy_n at the final stage.

Case 2: $R_1 > R_2$

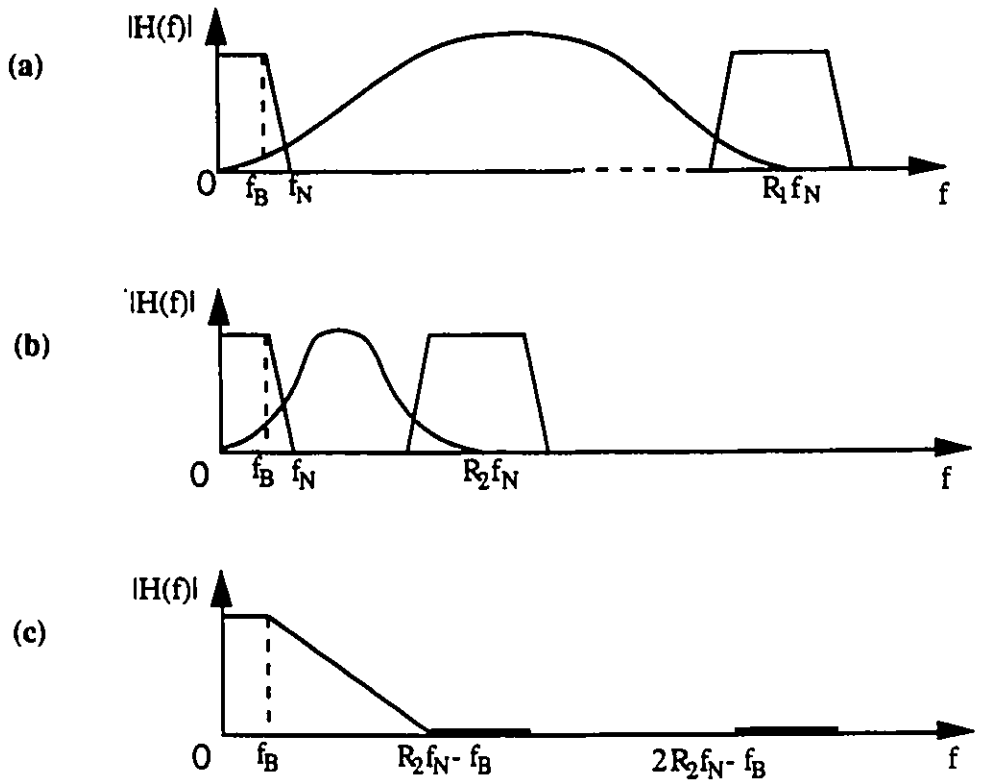

Figure 3.3.2 (a) FIR filtering output at oversampling ratio R_1, (b) adaptive filtering input at oversampling ratio R_2, (c) designed digital filter to simplify the shaded block.

This is the case for AIC as explained earlier. The FIR filtering part uses a high oversampling ratio R_1, but R_2 can be as low as 4, which has been shown to be sufficient in section 3.2. The block of decimator 1 (containing a lowpass and a R_1 downsampler) and R_2 upsampler can be simplified into a simple lowpass followed by a R_1/R_2 downsampler. The function of the lowpass is to avoid aliasing when signal is downsampled, by bandlimiting the high frequency band quantization noise shown in Fig.3.3.2(a). Taking into consideration of the fact that the signal will be decimated to a sampling frequency $R_2 f_N$ as shown in Fig.3.3.2(b), the decimator thus becomes a multi-stopband filter with a fairly wide transition band from f_B up to $R_2 f_N - f_B$ as shown in Fig.3.3.2(c).

Case 3: R1<R2

It has been argued earlier in this section that this third possibility is not practically relevant.

In the next two chapters, we will discuss the subbanded sigma-delta modulated adaptive system for the application of AIC and ANC respectively.

4 Performance of Modulated Subbanded Adaptive Interference Cancellation

It has been shown in chapter 3 that subbanded AIC using sigma-delta modulation provides an efficient alternative to the conventional implementation. To test the performance of proposed interference canceller, simulations were run for the proposed and the conventional structure using the same data. The objective is to achieve similar performance at a reduced cost.

First we start with the results for the conventional (non-modulated) structure in section 4.1 as comparison criterion. Next, the subbanded structure with only the adaptive filtering part sigma-delta modulated is considered in section 4.2. Section 4.3 studies the case when both filter bank and adaptive parts are modulated. A separate series of simulations investigating the effect of the oversampling ratio is given in section 4.4. The effect of the decimator quality will also be discussed. Section 4.5 summarizes the conclusions of this chapter.

The corresponding performance of proposed ANC is discussed in chapter 5.

4.1 Conventional Subbanded AIC without Modulation (R1=R2=1)

The basic subbanded interference canceller is repeated here in Fig.4.1.1. The simulation results of this structure are used as the criterion for comparison with the

performance of the proposed system in section 4.2 and 4.3. The comparison will be made regarding complexity, convergence speed and steady state error. The effect of the oversampling ratios R1 and R2 used in the sigma-delta modulation as well as the quality of the decimator will also be considered in section 4.4.

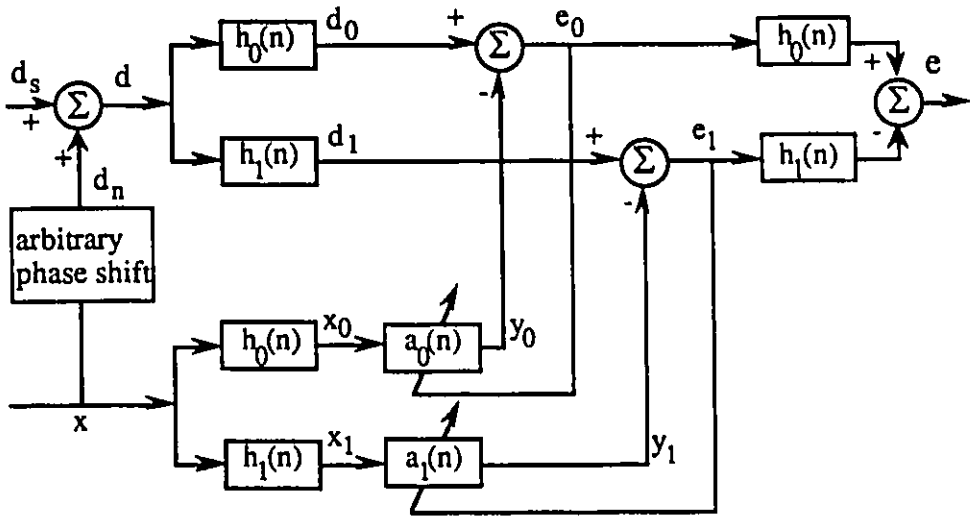

Figure 4.1.1 Conventional subbanded adaptive interference cancellation.

The simulation setup is as follows. The Nyquist sampling frequency is normalized to f_N=1Hz. The reference input signal x(n) contains two sinusoidal waves of 1/8 Hz and 3/9 Hz located in the lower (low frequency) and upper (high frequency) bands respectively.

The primary signal d(n) is a combination of a Gaussian white noise $d_s(n)$ bandlimited up to 1/2 Hz with zero mean and 0.05 standard deviation, and an interference signal $d_n(n)$ consisting of two sinusoidal waves of 1/8 Hz and 3/9 Hz with arbitrary phase shifts relative to x(n). The amplitude of the sinusoid is chosen to be 0.8, resulting in the power of the bandlimited white noise being roughly 21dB lower than the sinusoidal interference in each individual band:

$$10 \log_{10} \frac{(1/2)(0.8)^2}{(0.05)^2} \approx 21\text{dB}$$

The impulse and frequency responses of the lowpass filter $h_0(n)$ in the lower band are shown in Fig.4.1.2(a) and (b) respectively. The filter length is an even number 64 as discussed in Chapter 2. The highpass filter $h_1(n)$ in the upper band is a "π-shifted version" of $h_0(n)$. The length of the adaptive filters in both bands is 32.

The plot showing the ensemble average of the squared error as a function of the number of iterations is known as "learning curve". In the following, the learning curve is obtained by taking the average over an ensemble of 5 simulations, all starting with the same initial coefficients a=0 for different inputs.

Fig.4.1.3(a) and (c) show the lower band and upper band error signal respectively. Fig.4.1.3(b) and (d) show the lower band and upper band learning curves of conventional AIC. The number of iterations required for convergence is about 300. Fig.4.1.4(a) shows the power spectrum of the primary input, and (b) shows the power spectrum of the system output after convergence. Based on Fig.4.1.4, one can see that the sinusoidal interference is suppressed down by approximately 40dB.

Since our primary objective is to achieve similar performance using the sigma-delta modulated structure at a reduced cost, we now proceed to define a cost function that will be computed and compared for both the sigma-delta modulated and conventional structure. Assuming that cost unit is the cost for one single-bit adder at Nyquist rate, the cost function for the realization of the subbanded adaptive structure is defined as

$$C = P^* \sum \#\text{ of multipliers}^*\text{precision}^*\text{rate} + \sum \#\text{ of adders}^*\text{precision}^*\text{rate}$$

where P is the cost ratio between a multiplier and an adder, both are 1-bit precision and at Nyquist rate.

Table 4.1 shows the complexity per band in terms of the number of adders and multipliers, where

M(B3 R0)--- full precision multiplier with B3 bits and R0=1 (at Nyquist rate)

A(B4 R0)--- full precision adder with B4 bits and R0=1 (at Nyquist rate)

The cost function is

C=P*160*B3*R0+252*B4*R0

Table 4.1 Complexity for conventional subbanded AIC per band (R1=R2=1).

		# of M(B3R0)	# of A(B4R0)
AFB & SFB	x_0	64/2	64-1
	d_0	64/2	64-1
	e	64/2	64-1
AF	filtering y_0	32	32-1
	updating a_0	32	32
total		160	252

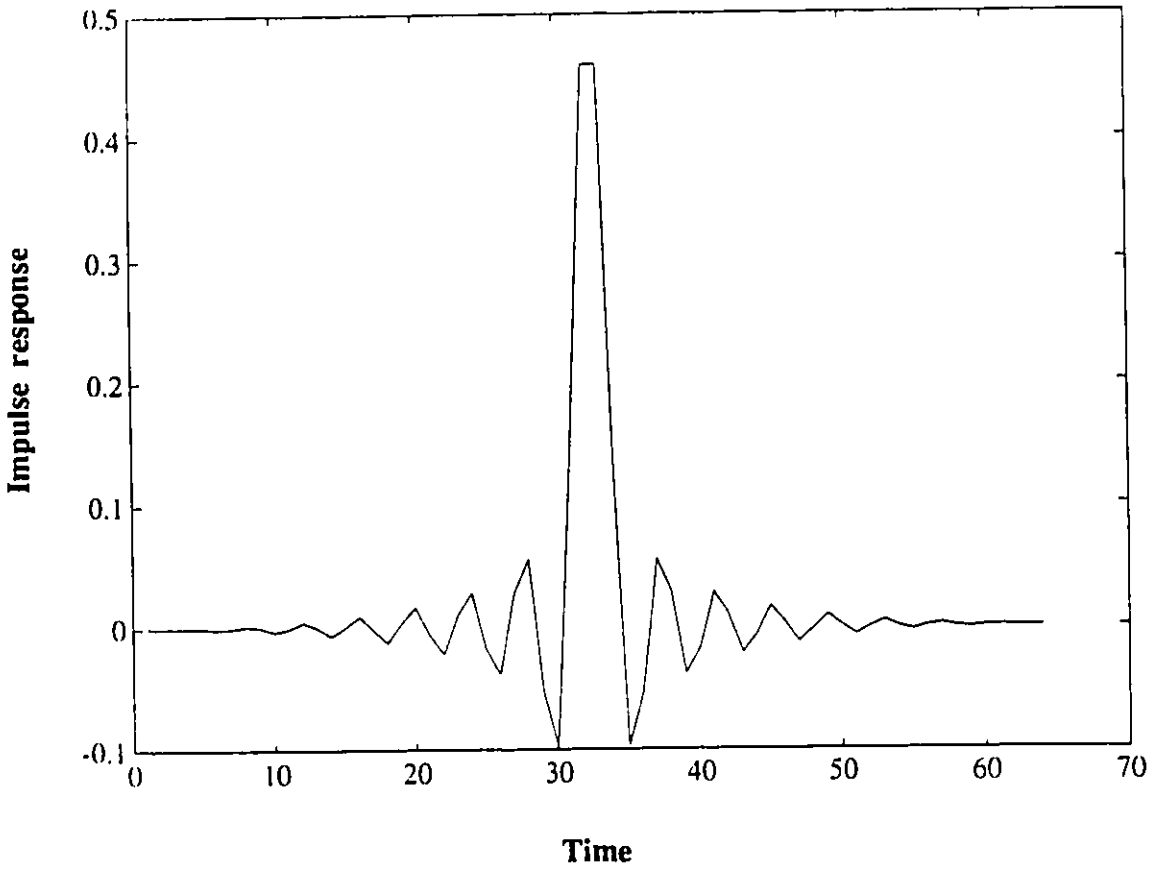

Figure 4.1.2 Lowpass filter in filter bank. The filter length is 64. (a) impulse response.

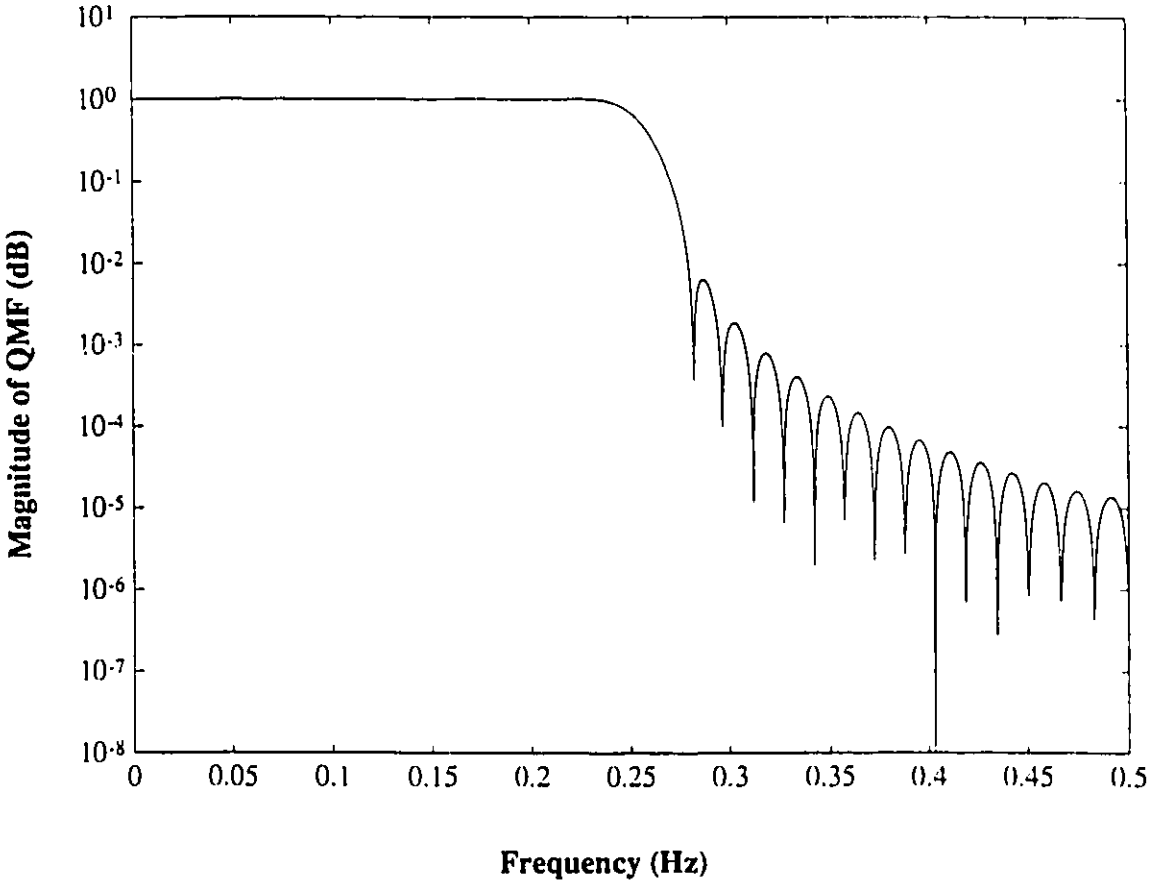

Figure 4.1.2 Lowpass filter in filter bank. The filter length is 64. (b) frequency response.

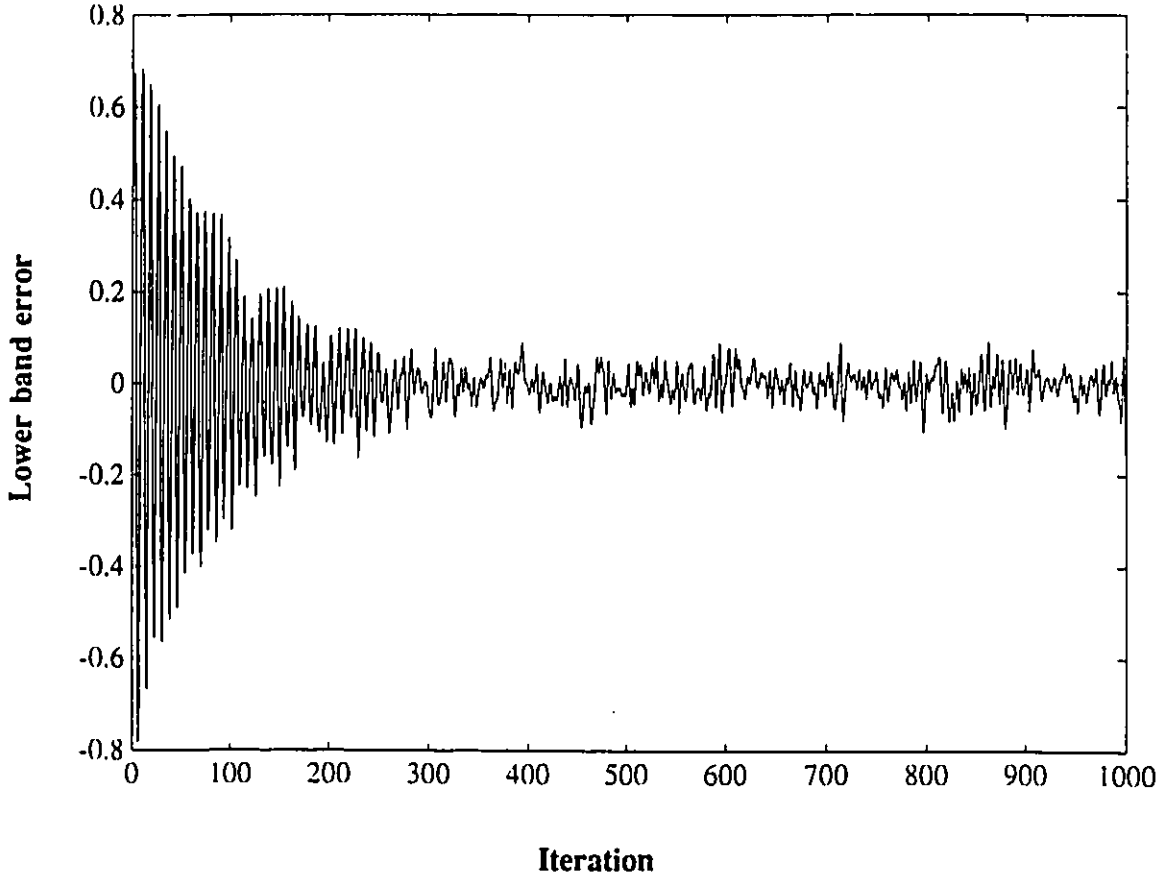

Figure 4.1.3 Conventional subbanded AIC (R1=1, R2=1).
(a) time evolution of lower band error signal.

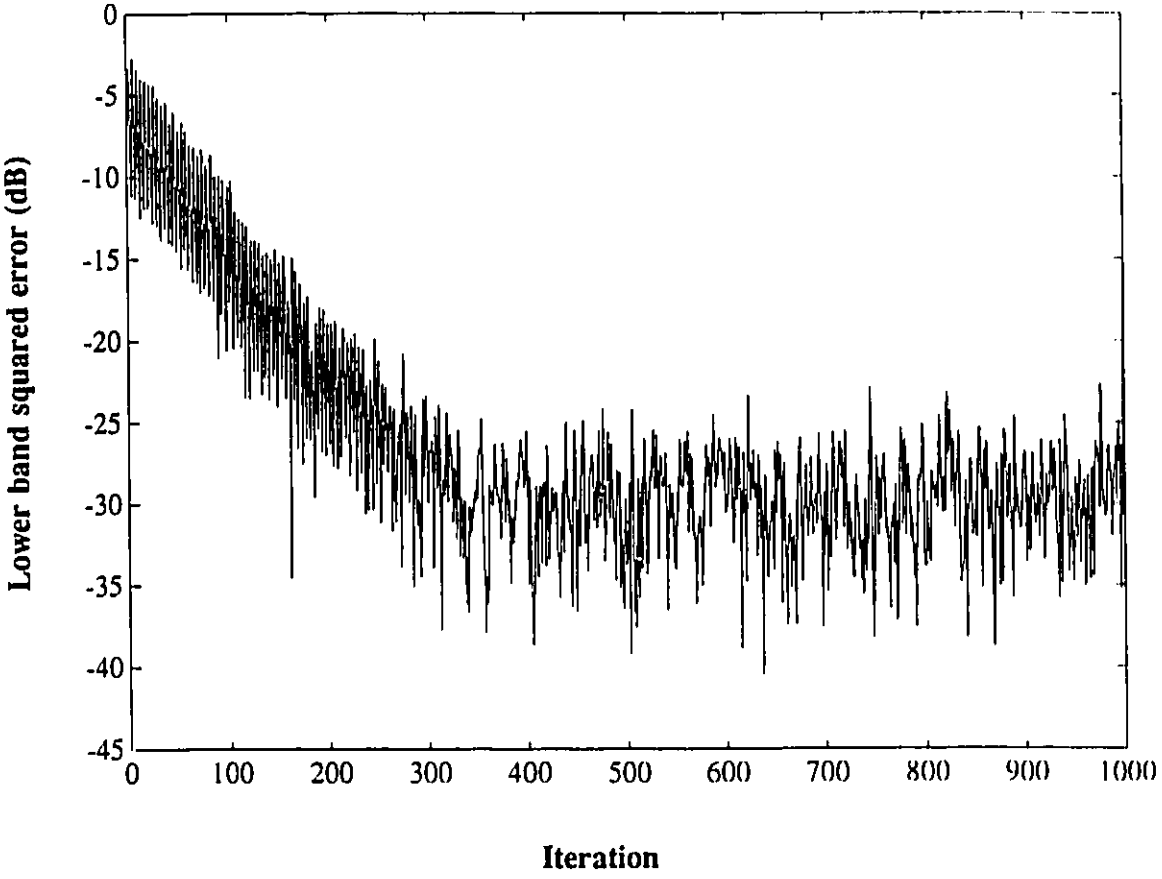

Figure 4.1.3 Conventional subbanded AIC (R1=1, R2=1).
(b) time evolution of lower band squared error.

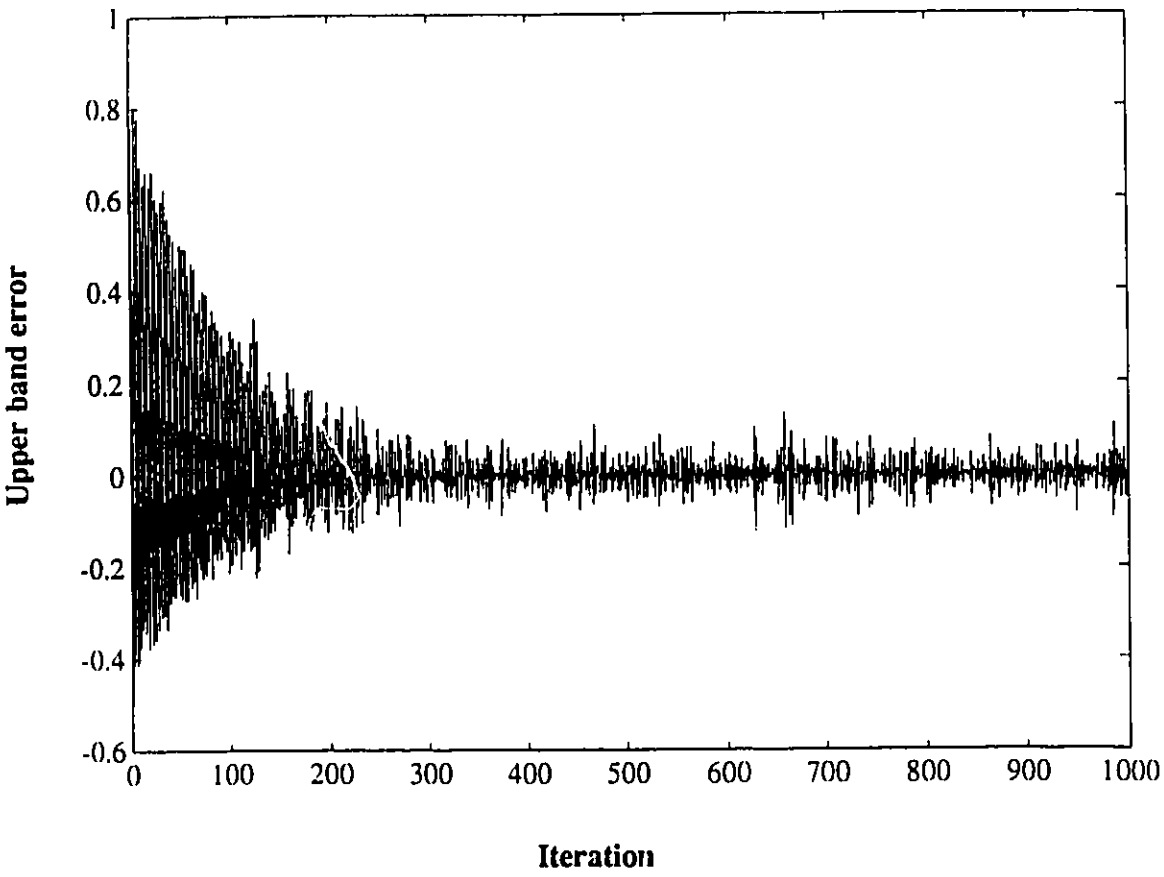

Figure 4.1.3 Conventional subbanded AIC (R1=1, R2=1).
(c) time evolution of upper band error signal.

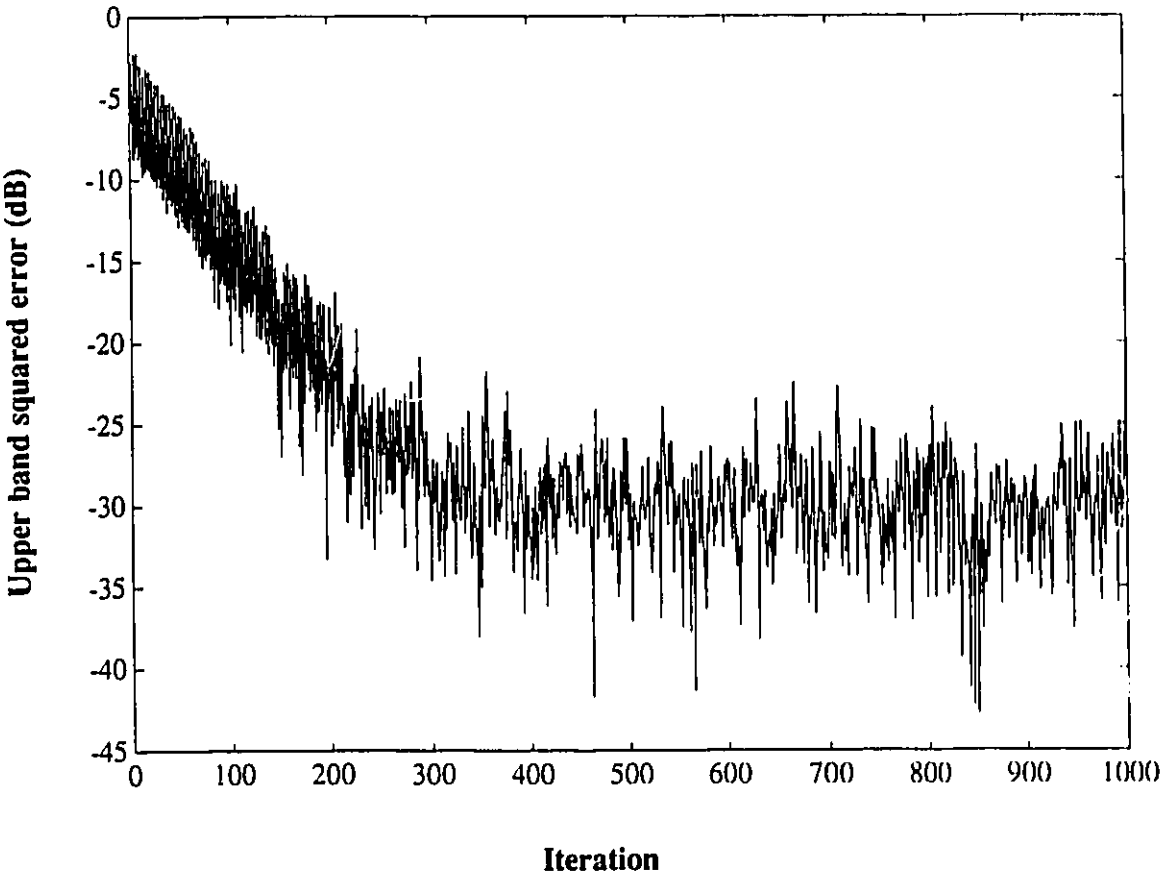

Figure 4.1.3 Conventional subbanded AIC (R1=1, R2=1).
(d) time evolution of upper band squared error.

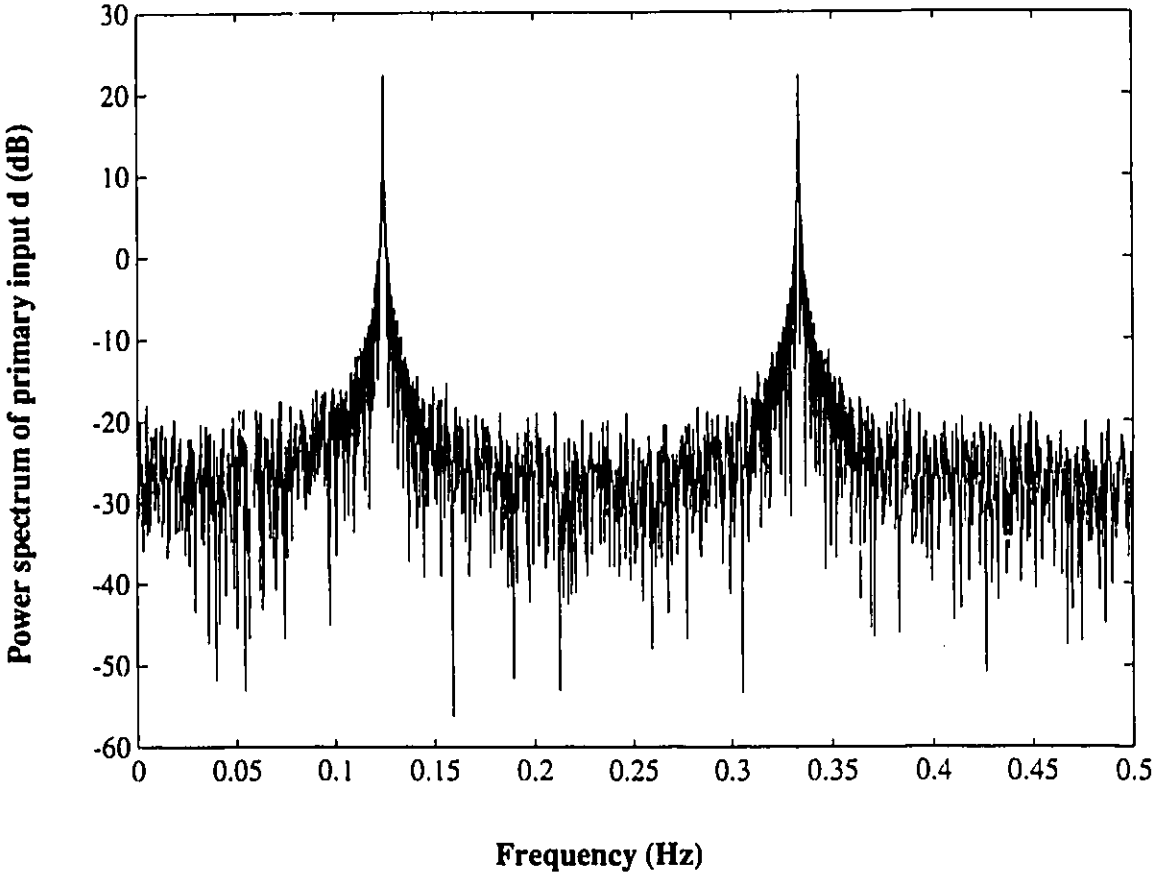

Figure 4.1.4 Power spectrum of conventional subbanded AIC (R1=1, R2=1). (a) primary input -- a combination of a Gaussian white noise as signal and two sinusoidal signals at 1/8Hz and 3/9Hz as noise.

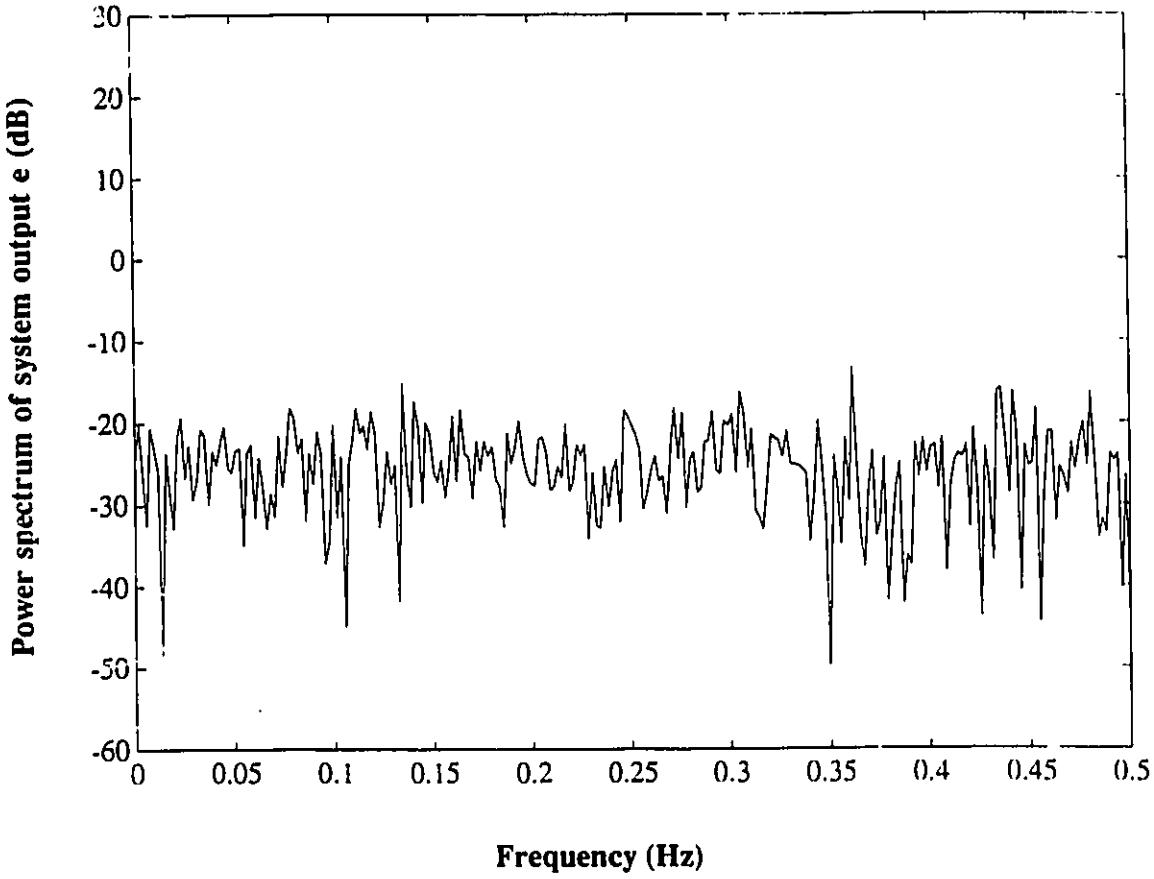

Figure 4.1.4 Power spectrum of conventional subbanded AIC (R1=1, R2=1). (b) system output with the sinusoidal interference being cancelled.

4.2 Proposed Partially Modulated Subbanded AIC (R1=1,R2=4)

Fig.4.2.1 shows the detailed block diagram of the proposed modulated system with the adaptive section sigma-delta modulated.

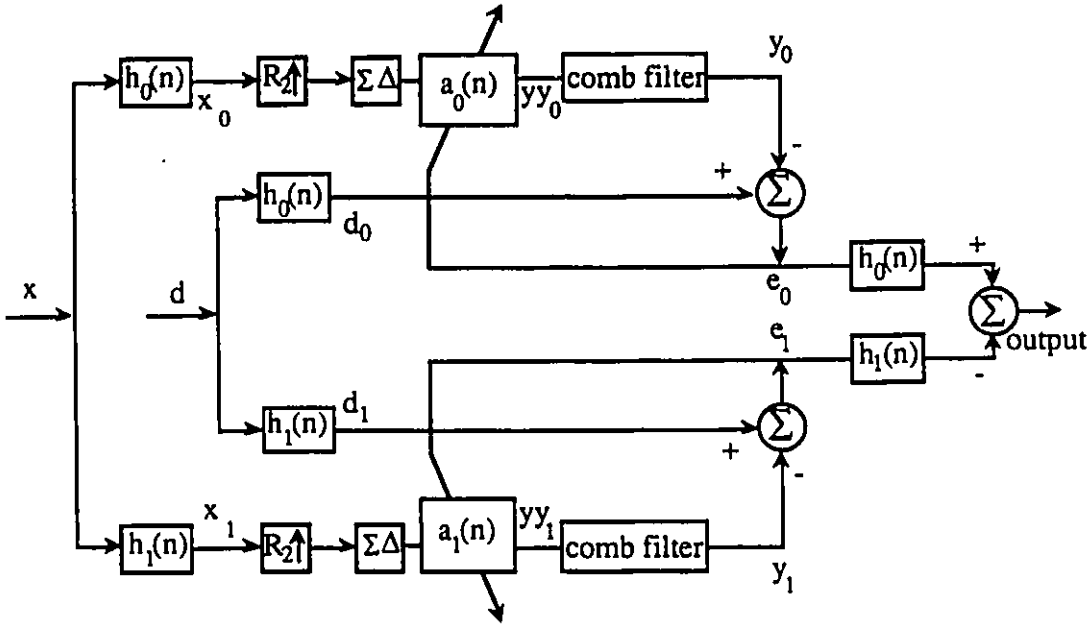

Figure 4.2.1 Partially modulated subbanded adaptive interference cancellation.

The oversampling ratio for modulated adaptive filtering is initially chosen at R2=4. The decimator used is an N=4 comb filter requiring no multipliers to implement. Fig.4.2.2(a) and (c) show the lower band and upper band error signal respectively. Fig.4.2.2(b) and (d) show the lower band and upper band learning curves of partially modulated subbanded AIC. The number of iterations required for convergence is about 400. Fig.4.2.3(a) shows the power spectrum of the primary input, and (b) shows the power spectrum of the system output after convergence. Based on Fig.4.2.3, one can

see that the sinusoidal interference is successfully suppressed down by approximately 40dB, the same as for the conventional case.

Table 4.2 shows the complexity of this partially sigma-delta modulated structure in terms of the number of adders and multipliers required by one band, where

M(B3 R0)--- full precision multiplier with B3 bits and R0=1 (at Nyquist rate)

A(B4 R0)--- full precision adder with B4 bits and R0=1 (at Nyquist rate)

A(B4 R2)--- full precision adder with B4 bits and R2=4

[S. Chu 1984] showed that, by applying the commutative rule, a comb filter needs only two registers, one adder at high rate, and one adder at the low rate regardless of the decimation ratio, i.e. regardless of the comb filter length. Thus, the overall cost function is

$$C=P*96*B3*R0+222*B4*R0+32*B4*R2$$

Table 4.2 Complexity for partially modulated subbanded AIC per band (R1=1, R2=4).

		# of M(B3R0)	# of A(B4R0)	# of A(B4R2)
AFB & SFB	x_0	64/2	64-1	0
	d_0	64/2	64-1	0
	e	64/2	64-1	0
AF	filtering y_0	0	0	32-1
	updating a_0	0	32	0
	comb filter	0	1	1
total		96	222	32

Comparing this to the conventional case, we can see that we are able to achieve basically the same performance (40dB cancellation) at a significantly lower complexity (96 as opposed to 160 full-precision multipliers in the conventional case).

The sigma-delta modulation resulted in reduced number of multipliers (by eliminating the multipliers required in the adaptive sections) at basically minimal cost (the cost of implementing the comb filter).

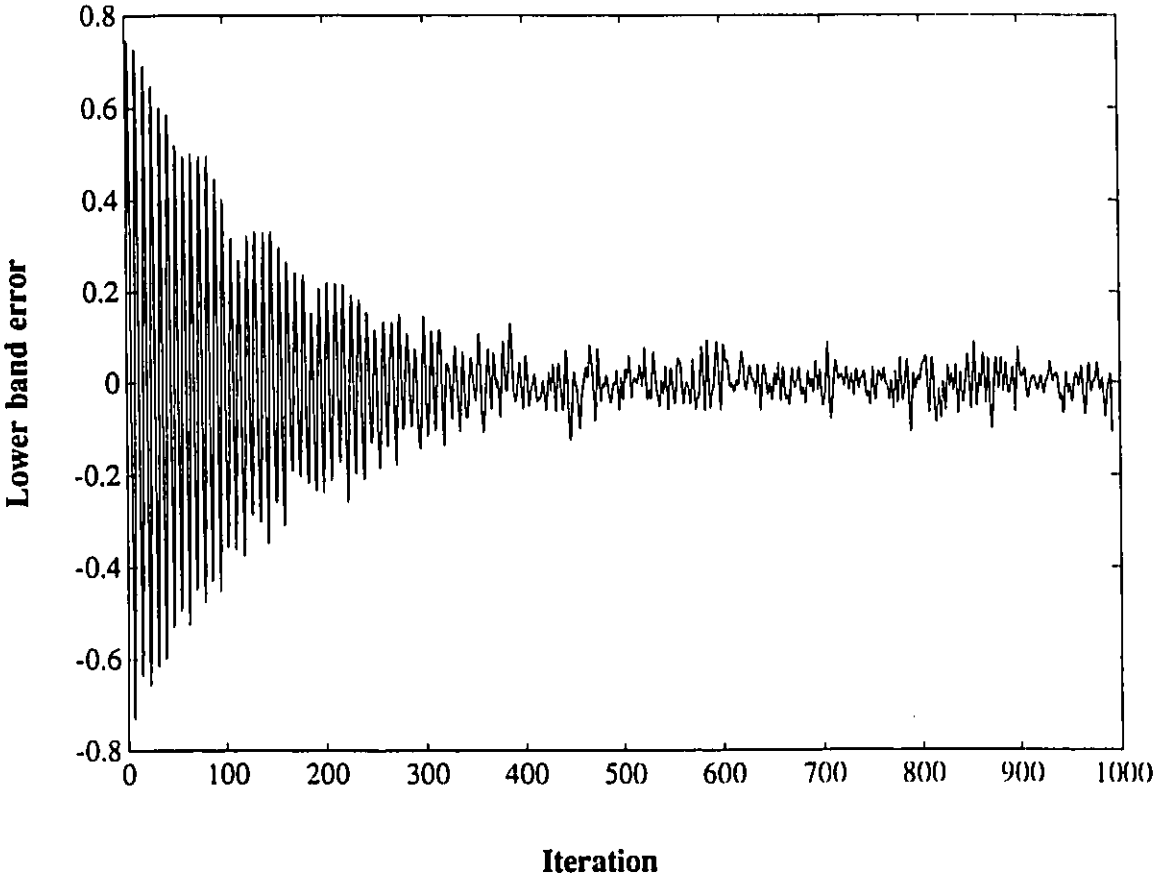

Figure 4.2.2 Subbanded AIC with adaptive part modulated (R1=1, R2=4). (a) time evolution of lower band error signal.

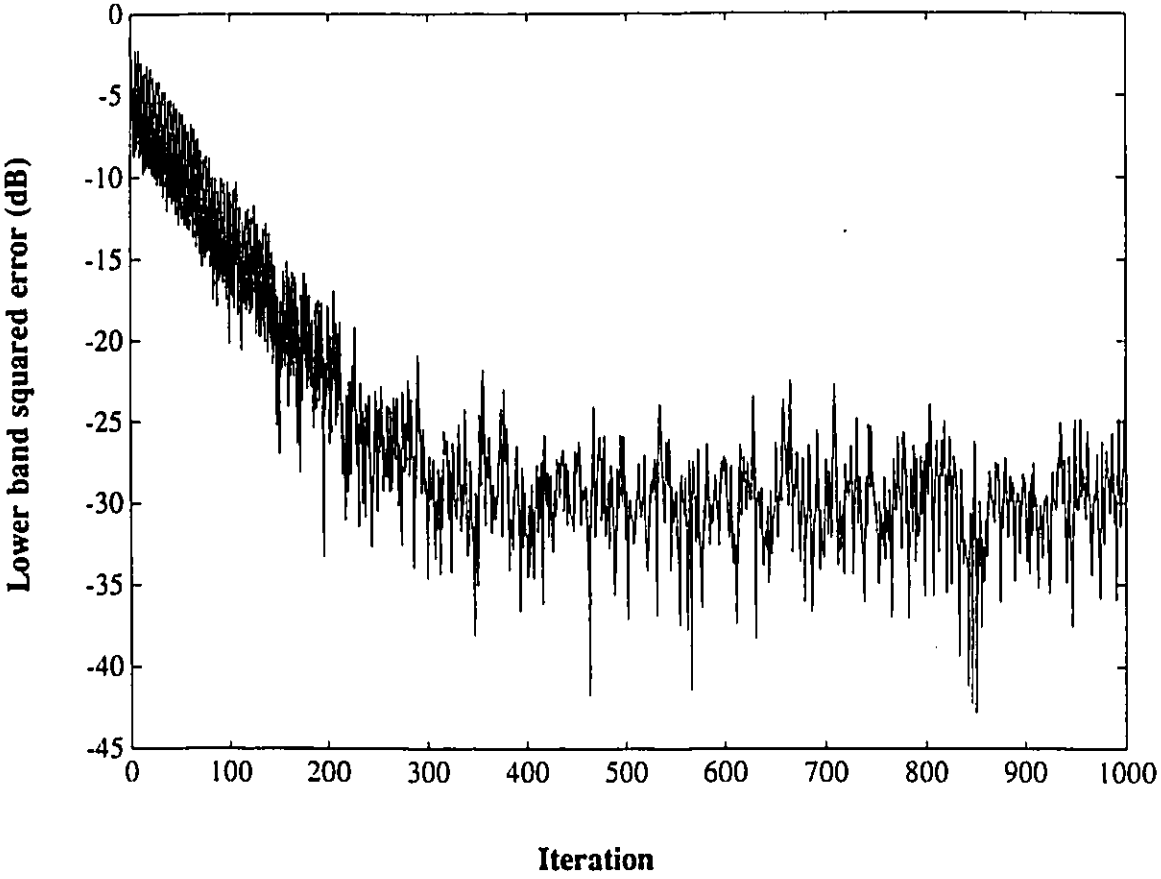

Figure 4.2.2 Subbanded AIC with adaptive part modulated (R1=1, R2=4). (b) time evolution of lower band squared error.

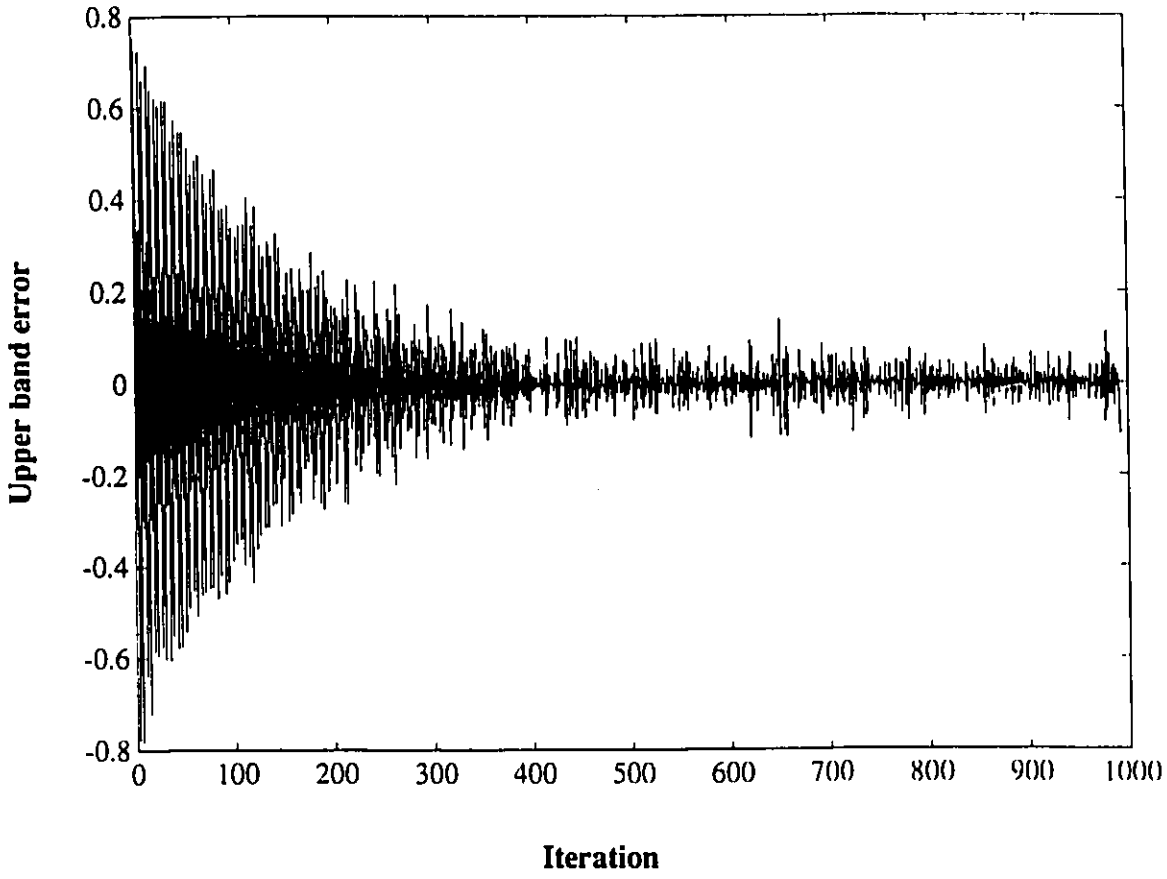

Figure 4.2.2 Subbanded AIC with adaptive part modulated (R1=1, R2=4). (c) time evolution of upper band error signal.

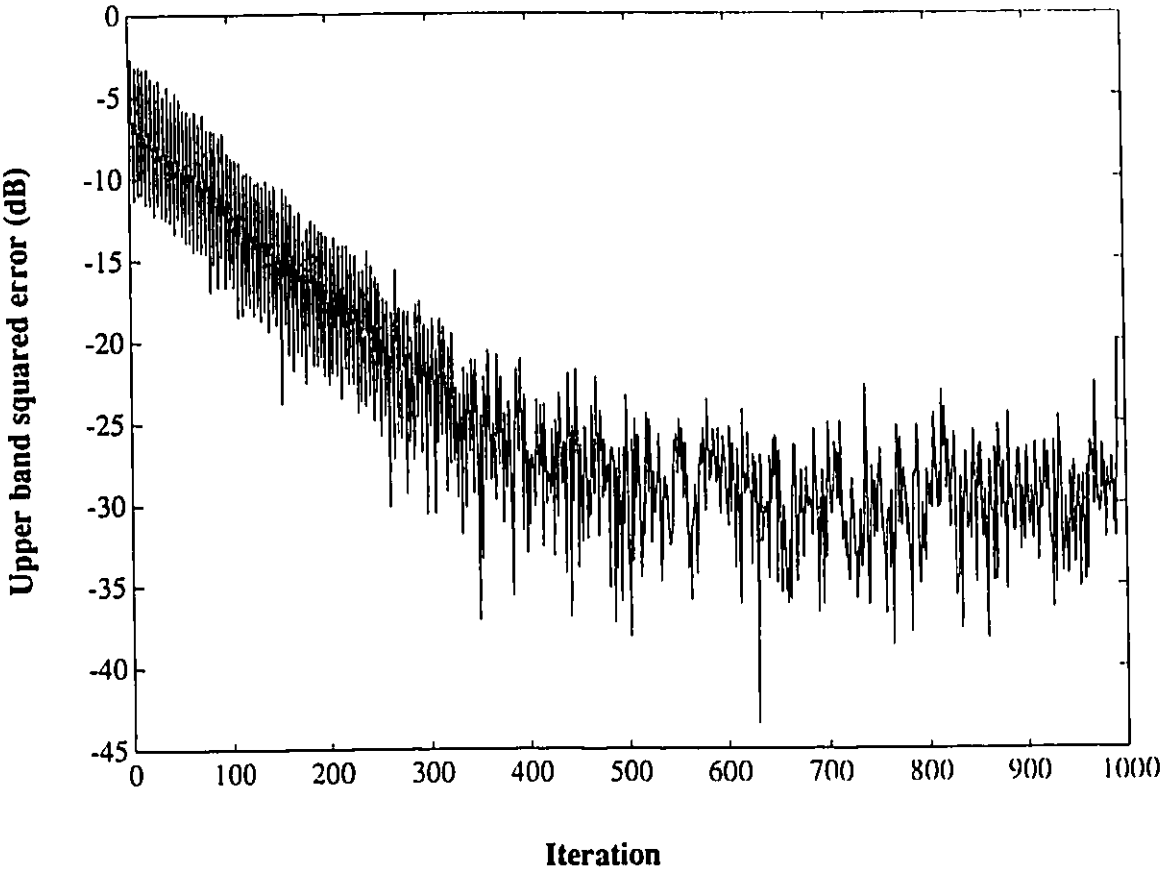

Figure 4.2.2 Subbanded AIC with adaptive part modulated (R1=1, R2=4). (d) time evolution of upper band squared error.

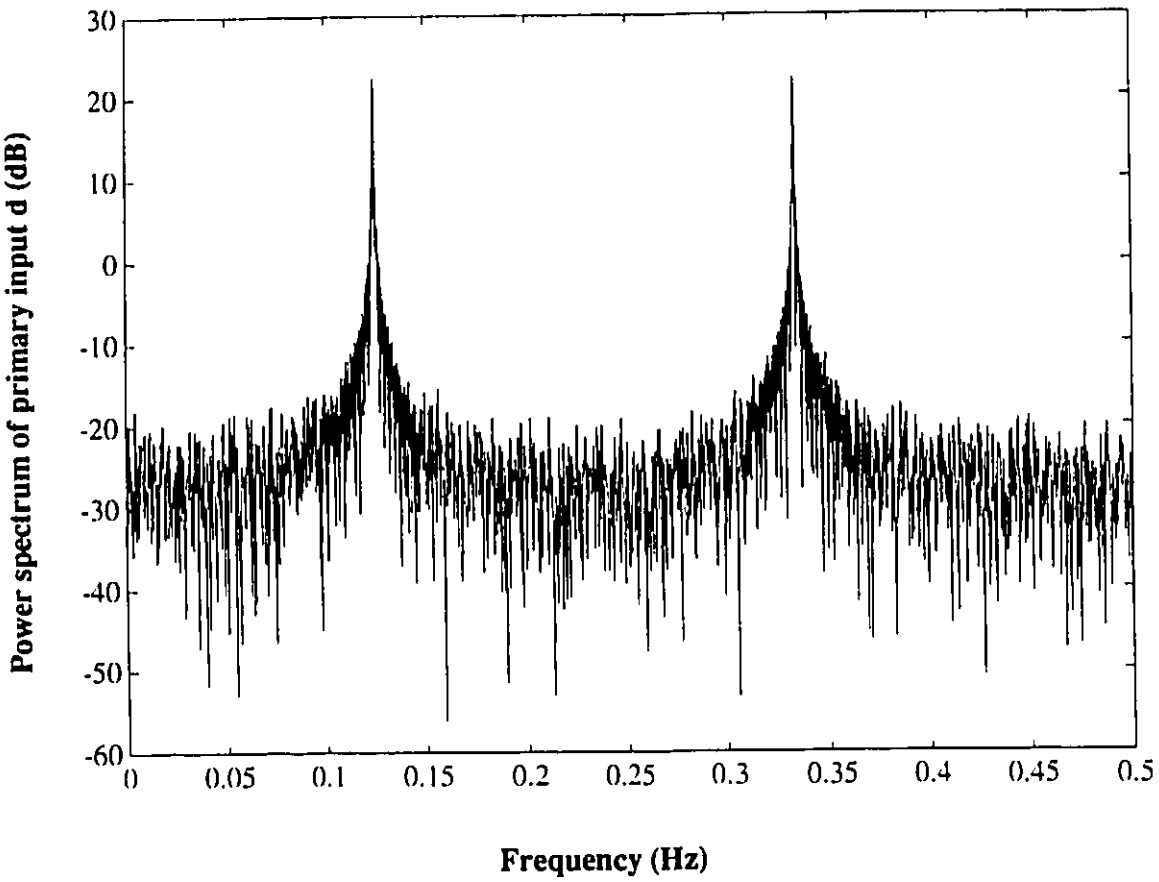

Figure 4.2.3 Power spectrum of subbanded AIC with adaptive part modulated (R1=1, R2=4). (a) primary input -- a combination of a Gaussian white noise as signal and two sinusoidal signals at 1/8Hz and 3/9Hz as noise.

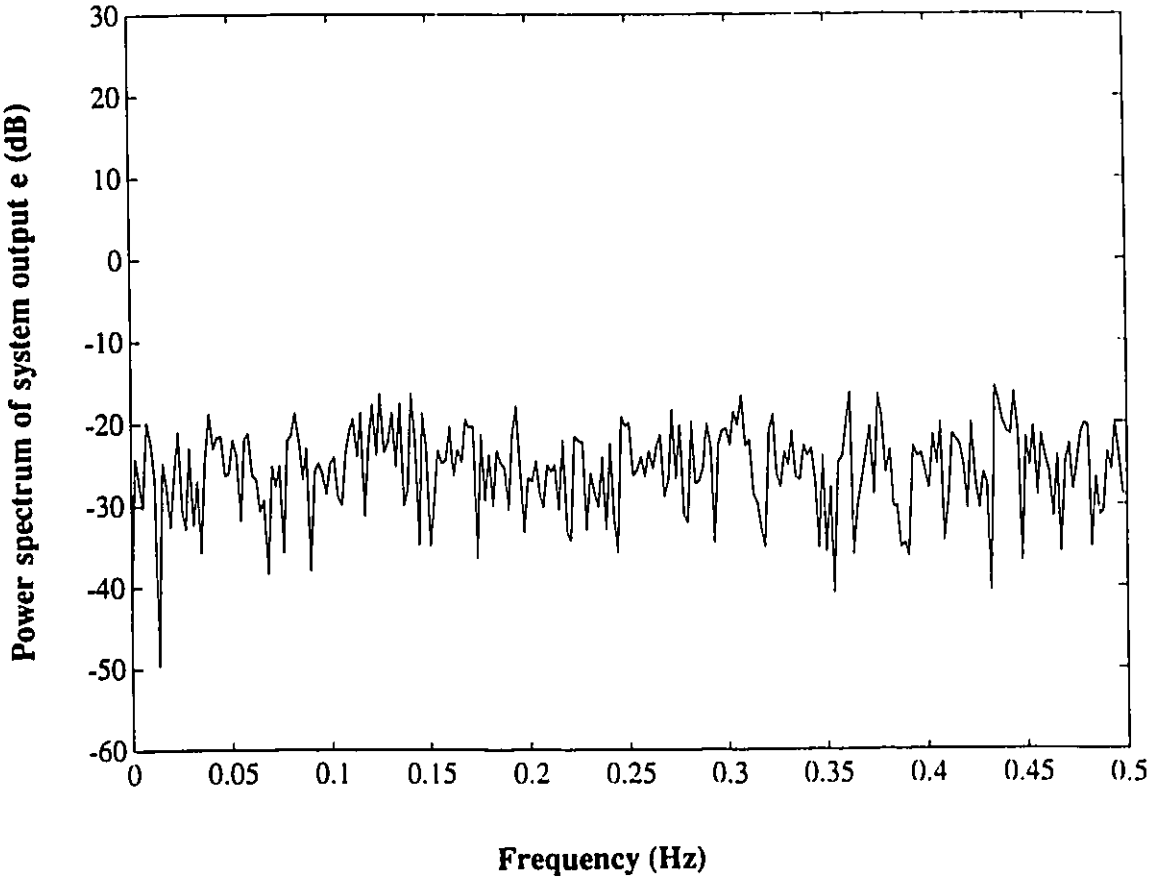

Figure 4.2.3 Power spectrum of subbanded AIC with adaptive part modulated (R1=1, R2=4). (b) system output with the sinusoidal interference being cancelled.

4.3 Proposed Fully Modulated Subbanded AIC (R1=64,R2=4)

In this section, the use of sigma-delta modulation in the filter implementation is extended to the analysis/synthesis filter bank to further increase the reduction required in hardware. Fig 4.3.1 shows the block diagram of this proposed fully sigma-delta modulated subbanded AIC.

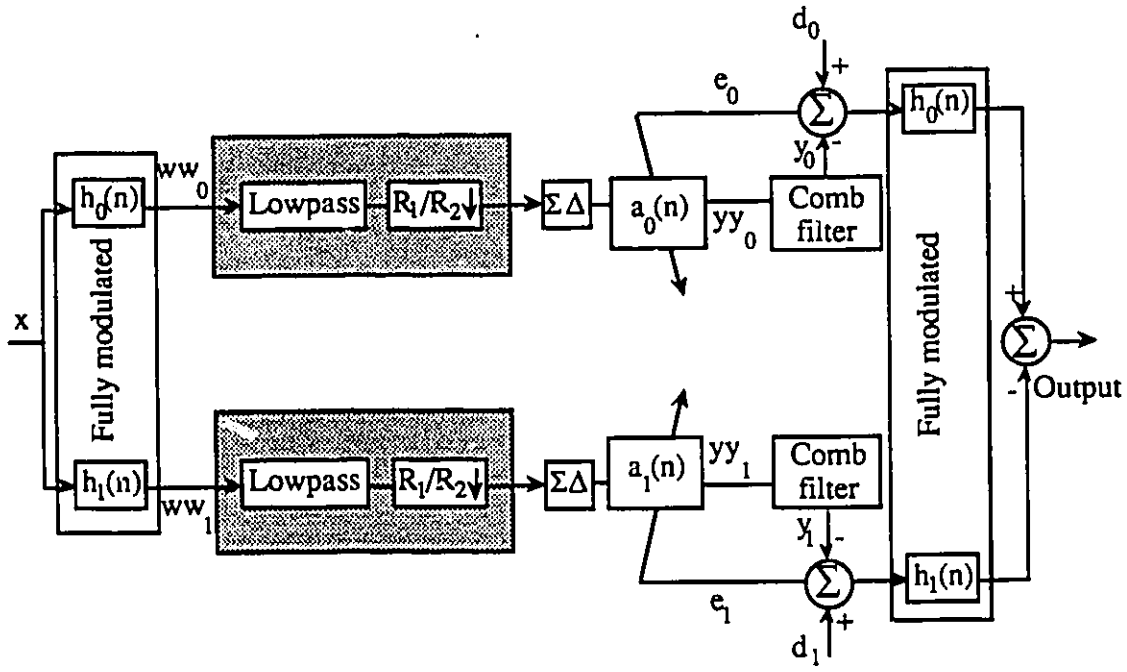

Figure 4.3.1 Fully modulated subbanded adaptive interference cancellation.

As discussed in chapter 3, R_1 is chosen as high as 64 to ensure proper representation of the subbanded signal. It was also shown in chapter 2 that R_2=4 is sufficient for AIC applications. The lowpass filter shown in the shaded block is needed to bandlimit the signal prior to the lower oversampling ratio R_2. In the case, we use a regular FIR filter. The signal is then decimated to the lower rate $R_2 f_N$. The output of

the decimator is obviously multi-bit and has to be transformed into the one-bit format using the sigma-delta modulated block identical to the in Fig.2.3.5.

Fig.4.3.2(a) and (c) show the lower band and upper band error signal respectively. Fig.4.3.2(b) and (d) show the lower band and upper band learning curves of fully modulated subbanded AIC. The number of iterations required for convergence is about 800. Fig.4.3.3(a) shows the power spectrum of the primary input, and (b) shows the power spectrum of the system output after convergence. Based on Fig.4.3.3, one can see that the sinusoidal interference is suppressed down by the required 40dB.

Table 4.3 Complexity for fully modulated subbanded AIC per band (R1=64, R2=4).

		# of M (B3R0)	# of M (B2R2)	# of A (B4R1)	# of A (B4R0)	# of A (B4R2)	# of A (B1R1)
AFB & SFB	x_0	0	0	0	0	0	64-1
	d_0	0	0	0	0	0	64-1
	e	0	0	0	0	0	64-1
	decimator A	60/4	0	0	60/4	60/4	0
	decimator C	60/2	0	0	60/2	60/2	0
AF	filtering y_0	0	0	0	0	32-1	0
	updating a_0	0	0	0	32	0	0
	comb filter	0	0	0	1	1	0
additional	lowpass	0	(19+1)/2	(19-1)/2	0	(19-1)/2	0
total		45	10	9	78	86	189

Table 4.3 shows the complexity in terms of the number of adders and multipliers for one band, where decimator A denotes the decimator in synthesis filter

bank (SBF) part, decimator C denotes the decimator for the modulated primary signal d and

M(B3 R0)--- full precision multiplier with B3 bits and R0=1 (at Nyquist rate)

M(B2 R2)--- multibit multiplier with B2=$\log_2 64+1$=7bits and R2=4

A(B4 R1)--- full precision adder with B4 bits and R1=64

A(B4 R0)--- full precision adder with B4 bits and R0=1 (at Nyquist rate)

A(B4 R2)--- full precision adder with B4 bits and R2=4

A(B1 R1)--- 1-bit adder with B1=1bit and R1=64

The fully modulated AIC structure proposed here contains modulated filter bank part (both AFB and SBF) and modulated adaptive filtering part. For the adaptive filter part, comb filter is sufficient as decimator. But regular decimators A and C are needed for filter bank part with the same specifications. Since the decimation at the SFB stage can be performed at the system output as opposed to at the output of each band, in other words, one filter rather than two is needed for SFB, only one half of the decimator A's complexity should be calculated as far as the complexity per band in concerned in Table 4.3.

For both Table 4.2 and 4.3, the number of multipliers and adders are calculated taking into consideration the difference in speed. It has been shown in chapter 2 that filters used as decimators in multirate system can be designed to run at the lower rate. This is assumed in the calculation in Table 4.2 and 4.3. Referring to Fig.2.3.11, we implement the lowpass filter (needed for rate changing from R1 to R2) and the decimators needed for synthesis filter bank with all multipliers operating at low rate, half adders operating at low rate, and the other half at high rate. This is similar to a comb filter implementation with one adder at high rate, one adder at low rate after applying the commutative rule.

The cost function is

C=P*(45*B3*R0+10*B2*R2)+9*B4*R1+78*B4*R0+86*B4*R2+189*B1*R1

Comparing this to the results in section 4.1 and 4.2, we can see that we achieve the same performance (40dB cancellation) at much lower complexity (45 as opposed to 96 and 160 full-precision multipliers for the half modulated and conventional case respectively). The fully modulated AIC is the most desirable among three structures in terms of cost efficiency.

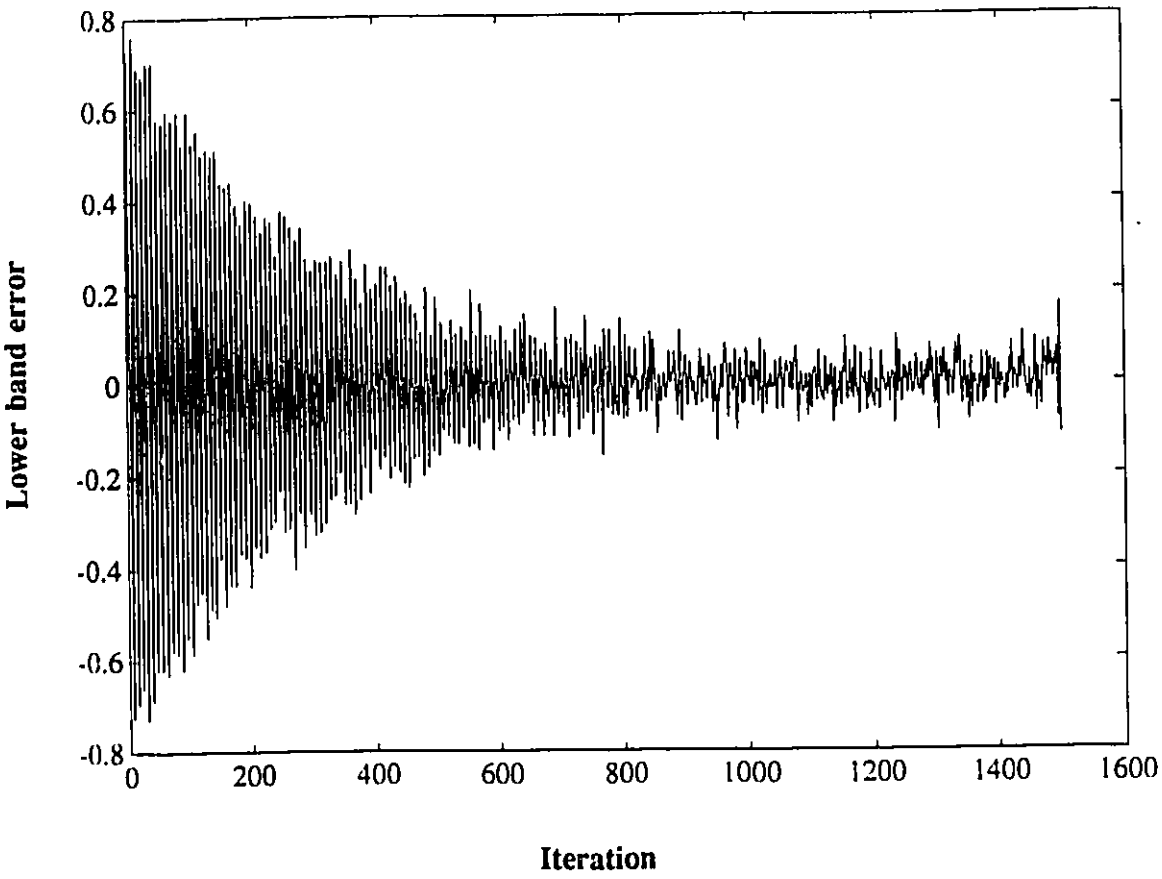

Figure 4.3.2 Subbanded AIC with both filter bank and adaptive part modulated (R1=64, R2=4). (a) time evolution of lower band error signal.

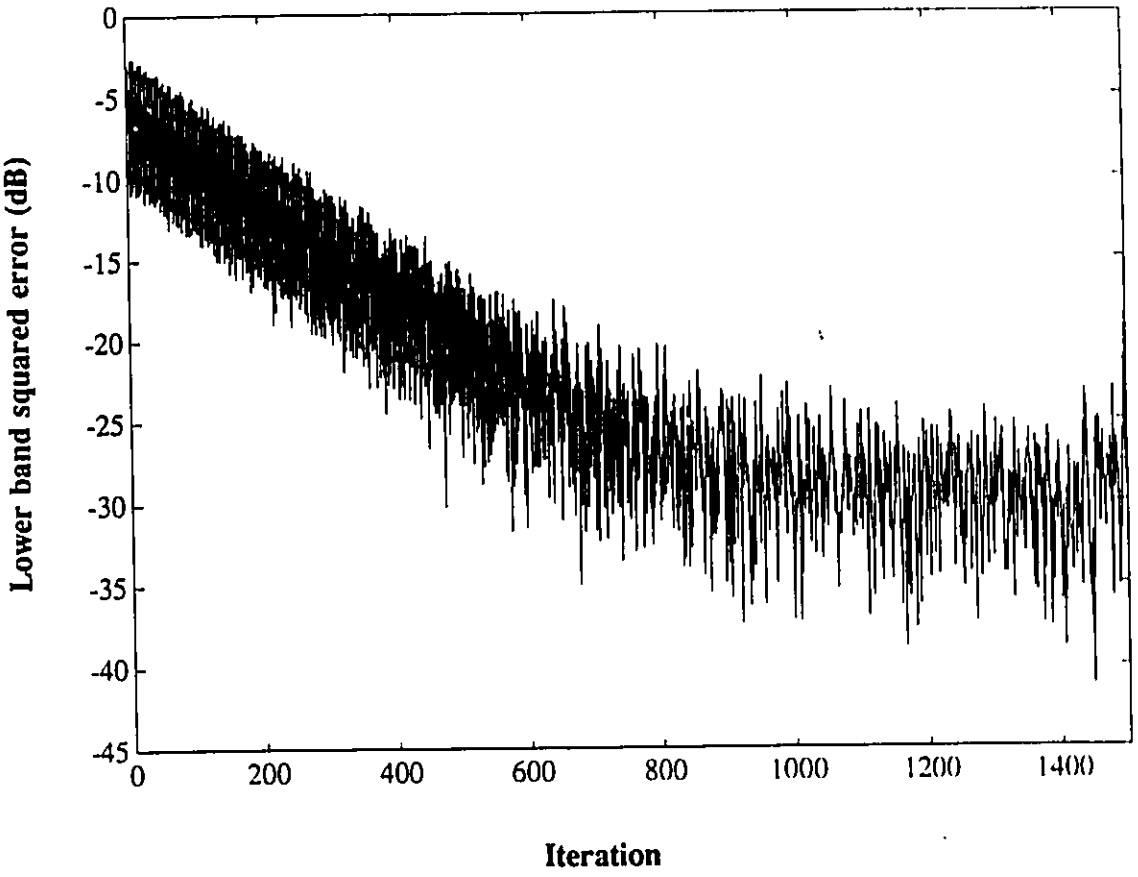

Figure 4.3.2 Subbanded AIC with both filter bank and adaptive part modulated (R1=64, R2=4). (b) time evolution of lower band squared error.

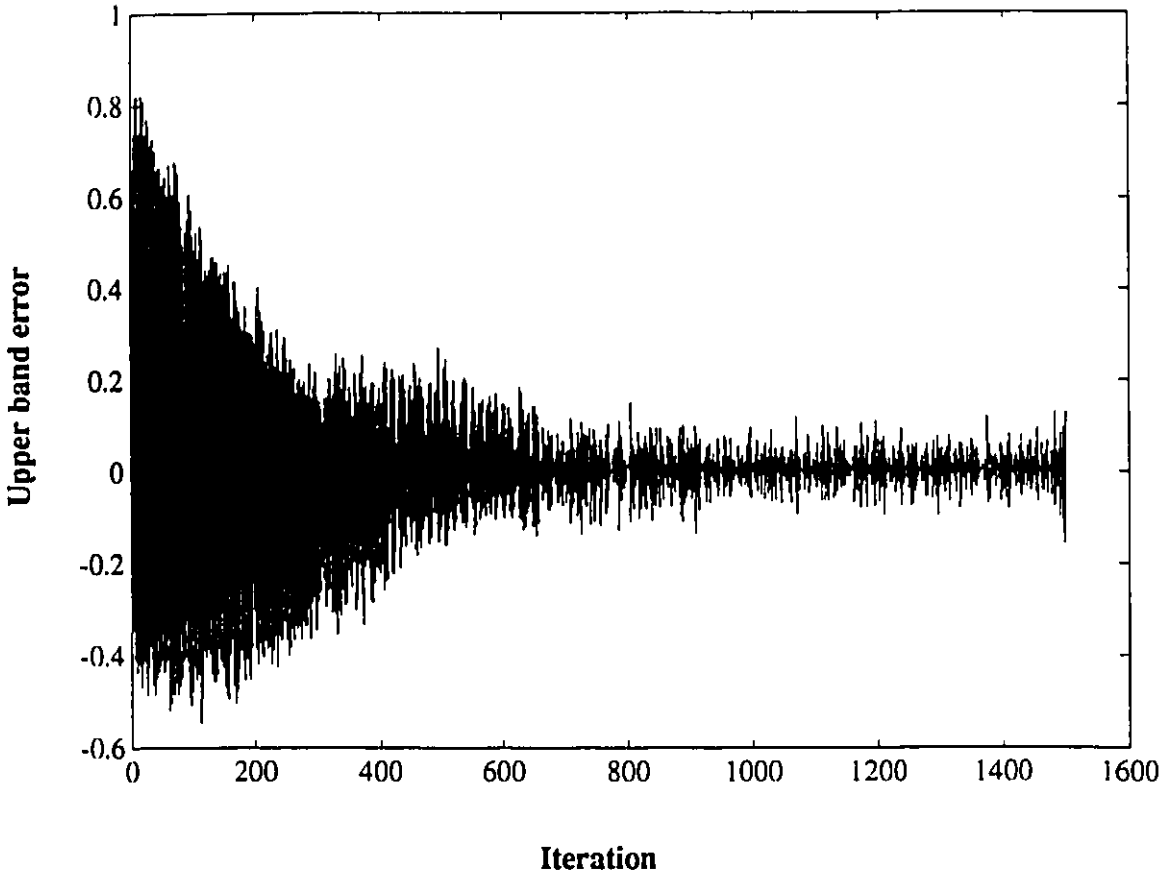

Figure 4.3.2 Subbanded AIC with both filter bank and adaptive part modulated (R1=64, R2=4). (c) time evolution of upper band error signal.

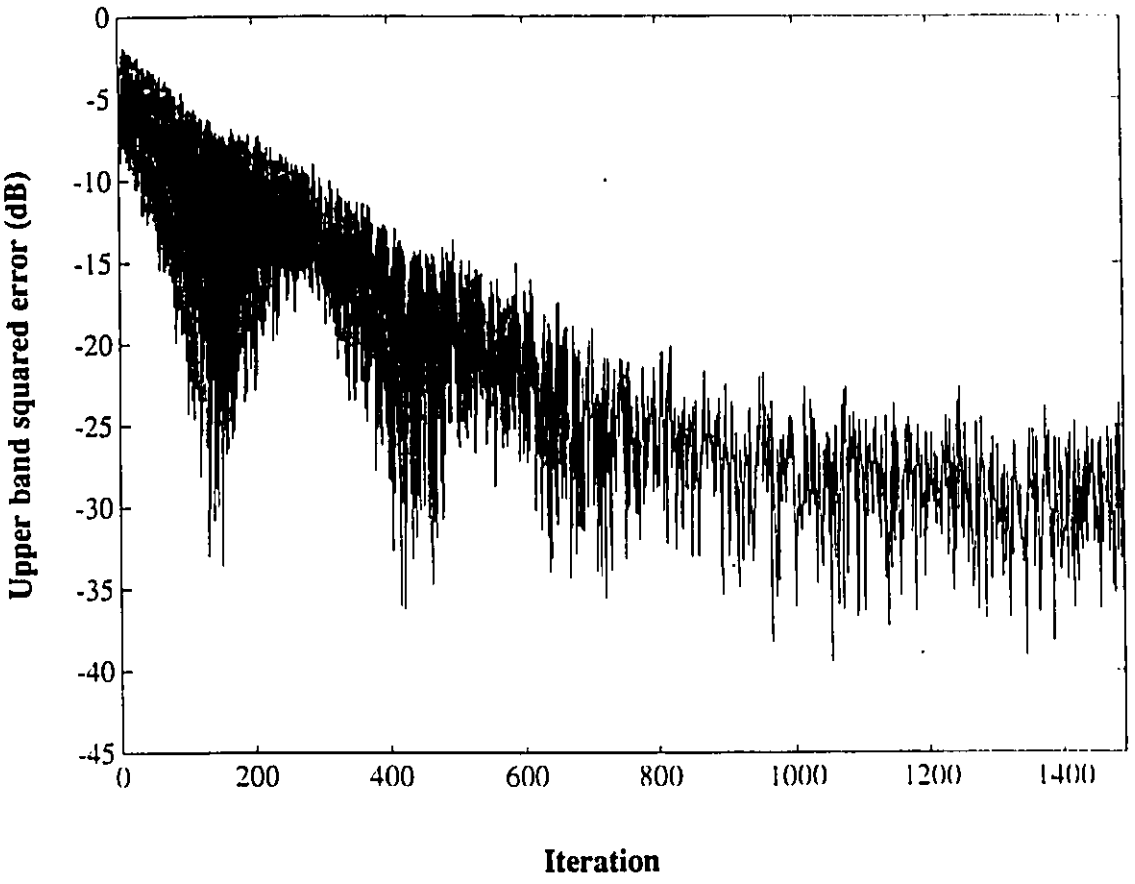

Figure 4.3.2 Subbanded AIC with both filter bank and adaptive part modulated (R1=64, R2=4). (d) time evolution of upper band squared error.

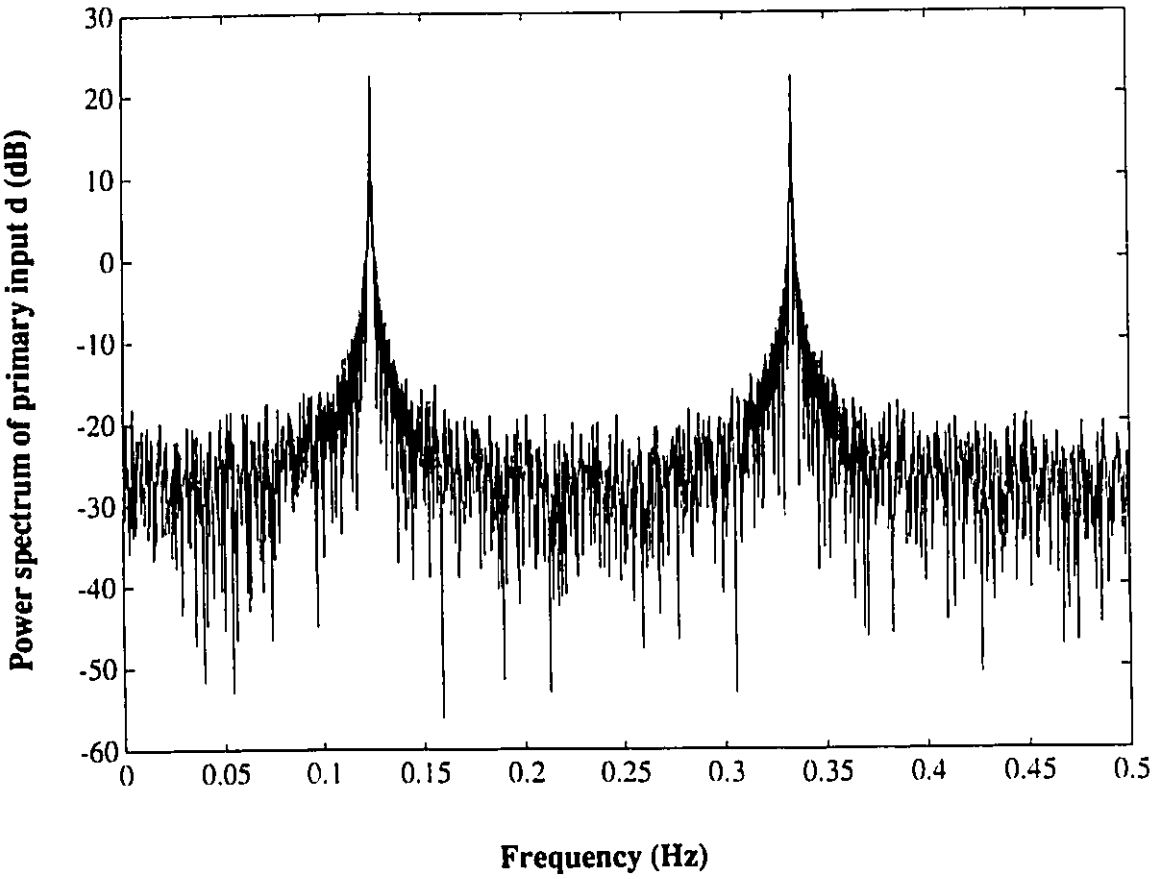

Figure 4.3.3 Power spectrum of subbanded AIC with both filter bank and adaptive part modulated (R1=64, R2=4). (a) primary input -- a combination of a Gaussian white noise as signal and two sinusoidal signals at 1/8Hz and 3/9Hz as noise.

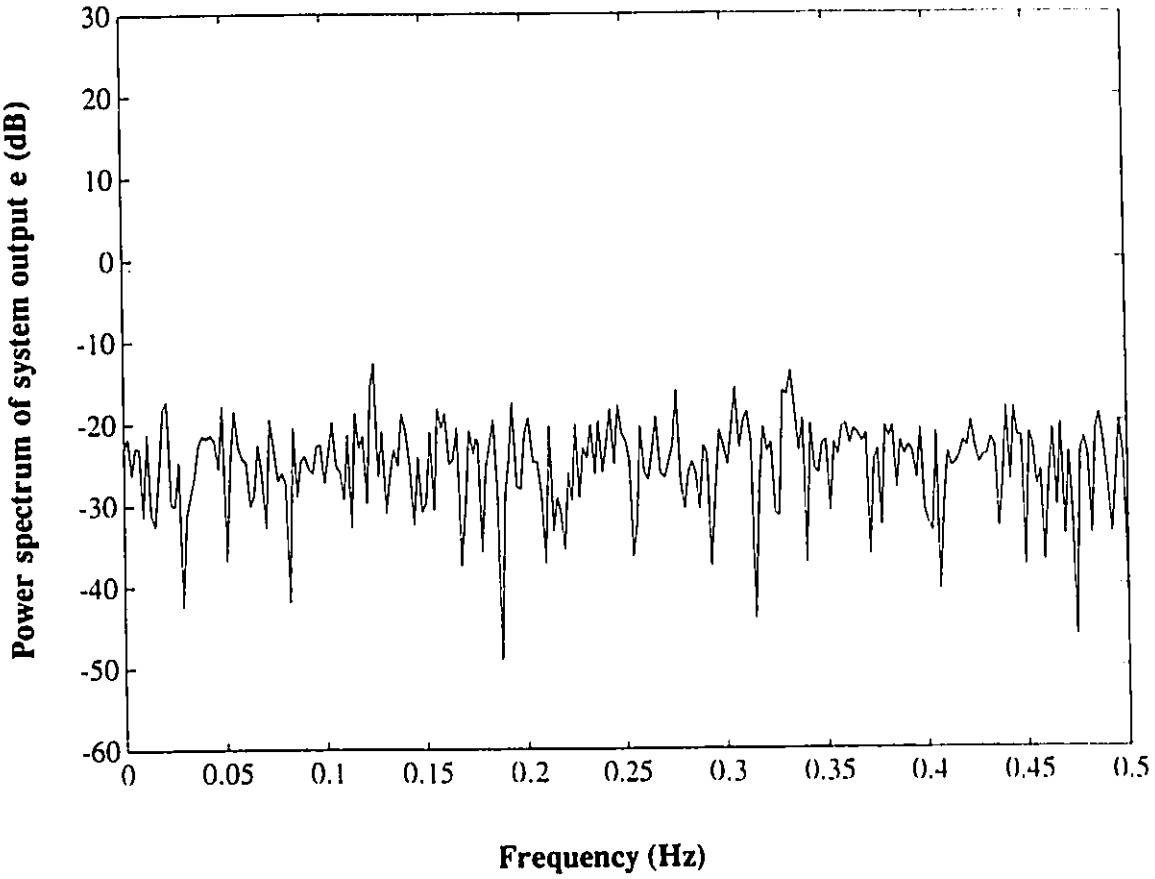

Figure 4.3.3 Power spectrum of subbanded AIC with both filter bank and adaptive part modulated (R1=64, R2=4). (b) system output with the sinusoidal interference being cancelled.

4.4 Effect of Oversampling Ratios R1 and R2 and Decimator Quality

The oversampling ratio R1 for fixed FIR filtering is chosen to be 64 in the previous simulations. As discussed in chapter 3, if R1 is too small, it will fail to represent the input signal or filter coefficient at 1-bit precision. Thus, even after noise shaping, the quantization noise residual in baseband might be significantly large to distort the baseband signal. Improving the decimator quality cannot make up for this "baseband" distortion.

To verify this, a simulation was run for the same structure in Fig.4.1.3 but using R1=16 and R2=4. The convergence of error signals and squared error signals for both bands are shown in Fig.4.4.1(a)(b)(c)(d). The power spectrum of the primary input and the system output are shown in Fig.4.4.2(a) and Fig.4.4.2(b) respectively. We can see that the error signals are much larger after convergence compared to R1=64 case. The sinusoidal interference is suppressed down by approximately 25dB as opposed to 40dB when R1=64, R2=4.

Next, to test the effect of R2 on the overall performance, we chose R1=64 and R2=8 and run the simulation again. Since R1=64 and R2=4 are values which give satisfactory results for the proposed structure comparable to that for the conventional case, it is quite reasonable to conclude that bringing R2 higher than 4 will not be much benefit. Results in section 4.1.1 for conventional case are close to optimum, so no matter how high R2 is, performance of proposed case cannot be significantly better than the optimal reference.

The convergence of error signals and squared error signals for both bands are shown in Fig.4.4.3(a)(b)(c)(d). The power spectrum of the primary input and the system output are shown in Fig.4.4.4(a) and Fig.4.4.4(b) respectively. These results

confirm what has been discussed above. The learning curve is an average of 2 simulations, so it is quite noisy, but it can be seen from Fig.4.4.4(b) that the sinusoidal interference is suppressed down by the desired 40dB.

Then, a third set of simulation was run for R1=16 and R2=8. The purpose is to testify if the performance of the overall system can be compensated by a high oversampling ratio for adaptive filtering part when the oversampling ratio for filter bank section is low. The convergence of error signals and squared error signals for both bands are shown in Fig.4.4.4(a)(b)(c)(d). The power spectrum of the primary input and the system output are shown in Fig.4.4.5(a) and Fig.4.4.5(b) respectively. We can see that the error signals are larger after convergence compared to R1=64 R2=4 case. The sinusoidal interference is suppressed down by approximately 25dB as opposed to 40dB when R1=64, R2=4. This recomfirms our statement that a high R2 would not possibly make up for the unsatisfatory performance when R1 is low.

Finally, we have shown in section 3.2.2 that a comb filter is sufficient as a decimator for adaptive filtering part in an interference cancellation system. A comb filter is especially favorable in this application, as our aim is to maintaining reasonable performance while bringing down the hardware complexity. The adequacy of this simple decimator was verified when the same performance was achievable compared to conventional case. For other sigma-delta modulation applications, like the ANC to be discussed in chapter 5, This simple comb filter may no longer be sufficient.

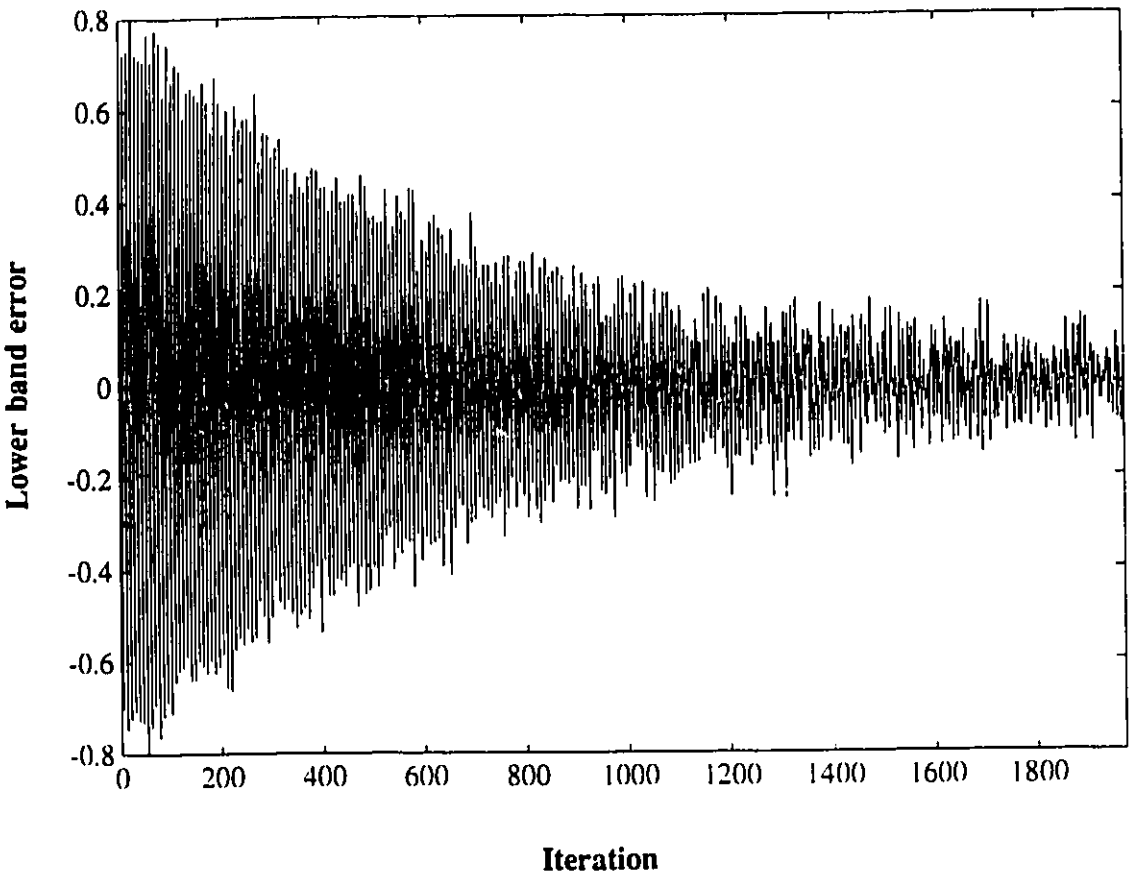

Figure 4.4.1 Subbanded AIC with both filter bank and adaptive part modulated (R1=16, R2=4). (a) time evolution of lower band error signal.

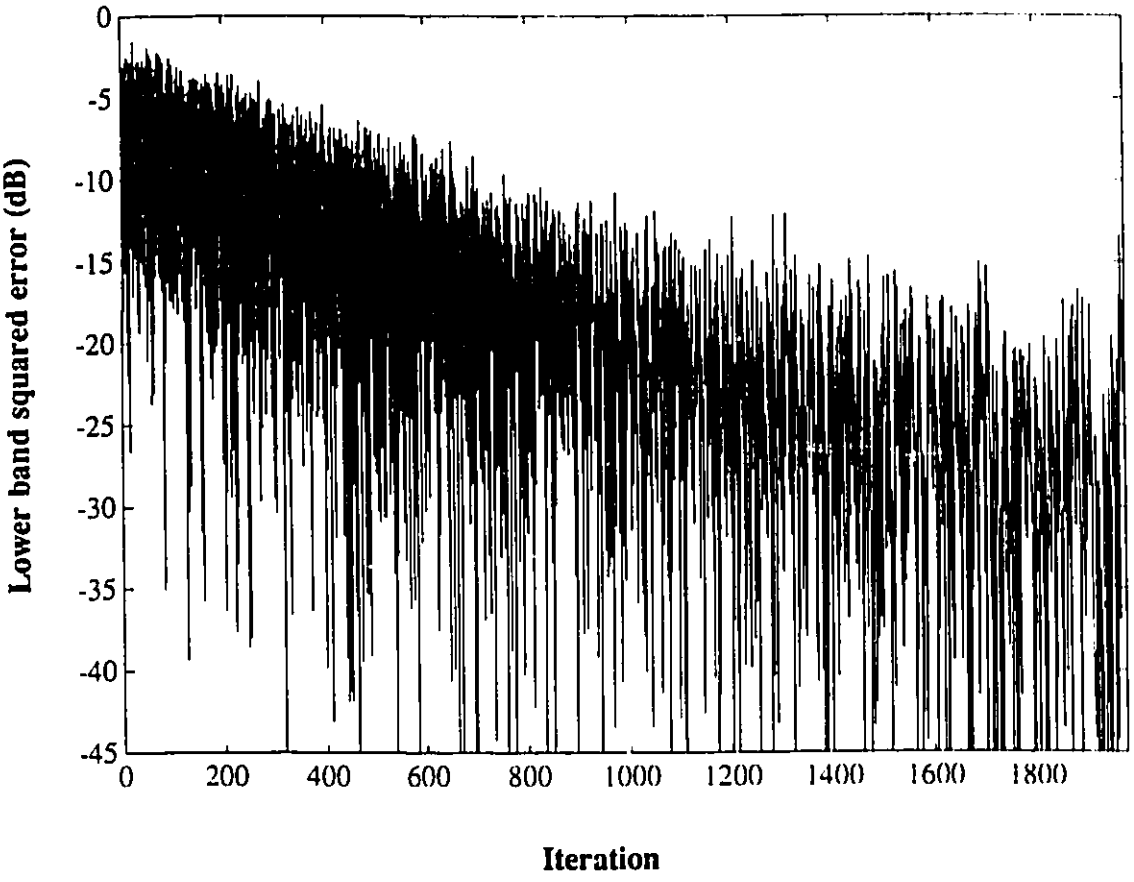

Figure 4.4.1 Subbanded AIC with both filter bank and adaptive part modulated (R1=16, R2=4). (b) time evolution of lower band squared error.

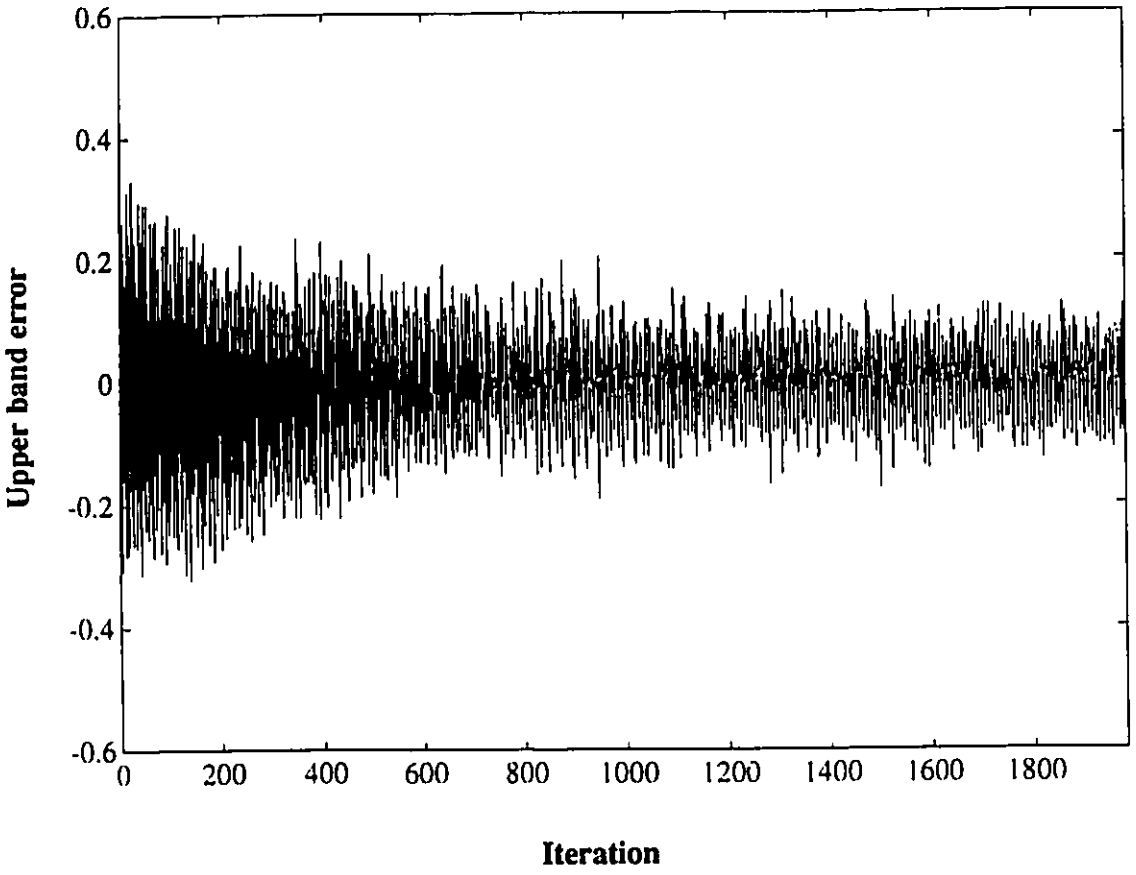

Figure 4.4.1 Subbanded AIC with both filter bank and adaptive part modulated (R1=16, R2=4). (c) time evolution of upper band error signal.

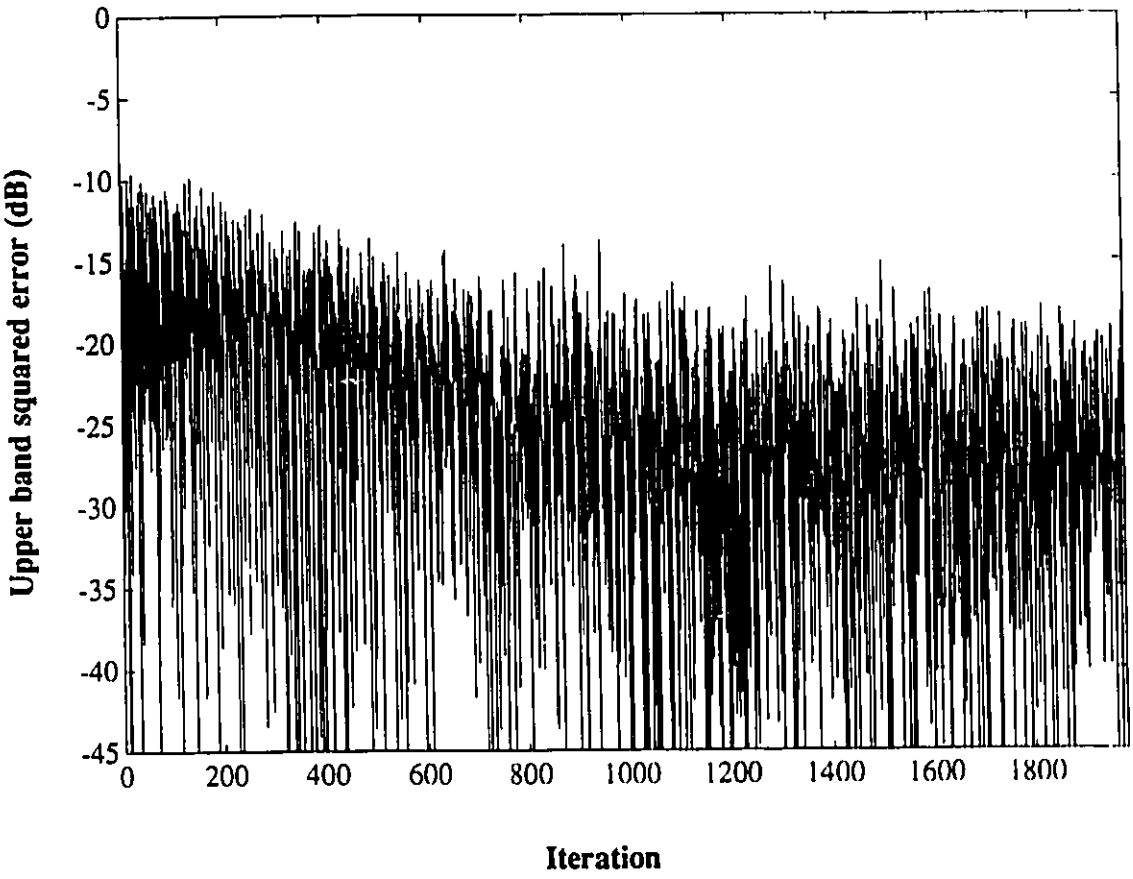

Figure 4.4.1 Subbanded AIC with both filter bank and adaptive part modulated (R1=16, R2=4). (d) time evolution of upper band squared error.

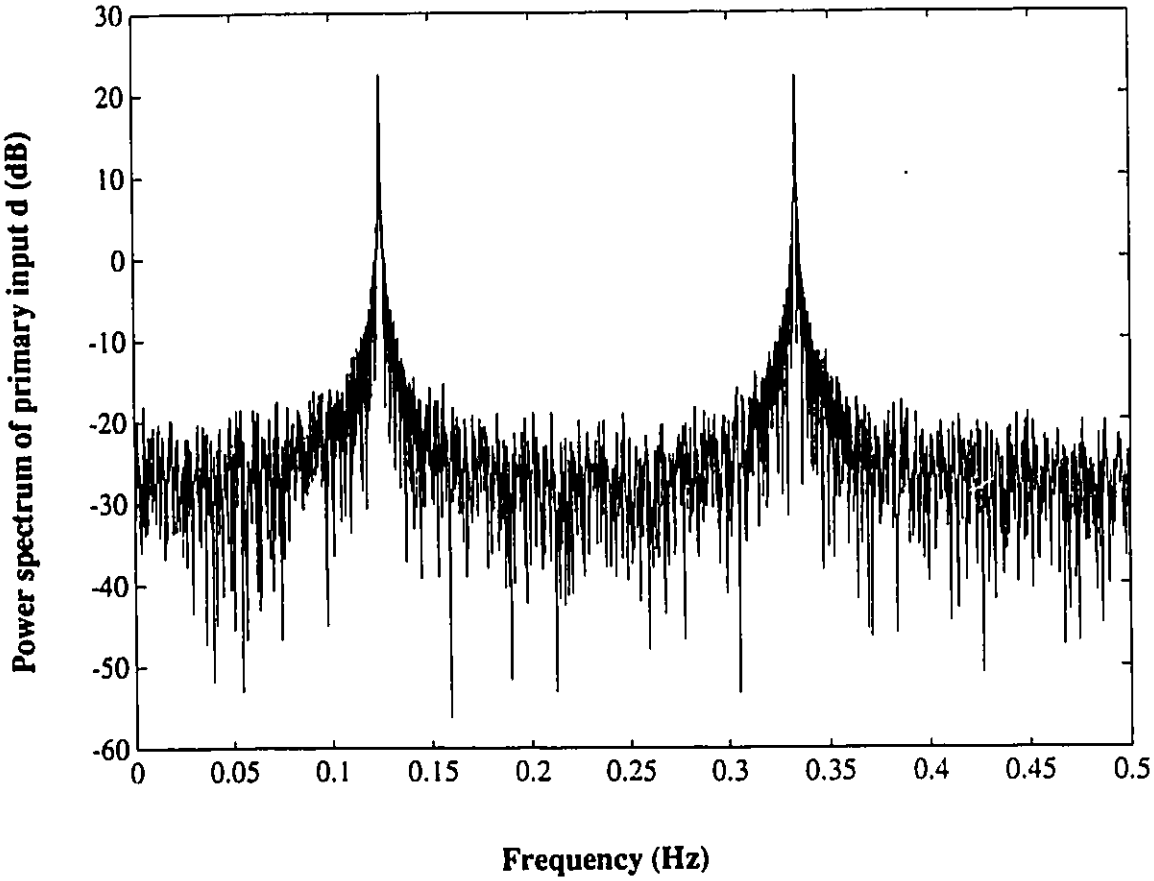

Figure 4.4.2 Power spectrum of subbanded AIC with both filter bank and adaptive part modulated (R1=16, R2=4). (a) primary input -- a combination of a Gaussian white noise as signal and two sinusoidal signals at 1/8Hz and 3/9Hz as noise.

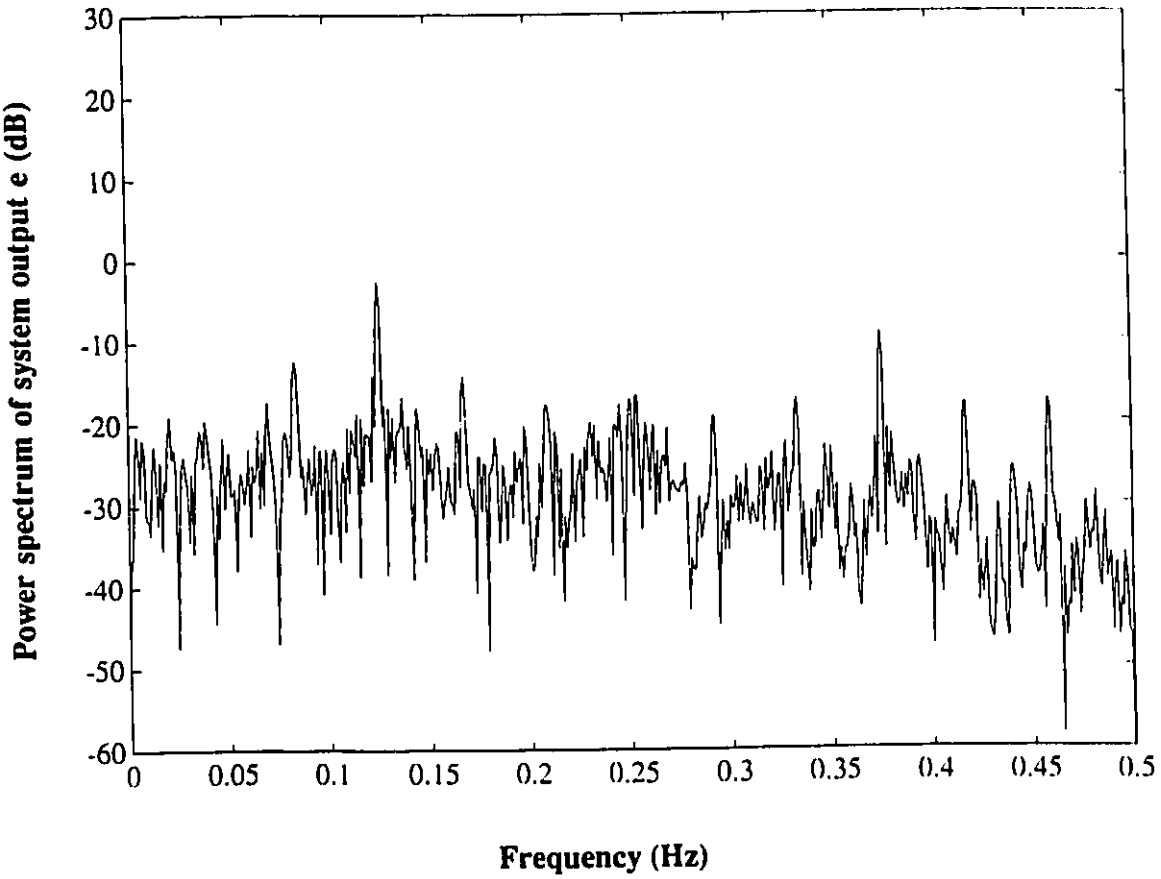

Figure 4.4.2 Power spectrum of subbanded AIC with both filter bank and adaptive part modulated (R1=16, R2=4). (b) system output with the sinusoidal interference being cancelled.

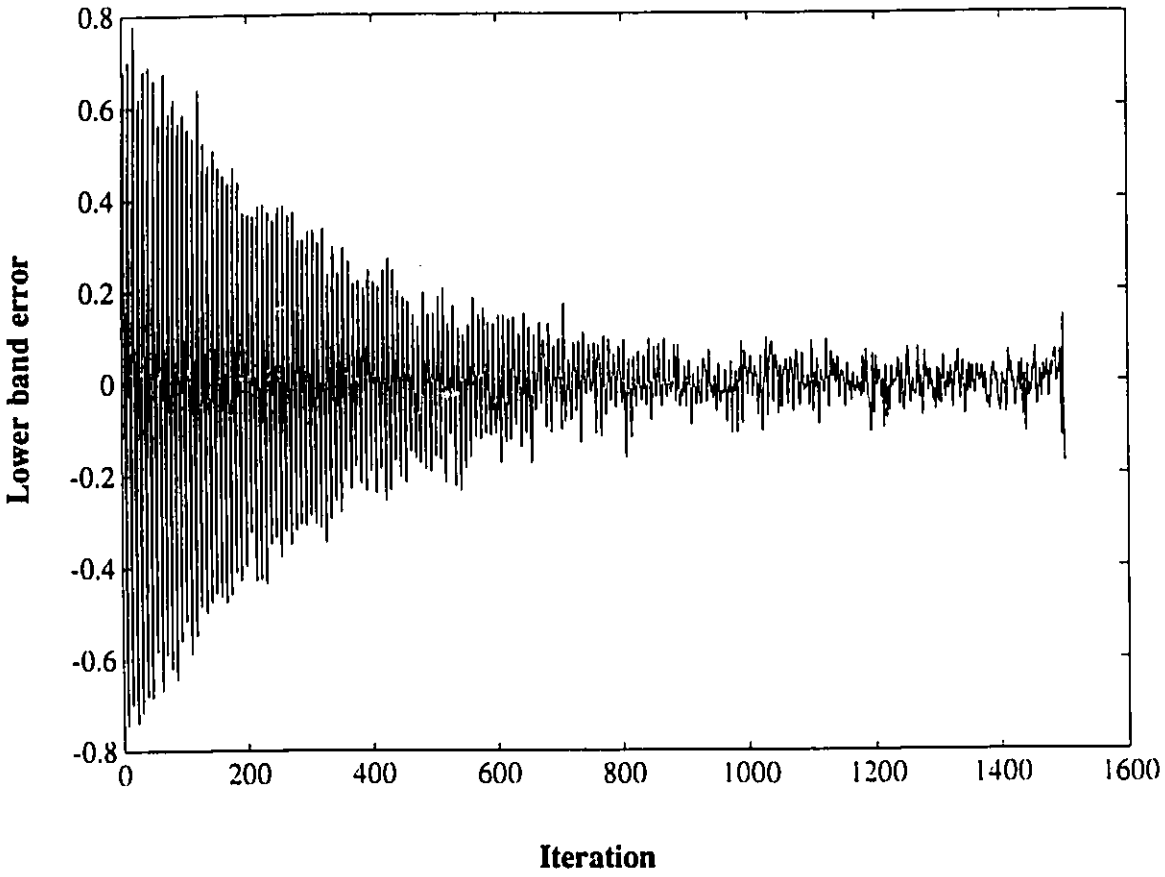

Figure 4.4.3 Subbanded AIC with both filter bank and adaptive part modulated (R1=64, R2=8). (a) time evolution of lower band error signal.

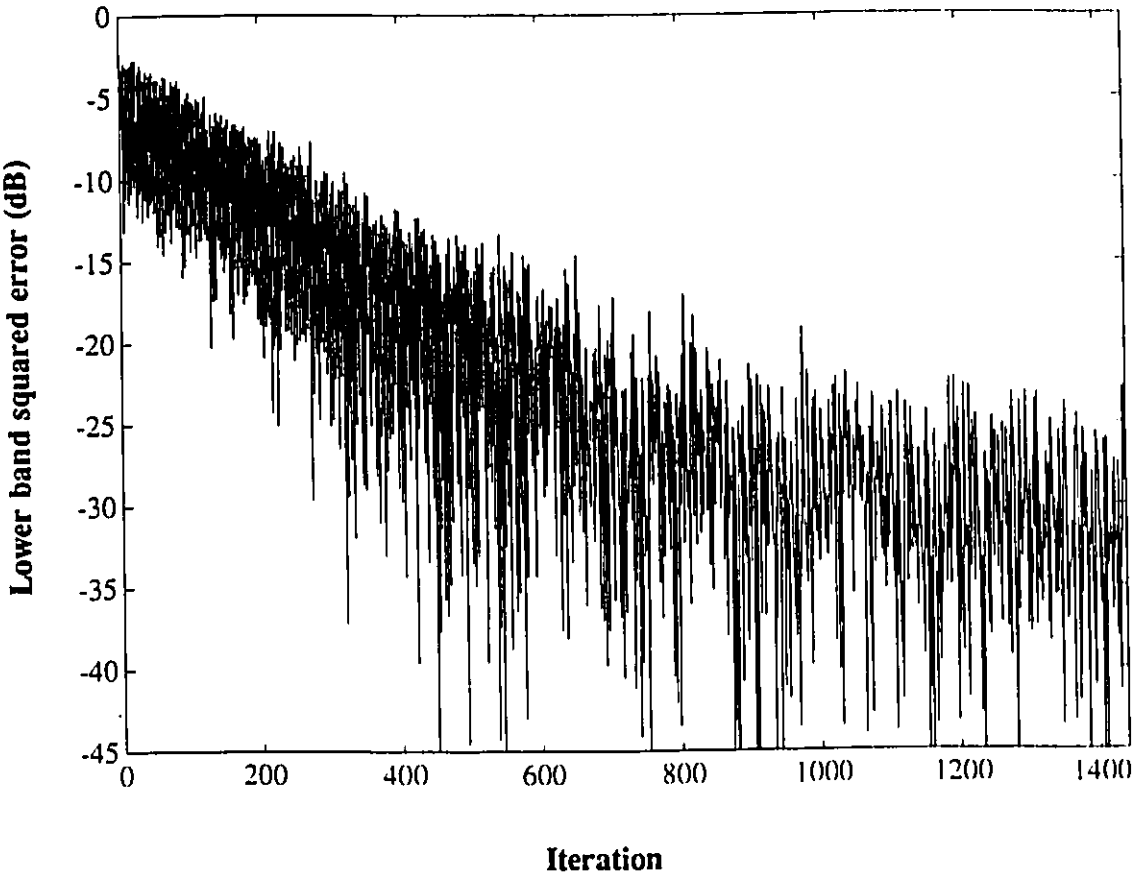

Figure 4.4.3 Subbanded AIC with both filter bank and adaptive part modulated (R1=64, R2=8). (b) time evolution of lower band squared error.

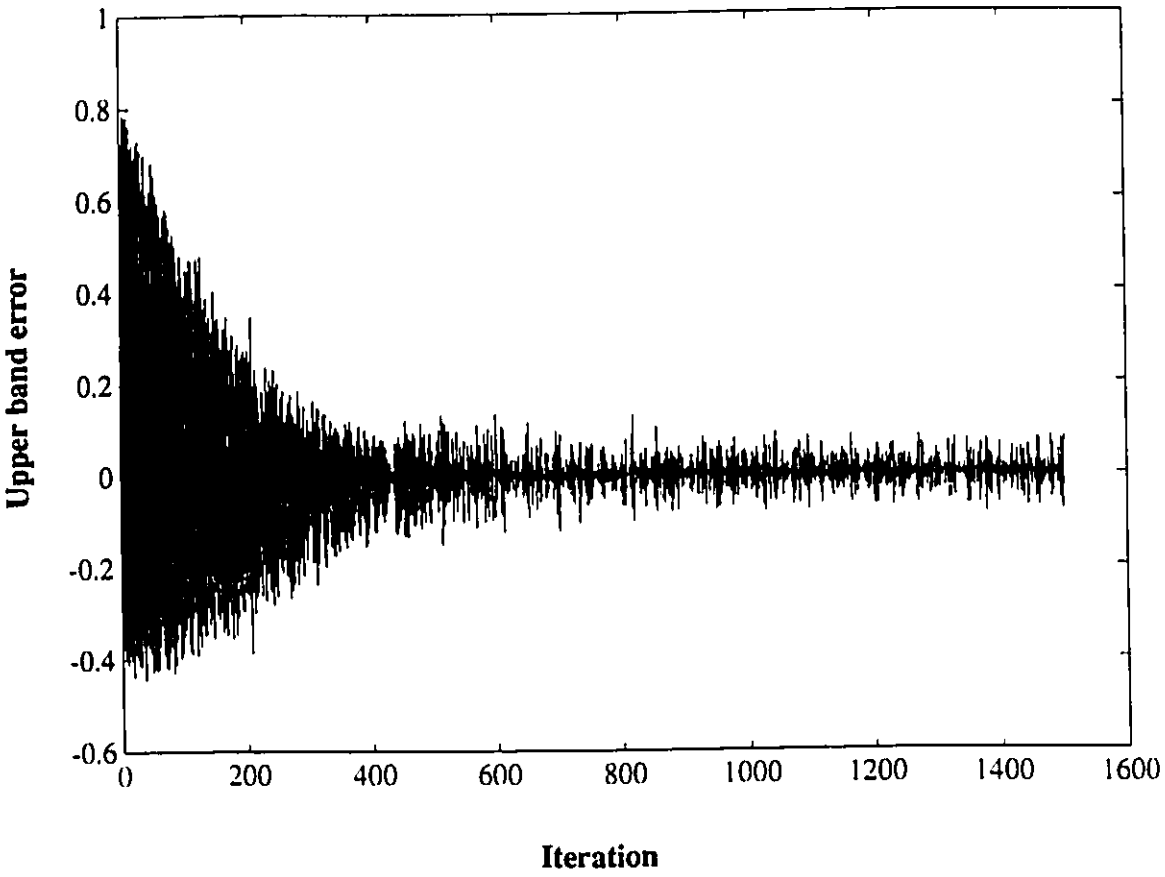

Figure 4.4.3 Subbanded AIC with both filter bank and adaptive part modulated (R1=64, R2=8). (c) time evolution of upper band error signal.

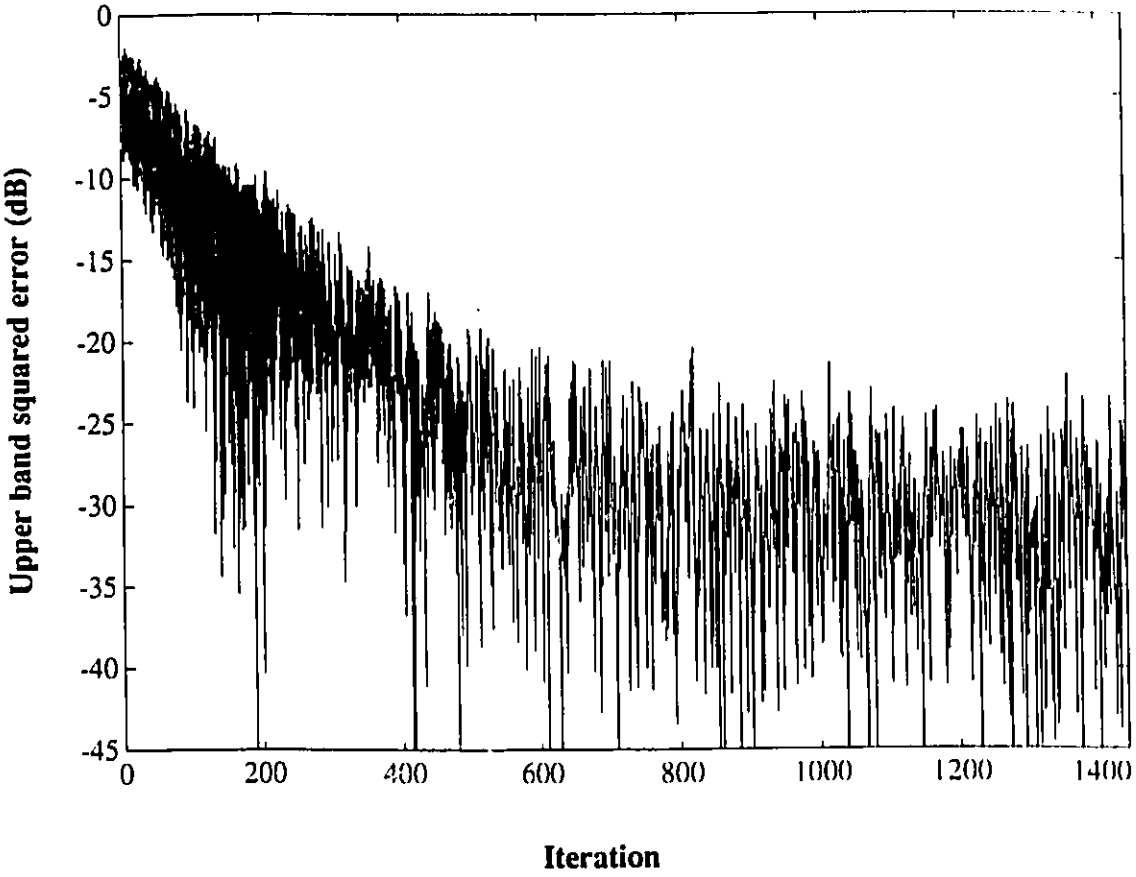

Figure 4.4.3 Subbanded AIC with both filter bank and adaptive part modulated (R1=64, R2=8). (d) time evolution of upper band squared error.

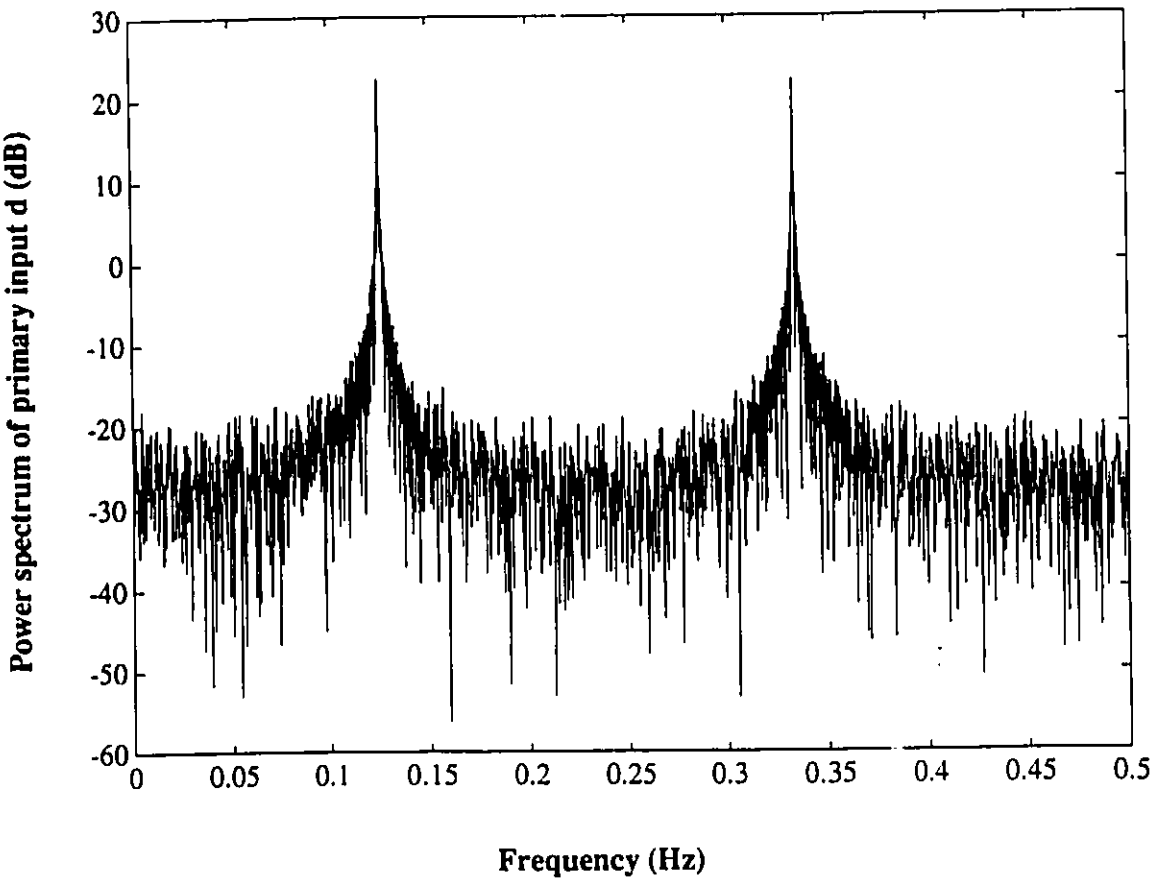

Figure 4.4.4 Power spectrum of subbanded AIC with both filter bank and adaptive part modulated (R1=64, R2=8). (a) primary input -- a combination of a Gaussian white noise as signal and two sinusoidal signals at 1/8Hz and 3/9Hz as noise.

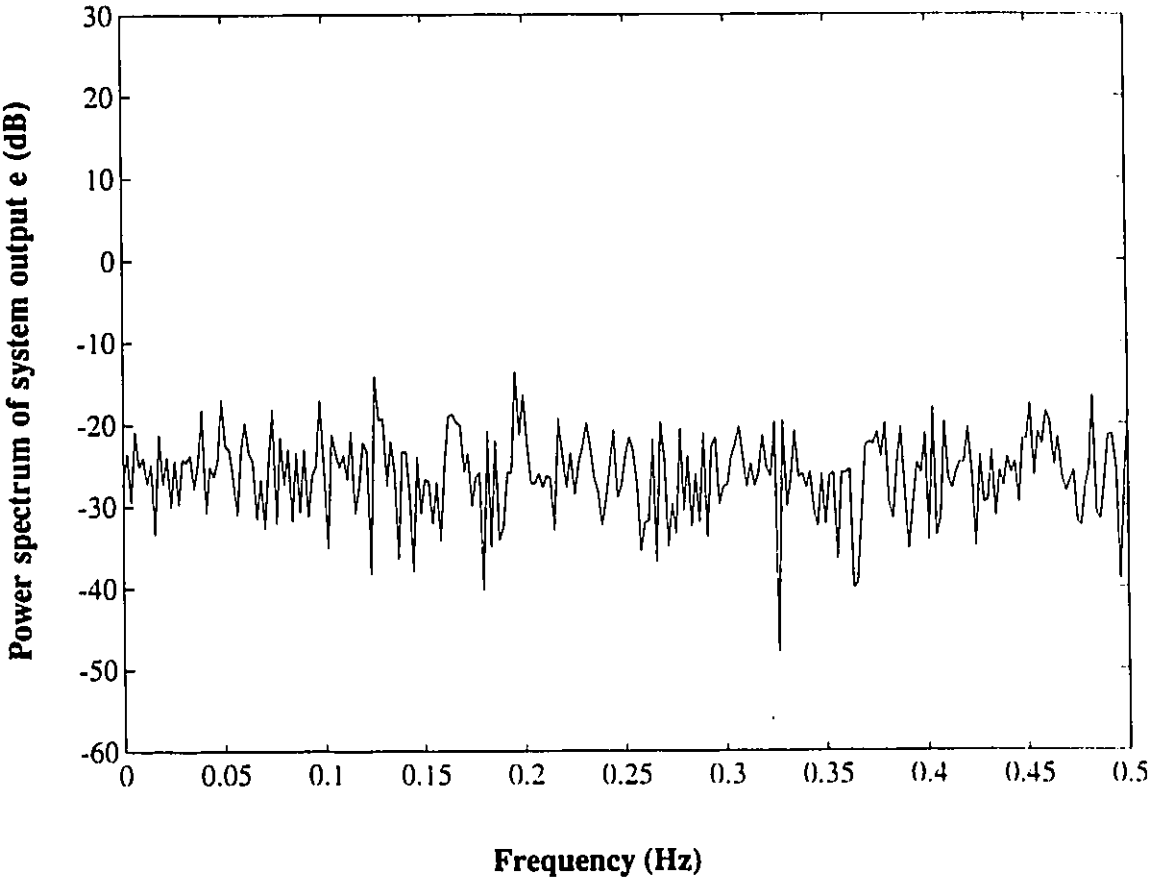

Figure 4.4.4 Power spectrum of subbanded AIC with both filter bank and adaptive part modulated (R1=4, R2=8). (b) system output with the sinusoidal interference being cancelled.

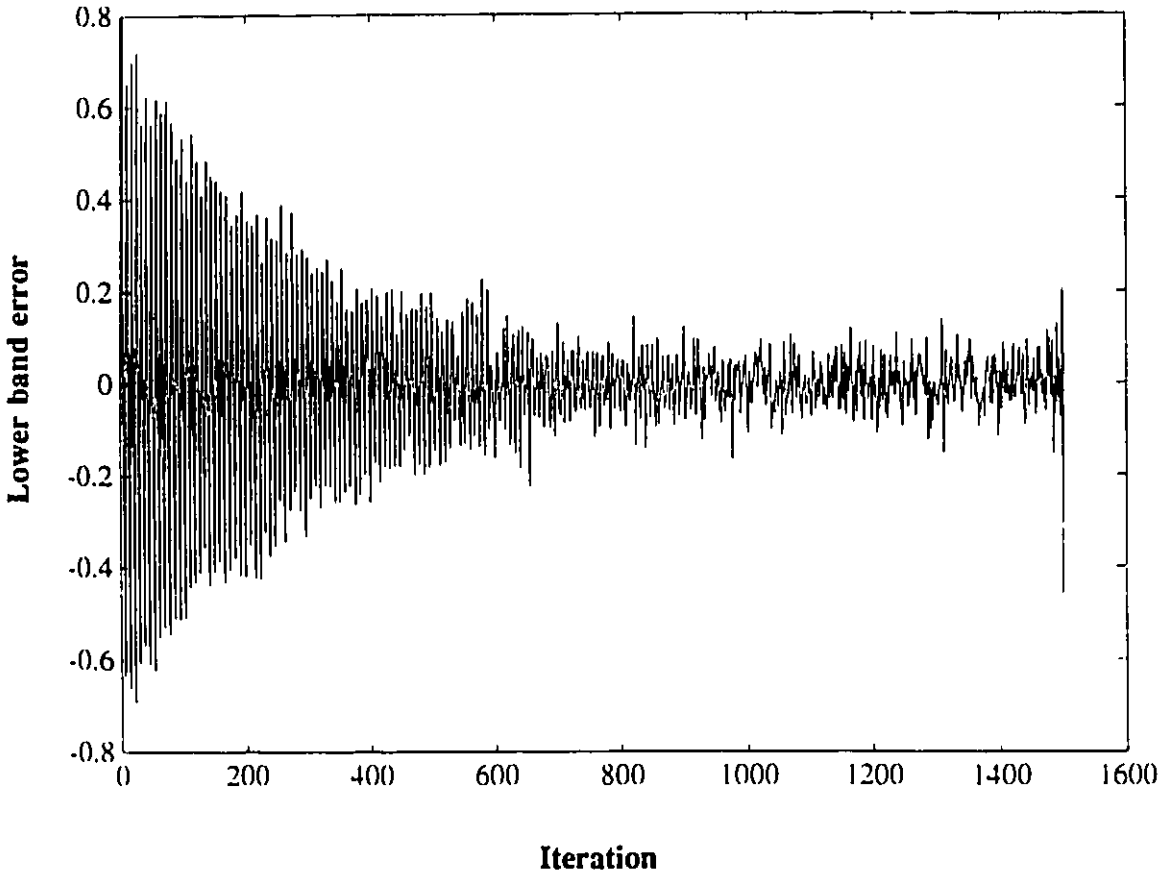

Figure 4.4.5 Subbanded AIC with both filter bank and adaptive part modulated (R1=16, R2=8). (a) time evolution of lower band error signal.

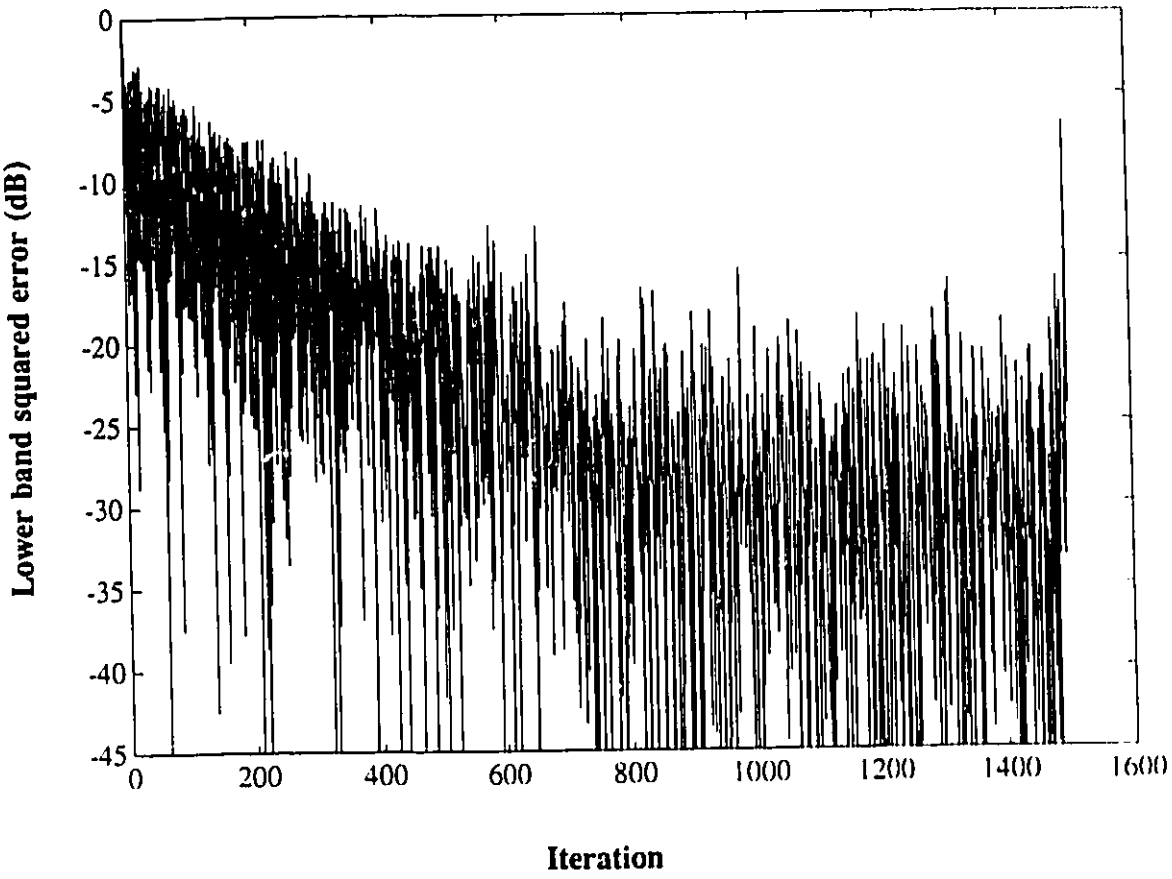

Figure 4.4.5 Subbanded AIC with both filter bank and adaptive part modulated (R1=16, R2=8). (b) time evolution of lower band squared error.

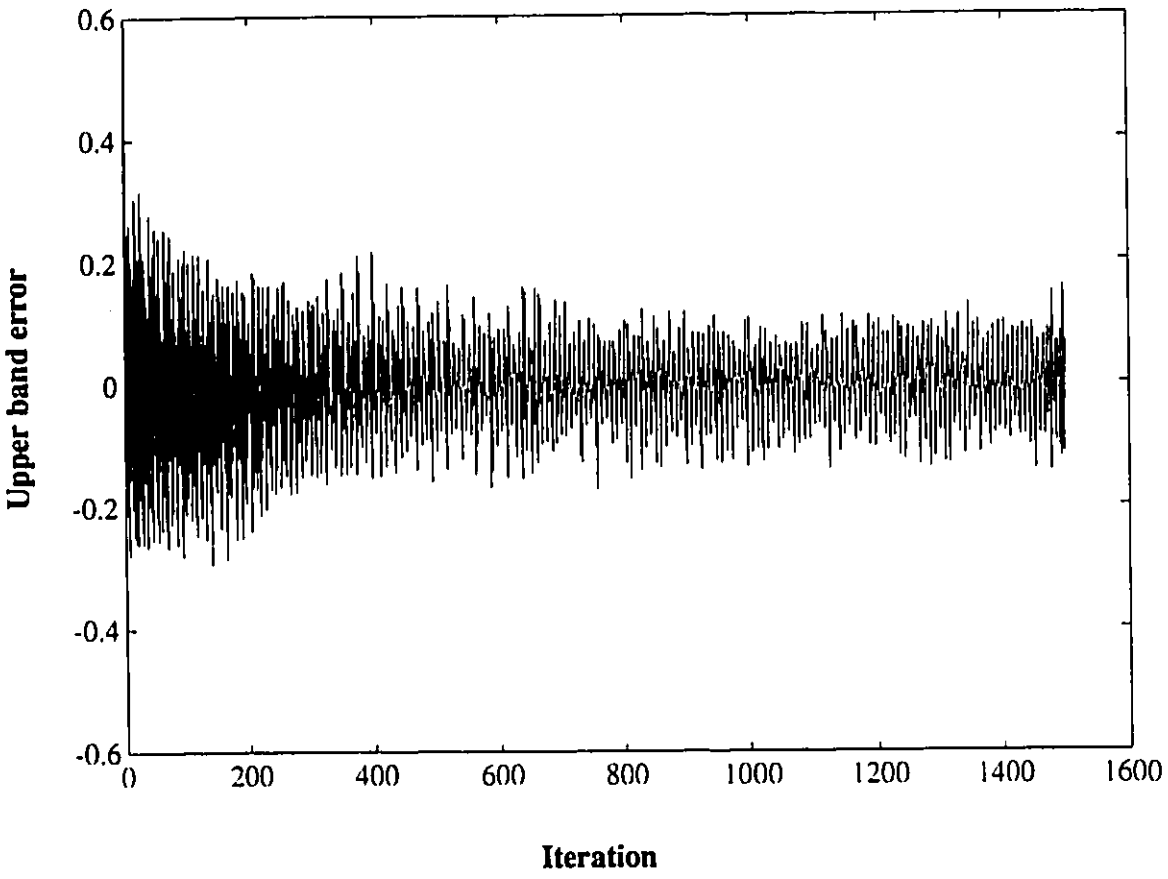

Figure 4.4.5 Subbanded AIC with both filter bank and adaptive part modulated (R1=16, R2=8). (c) time evolution of upper band error signal.

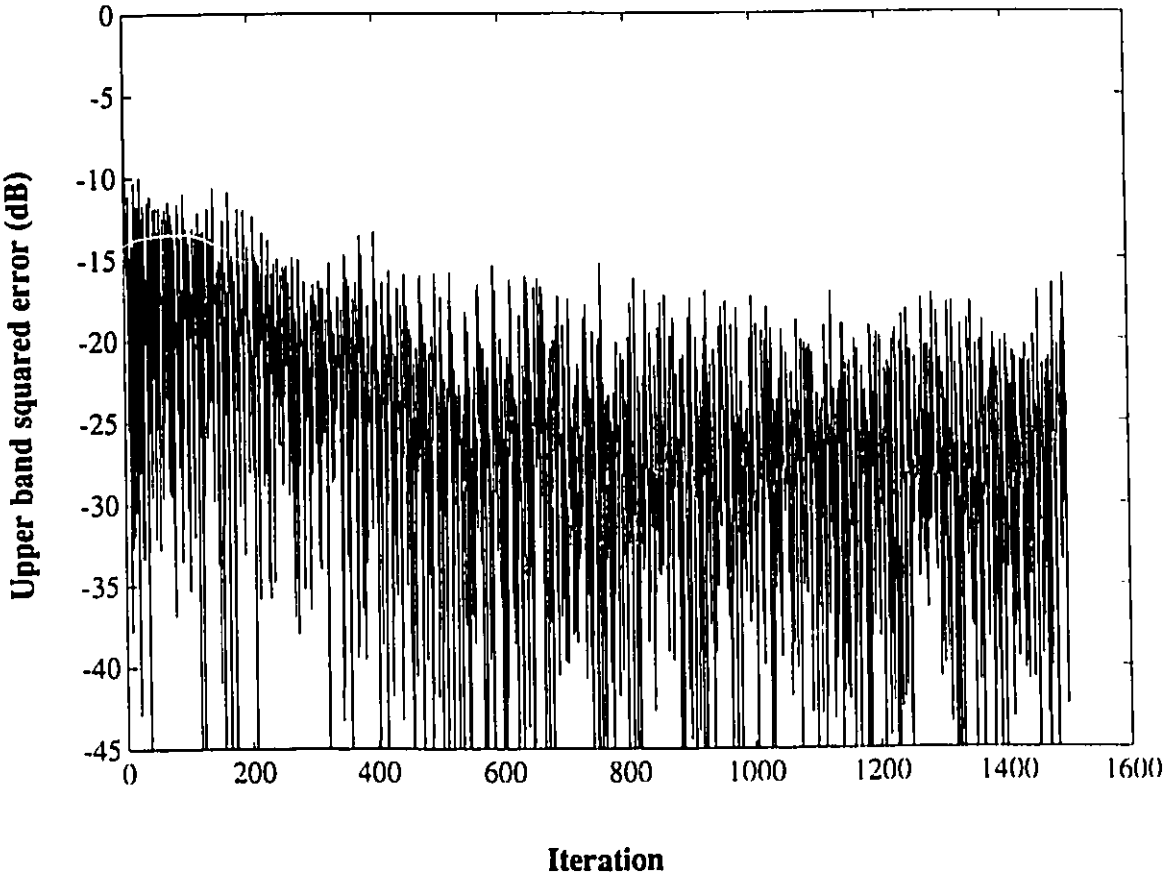

Figure 4.4.5 Subbanded AIC with both filter bank and adaptive part modulated (R1=16, R2=8). (d) time evolution of upper band squared error.

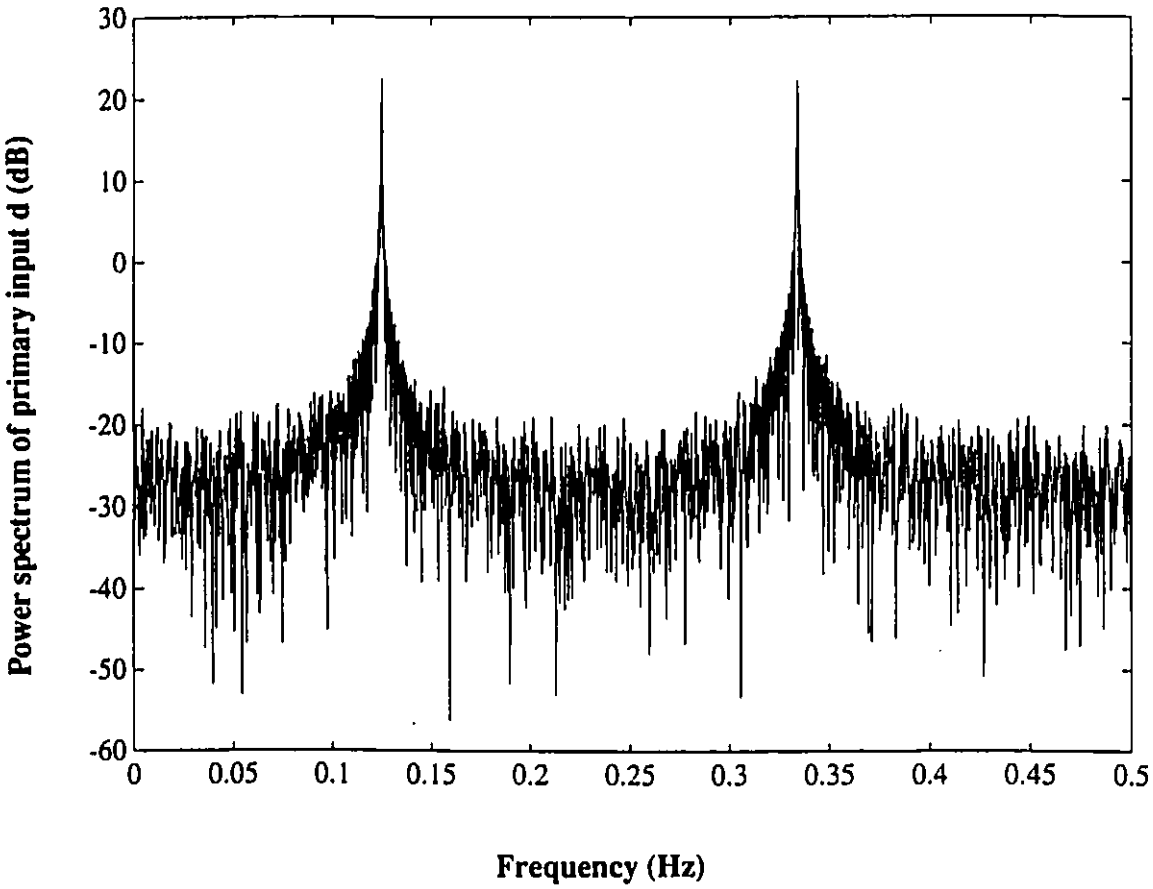

Figure 4.4.6 Power spectrum of subbanded AIC with both filter bank and adaptive part modulated (R1=16, R2=8). (a) primary input -- a combination of a Gaussian white noise as signal and two sinusoidal signals at 1/8Hz and 3/9Hz as noise.

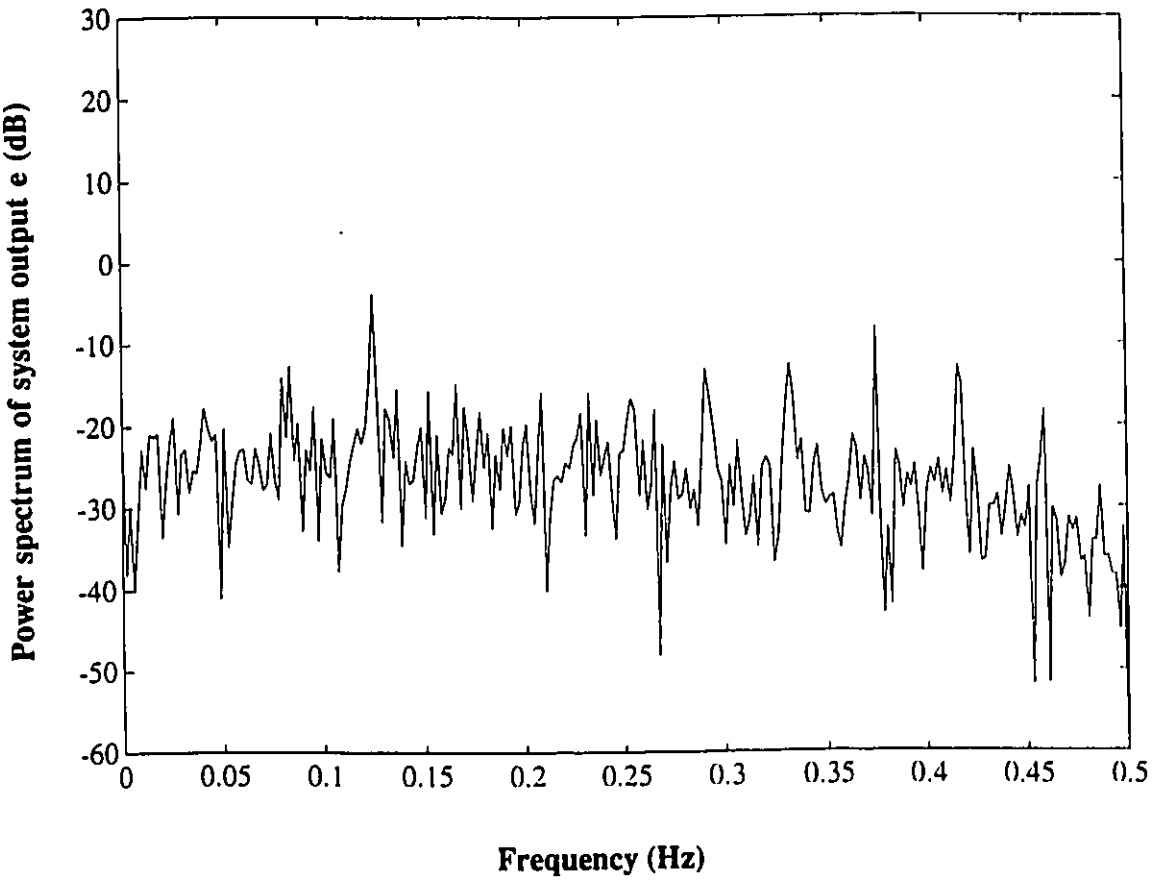

Figure 4.4.6 Power spectrum of subbanded AIC with both filter bank and adaptive part modulated (R1=16, R2=8). (b) system output with the sinusoidal interference being cancelled.

4.5 Conclusions

In this chapter, we propose the use of sigma-delta modulation implementations in subbanded adaptive interference cancellation. Two cases have been discussed, first when only the adaptive section is modulated, then when the whole system is modulated.

The simulation results show that modulated (partially or fully) subbanded adaptive interference cancellers can provide significant interference power reduction at a low cost compared to the conventional non-modulated structure. The savings are achieved by virtue of the fact that the modulators transfer the full-precision regular-rate PCM signals into 1-bit high-rate stream. All the signal processing being conducted on this 1-bit sequence requires very low precision adders working at higher speed. Thus, we are basically trading costly full-accuracy regular-rate of multipliers for much less expensive single-bit high-speed adders, that are needed for both FIR filtering and adaptive filtering operations.

It is also worth noting that depending on the application, the input signal may already be in the sigma-delta modulated format (as the output of a sigma-delta modulated A/D converter [R. W. Adams 1986] [V. Friedman 1989] [D. R. Welland 1989]). Processing this signal directly would provide further savings by eliminating the need to reconvert it to PCM format. In the proposed fully sigma-delta modulated structure, maintaining the sigma-delta modulated format throughout provides further saving for the oversampling ratio change as explained in section 3.3. Moreover, in most real applications, the actual impulse response length of the conventional adaptive filter in each band is very long, the modulated subbanded adaptive interference cancellers would be expected to be more cost-efficient then. We are able

to verify the performance of this system providing similar performance as the conventional one from the perspective of cancellation.

However, another important point illustrated by the simulation results is that the sigma-delta modulated implementation of the adaptive section results in slower convergence, i.e. more iterations compared with the conventional structure. The fully sigma-delta modulated system requires even more iterations. It is essential to note that a larger number of iterations does not automatically imply a longer convergence time in general. What we need to compare is the actual convergence time rather than the number of iterations, since the time needed for individual iterations for the above three structures is very different.

In our application, in order to get one system output per iteration, the partially modulated structure needs more full-precision multiplications compared to the fully modulated structure. And the conventional case needs even more. The multiplication generally takes longer time than the addition operation. Thus, though fully modulated structure requires more addition operations and more iterations to converge, it is quite possible that it can require less time to converge to the steady state. Based on the above, we believe sigma-delta modulated implementation of interference cancellation is a very efficient option.

5 Performance of Modulated Subbanded Adaptive Noise Cancellation

In this chapter, we consider the sigma-delta modulated subbanded ANC structure as an extension of the AIC application in chapter 4. The performance evaluation of the proposed structure is made based on simulation results.

First, we start with the results for the conventional non-modulated structure in section 5.1 as comparison criterion. Next, the subbanded structure with only the adaptive filtering part modulated is considered in section 5.2. Section 5.3 studies the case when both filter bank and adaptive part are modulated. Conclusions based on these results are summarized in section 5.4.

5.1 Conventional Subbanded ANC without Modulation (R1=R2=1)

The basic subbanded noise canceller is shown in Fig.5.1.1. The simulation results of this structure will be used as reference in comparison with the performance of the proposed systems in sections 5.2 and 5.3. The simulation data is provided as follows.

The sampling frequency is normalized to f_N=1Hz. The reference signal x(n) is a Gaussian white noise bandlimited up to 1/2Hz with zero mean. Its standard deviation is set to 1/4 of the full dynamic range [-1, 1], which gives the value of 0.5. This satisfies the 4σ rule suggested by [W. R. Bennett 1948] so that the probability of the sampled signal exceeding the dynamic range can be considered as zero. In the rare

case where the signal exceeds the dynamic range, it can be truncated to 1 or -1 depending on its sign.

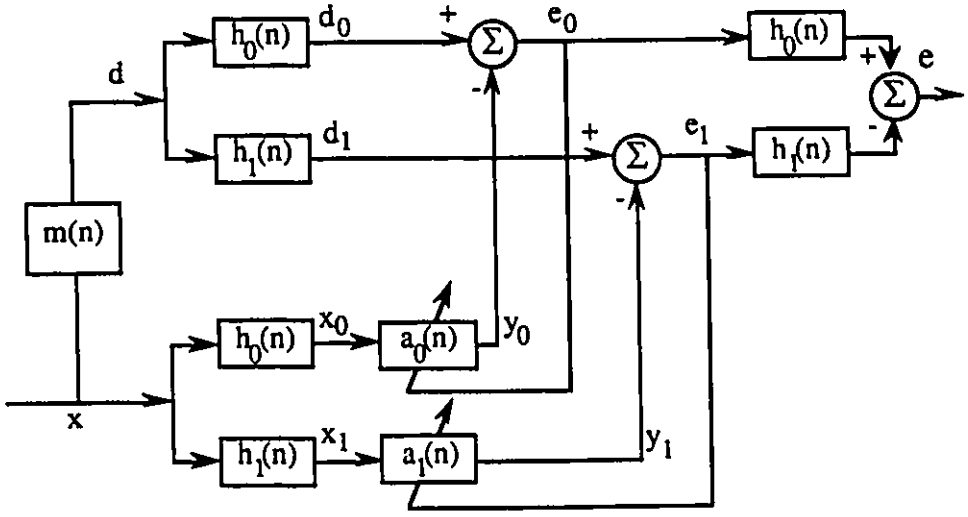

Figure 5.1.1 Conventional subbanded adaptive noise cancellation.

The primary signal d(n) is a corrupted version of the reference input x(n) by an unknown system which is modeled by a multiband FIR filter m(n) with 39 taps. The impulse response and frequency response of filter m(n) are shown in Fig.5.1.2(a) and (b) respectively. The analysis filter bank is made up from lowpass and highpass filters $h_0(n)$ and $h_1(n)$, the same as those used for AIC case in chapter 4. The length of the adaptive filter in each band is chosen to be 9. The learning curve is obtained by taking the average over an ensemble of several simulations. The number of simulations is indicated on each graph. Each simulation starts with the same initial coefficients a=0 for different inputs.

Fig.5.1.3(a) and (c) show the lower band and upper band error signal respectively. Fig.5.1.3(b) and (d) show the lower band and upper band learning curves of conventional ANC.

Notice that two types of input signals are used: bandlimited white Gaussian noise x(n) (reference input) with zero mean and 0.5 standard deviation, and bandlimited noise d(n) (primary input) passed through the multiband filter. The signal part in primary input d is assumed to be zero. Since there is no noise floor setup as for AIC case, we can not use illustrative input and output power spectrums to evaluate the system performance. So for this ANC system, the performance is measured in terms of adaptivity [R. Riegler 1973][T. Tjahjadi 1985], which is defined as

$$\text{ADAPTIVITY (dB)} = 10 \log_{10} (\bar{e}_k^2 / \bar{d}_k^2)$$

i.e. the ratio of the steady-state error variance $\bar{e}_k^2$ to the primary signal variance $\bar{d}_k^2$. It indicates how well the adaptive system can model the unknown system, the smaller its value, the better the quality of cancellation.

For the conventional case, the primary signal variance $\bar{d}_k^2$ =0.4512, and the variance of the steady-state system output e(n) is $\bar{e}_k^2$=0.0025, providing an adaptivity of -19.1dB.

Table 5.1 Complexity for conventional subbanded ANC per band (R1=R2=1).

		# of M(B3R0)	# of A(B4R0)
AFB & SFB	x_0	64/2	64-1
	d_0	64/2	64-1
	e	64/2	64-1
AF	filtering y_0	9	9-1
	updating a_0	9	9
total		114	206

Table 5.1 shows the complexity in terms of the number of adders and multipliers for subbanded ANC per band, where

M(B3 R0)--- full precision multiplier with B3 bits and R0=1 (at Nyquist rate)

A(B4 R0)--- full precision adder with B4 bits and R0=1 (at Nyquist rate)

The cost function is

C=P*114*B3+206*B4

where P is the cost ratio between a multiplier and an adder, both are 1-bit precision and at the Nyquist rate, the same as for the AIC case.

In this structure, since the length of adaptive filters is small, the system complexity is basically that of the filter bank part. In real applications where the unknown system is much more complicated than m(n), the length of the adaptive filter needs to be correspondingly larger so as to simulate the operation of the unknown system. Thus more complexity will be added due to the adaptive part.

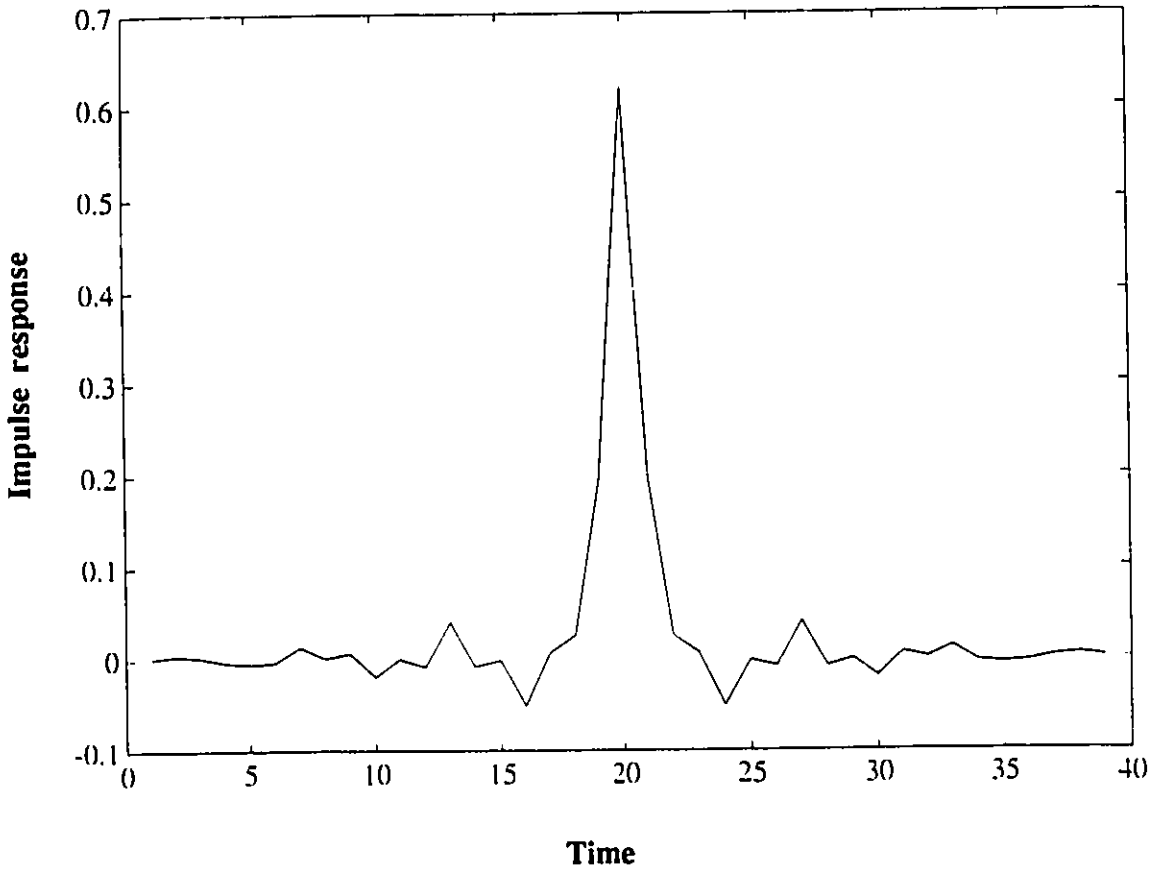

Figure 5.1.2 Multiband FIR filter as unknown system. The filter length is 39. (a) impulse response.

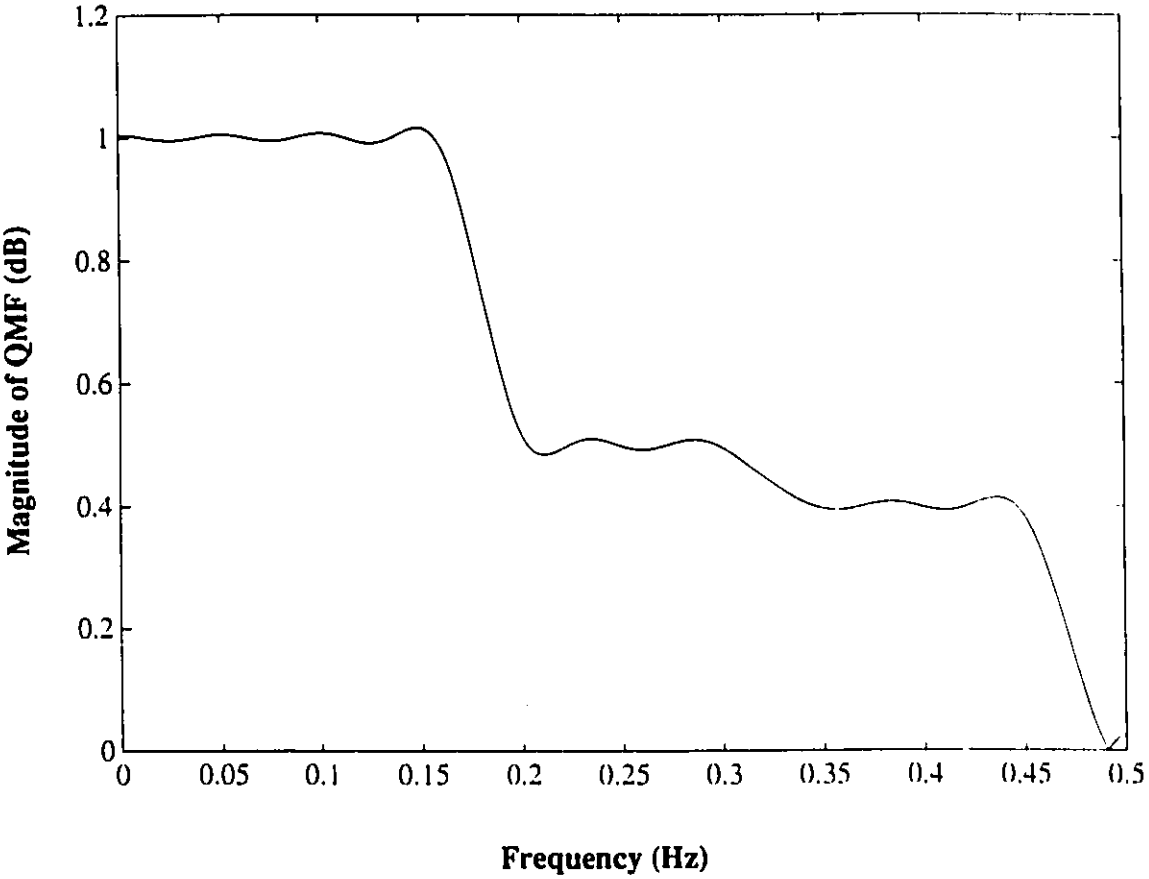

Figure 5.1.2 Multiband FIR filter as unknown system. The filter length is 39. (b) frequency response.

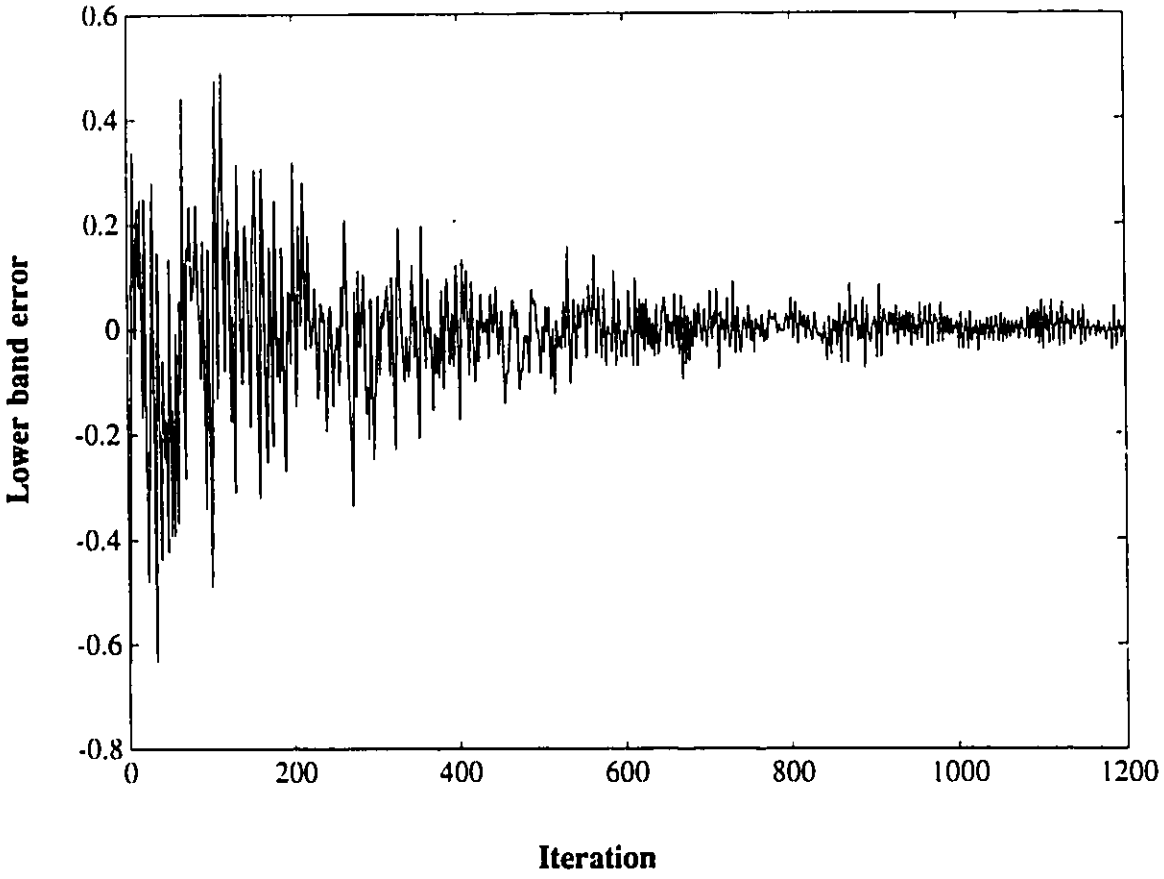

Figure 5.1.3 Conventional subbanded ANC (R1=1, R2=1).
(a) time evolution of lower band error signal.

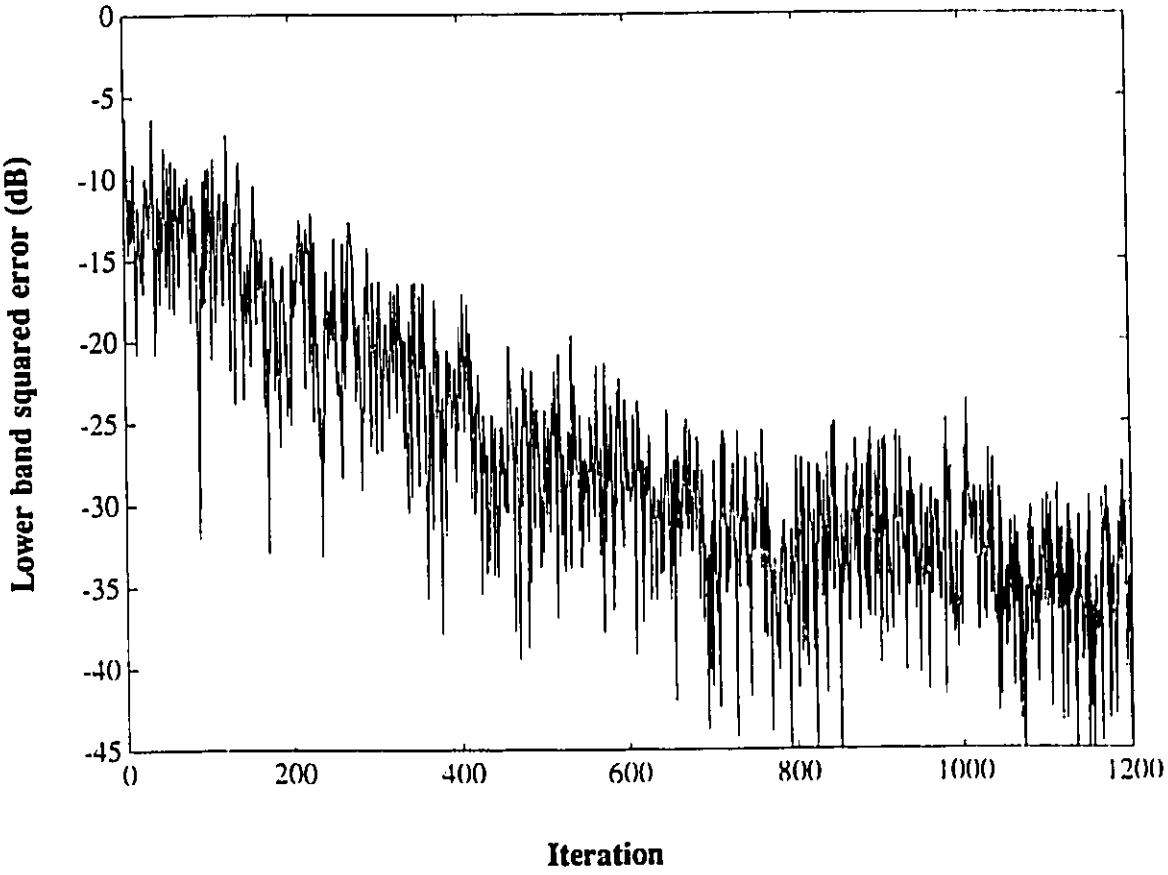

Figure 5.1.3 Conventional subbanded ANC (R1=1, R2=1).
(b) time evolution of lower band squared error. Average of 3 simulations.

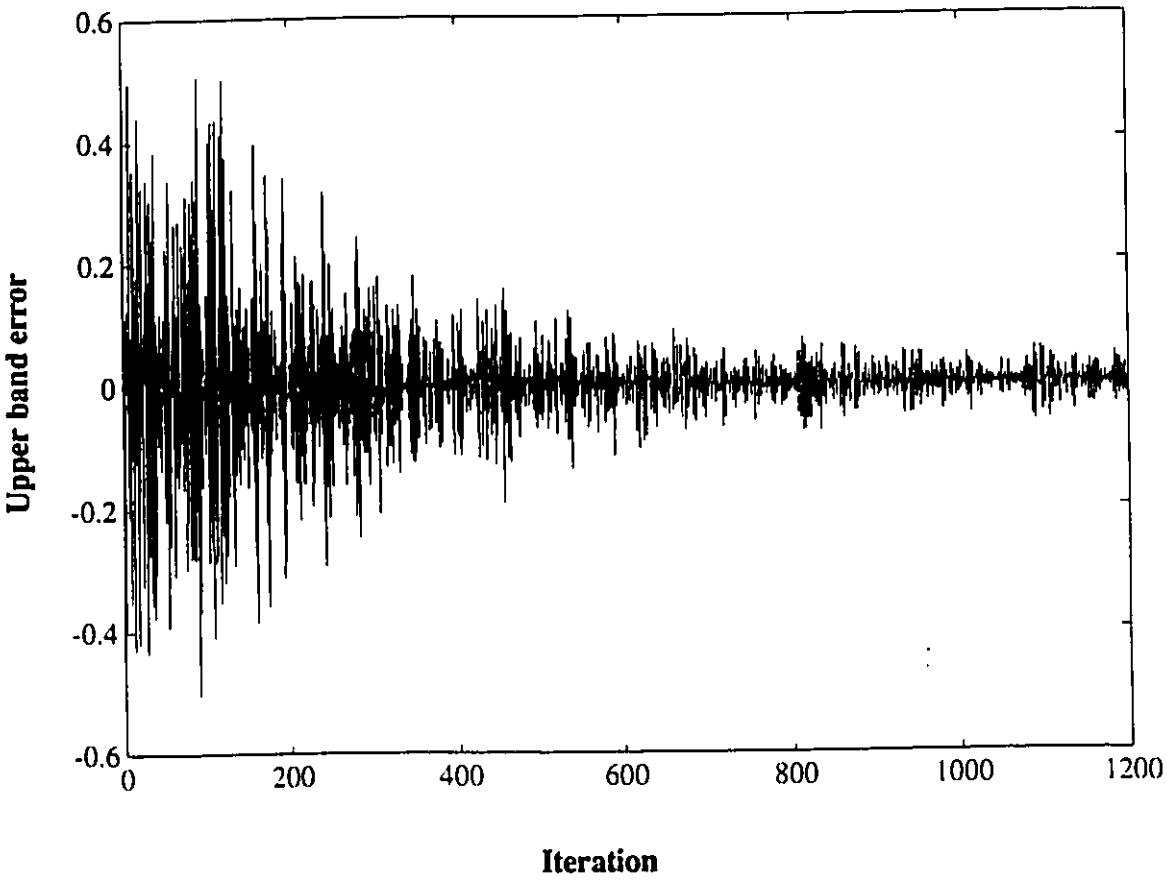

Figure 5.1.3 Conventional subbanded ANC (R1=1, R2=1).
(c) time evolution of upper band error signal.

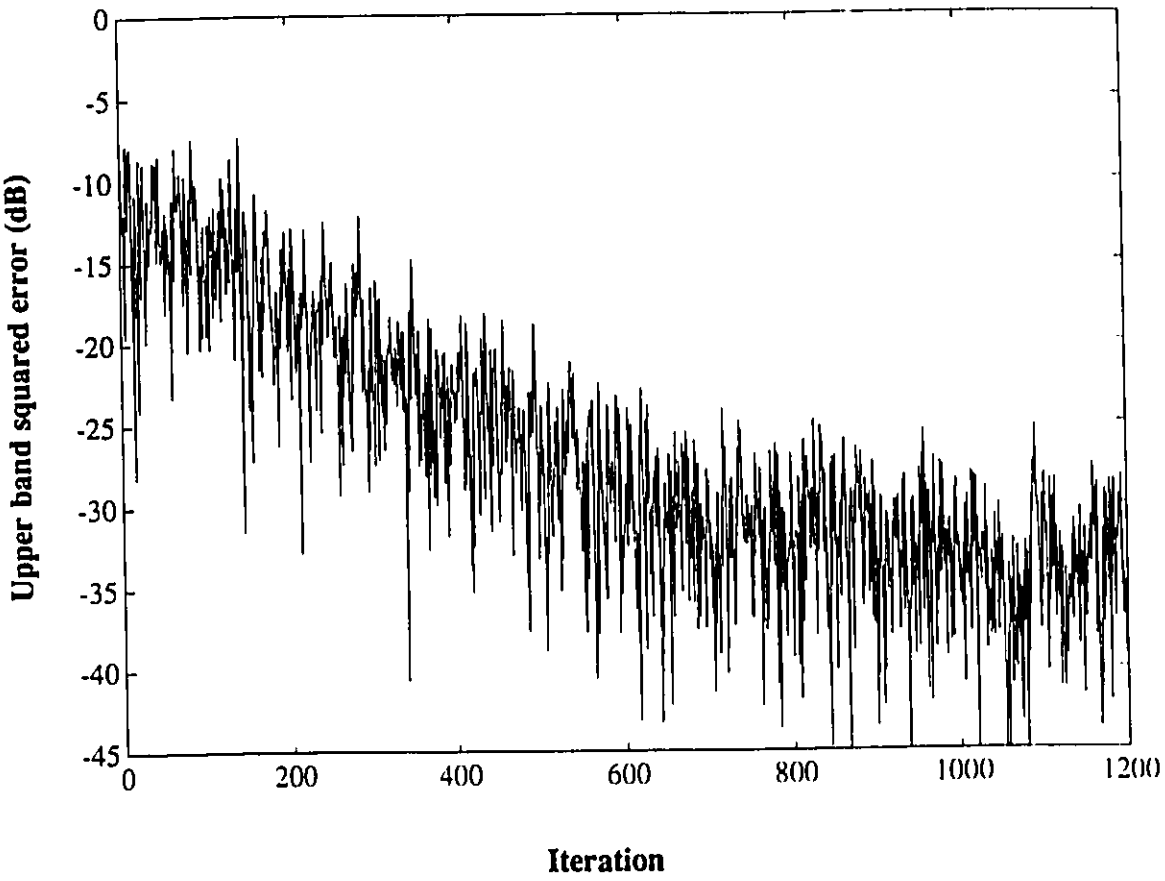

Figure 5.1.3 Conventional subbanded ANC (R1=1, R2=1).
(d) time evolution of upper band squared error. Average of 3 simulations.

5.2 Proposed Partially Modulated Subbanded ANC (R1=1,R2=64)

Fig.5.2.1 shows the detailed block diagram of the proposed modulated system with the adaptive section sigma-delta modulated.

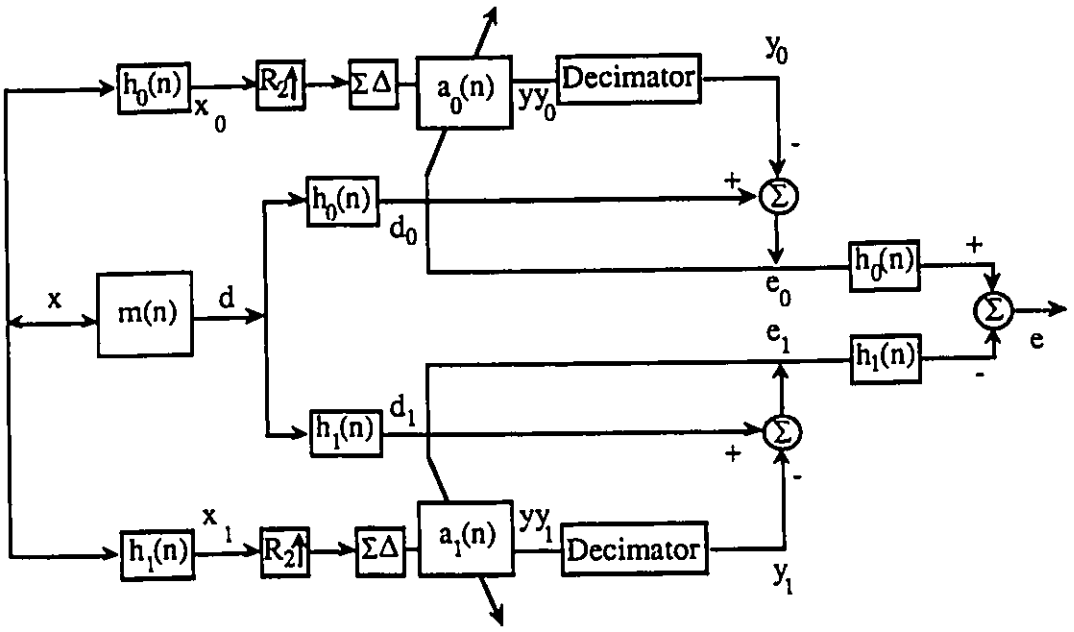

Figure 5.2.1 Partially modulated subbanded adaptive noise cancellation.

Simulation data is the same as in section 5.1. The oversampling ratio for modulated adaptive filtering part R2 is 64. Fig.5.2.2(a) and (c) show the lower band and upper band error signal respectively. Fig.5.2.2(b) and (d) show the lower band and upper band learning curves of partially modulated subbanded ANC. Based on these results, the primary signal variance $\bar{d}_k^2$ =0.4512, and the variance of the steady-state system output e(n) is $\bar{e}_k^2$=0.00655, providing an adaptivity of -14.9dB, compared to -19dB for the conventional case.

Table 5.2 shows the complexity in terms of the number of adders and multipliers for one band, where the decimator for the adaptive part is referred as to decimator A and

M(B3 R0)--- full precision multiplier with B3 bits and R0=1 (at Nyquist rate)

A(B4 R0)--- full precision adder with B4 bits and R0=1 (at Nyquist rate)

A(B4 R2)--- full precision adder with B4 bits and R2=64

Since the complexity of the system is mostly due to the filter bank, we can see that minor saving was achieved due to eliminating the multipliers in the filtering part while additional multiplications were required for the decimators. As explained in [T. Saramaki 1988 1990], more efficient multiplier-free implementation can be used for decimator. This will result in considerably less complexity than that in Table 5.2. Besides, in cases where the adaptive filters have more taps, the savings will be more significant.

Table 5.2 Complexity for partially modulated subbanded ANC per band (R1=1, R2=64).

		# of M(B3R0)	# of A(B4R0)	# of A(B4R2)
AFB	x_0	64/2	64-1	0
&	d_0	64/2	64-1	0
SFB	e	64/2	64-1	0
AF	filtering y_0	0	0	9-1
	updating a_0	0	9	0
	decimator D	100/2	100/2	100/2
total		146	248	58

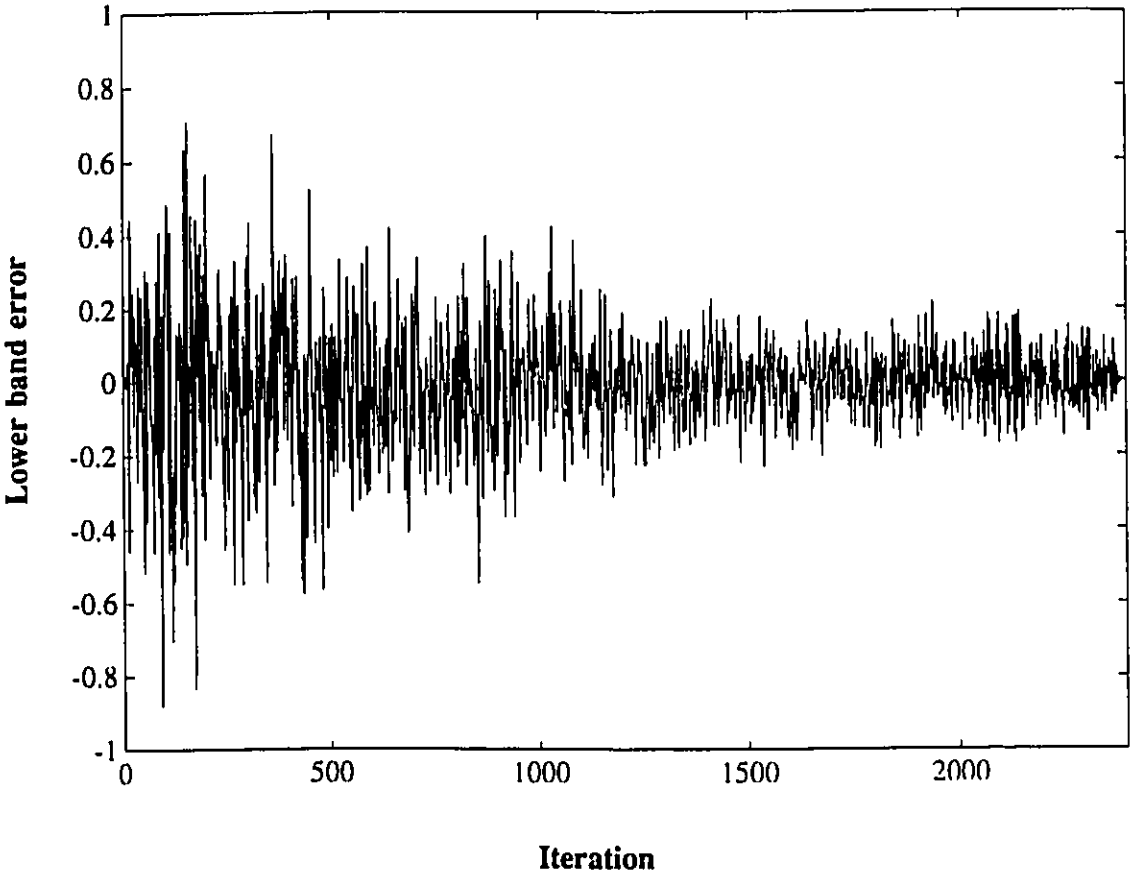

Figure 5.2.2 Subbanded ANC with adaptive part modulated (R1=1, R2=64). (a) time evolution of lower band error signal.

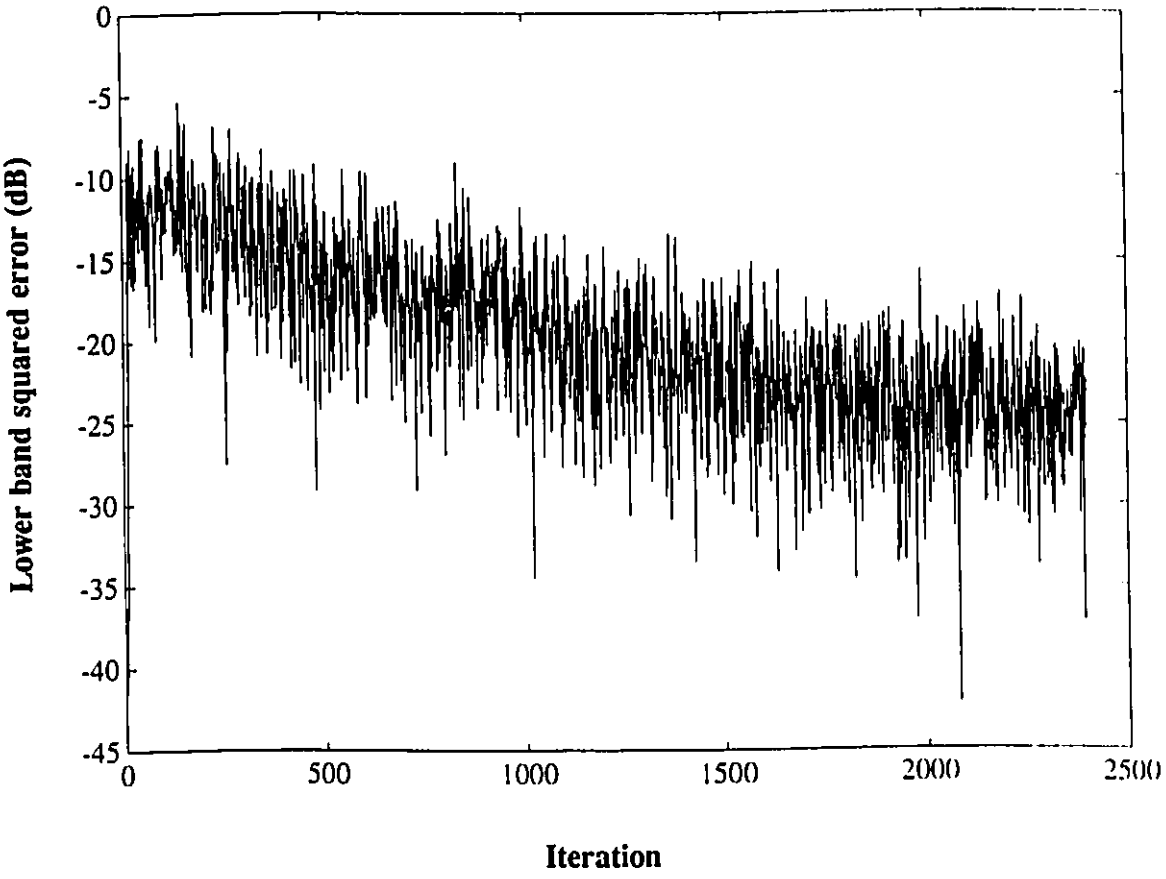

Figure 5.2.2 Subbanded ANC with adaptive part modulated (R1=1, R2=64). (b) time evolution of lower band squared error. Average of 6 simulations.

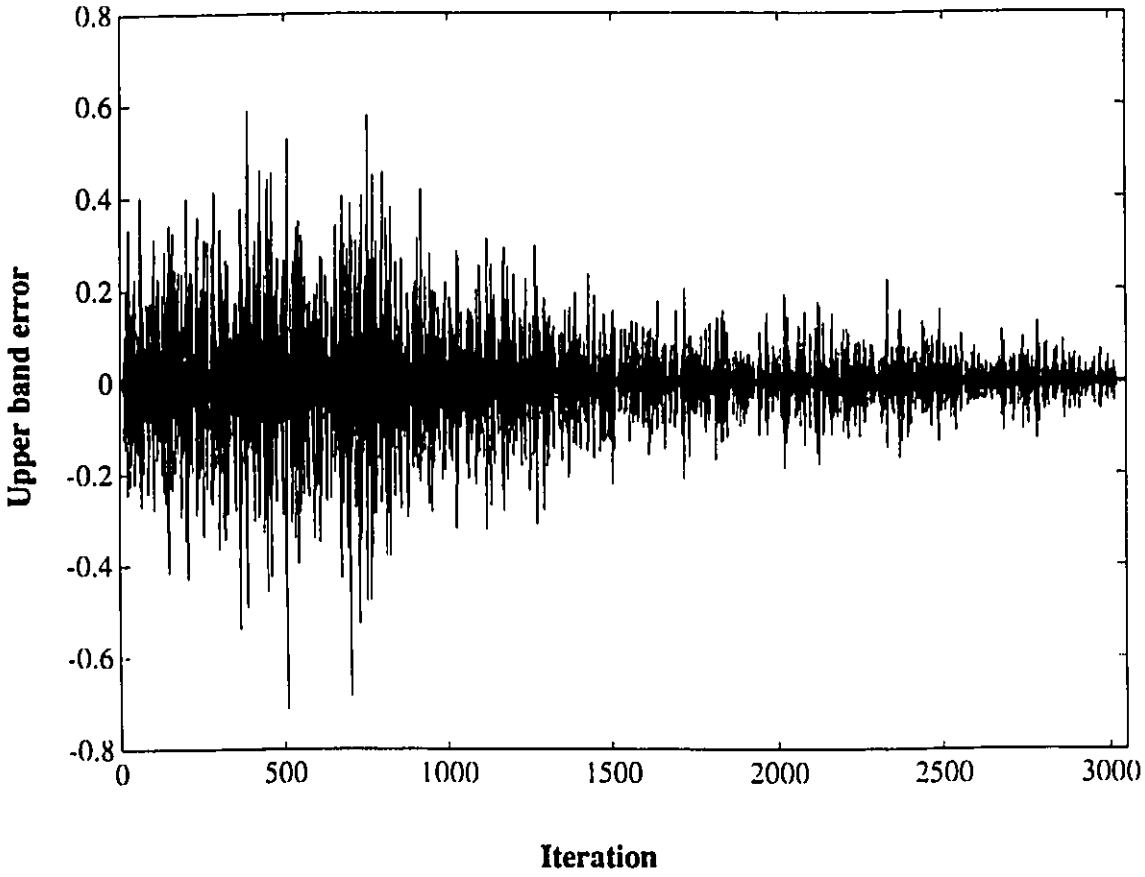

Figure 5.2.2 Subbanded ANC with adaptive part modulated (R1=1, R2=64). (c) time evolution of upper band error signal.

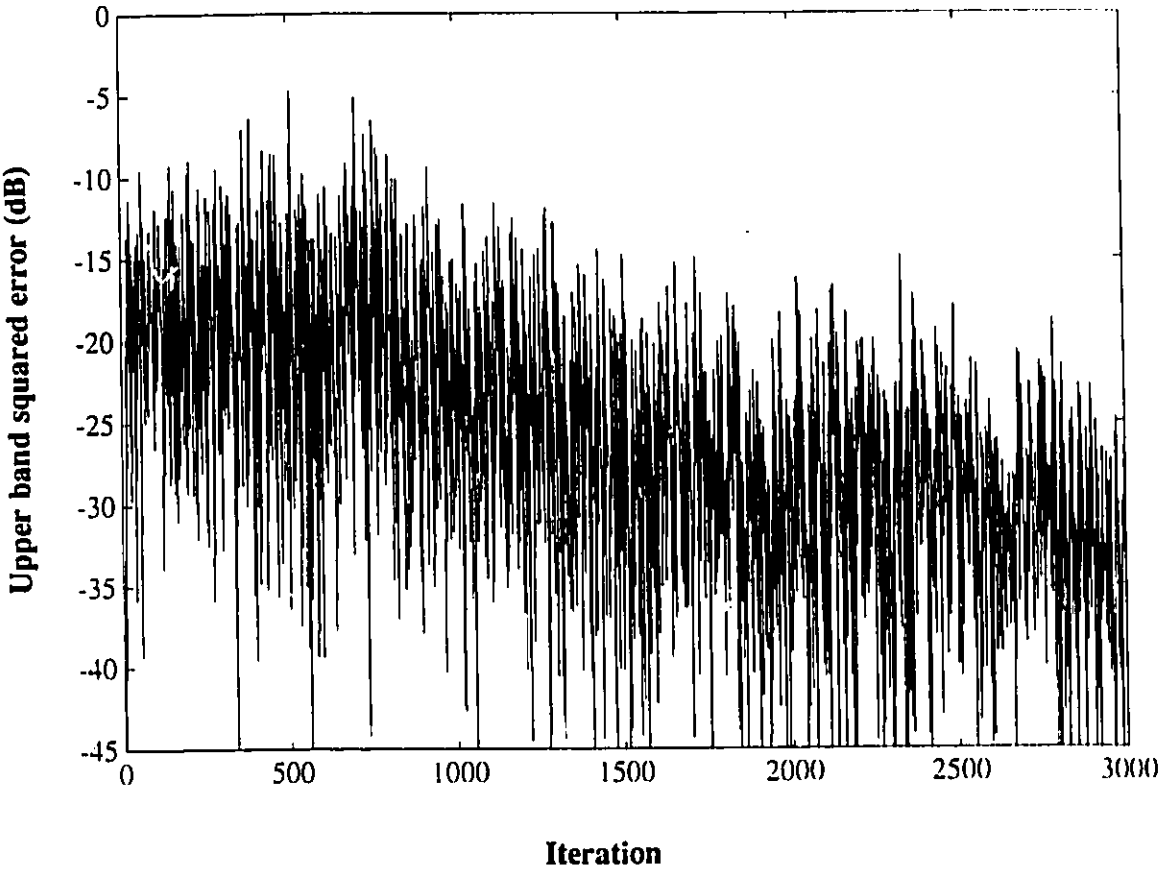

Figure 5.2.2 Subbanded ANC with adaptive part modulated (R1=1, R2=64). (d) time evolution of upper band squared error. Average of 3 simulations.

5.3 Proposed Fully Modulated Subbanded ANC (R1=64,R2=64)

From section 5.2, one can see that the majority of multipliers are in the filter bank section. Thus, implementing this part in sigma-delta modulated format has the potential of providing significant savings. This case is studied in this section. Fig.5.3.1 shows the block diagram of the proposed fully modulated subanded ANC.

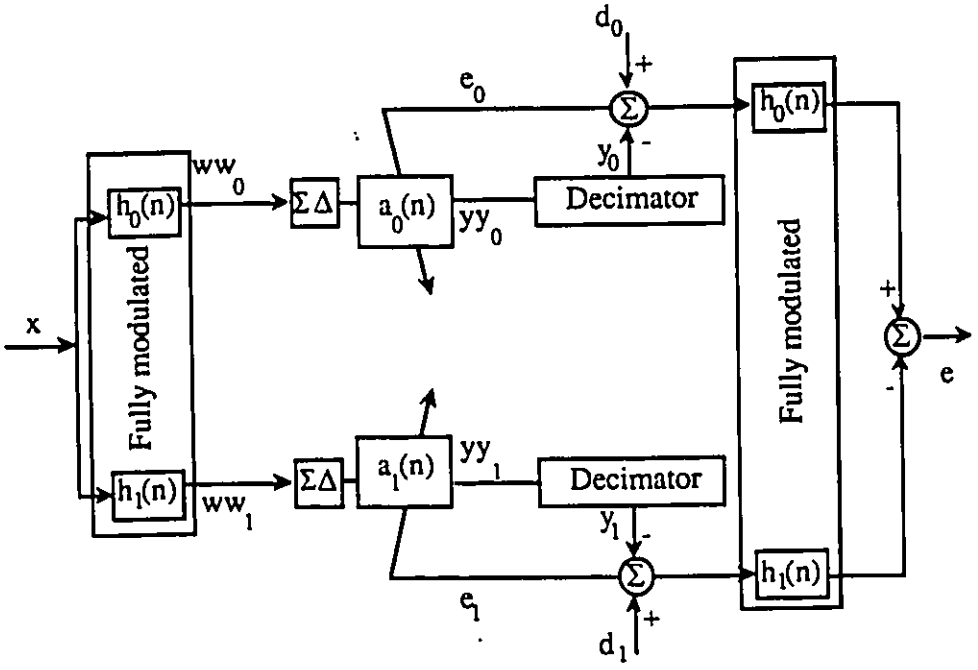

Figure 5.3.1 Fully modulated subbanded adaptive noise cancellation.

Recall that the typical oversampling ratio is from 64 to 1024. If we perceive the operation of the adaptive filtering at steady state as no more than usual FIR filtering operation, we believe it is reasonable to choose R1 and R2 to be the same value which has been shown as case 2 in section 3.3. Comparing Fig.5.3.1 and Fig.4.3.1, we note that because R1 and R2 are the same, the R1/R2 downsampler in Fig.4.3.1 for AIC

case is not needed. Besides, the lowpass filter in between can be eliminated as well, since the high-frequency modulation noise can be filtered out at the final stage by decimator after adaptive processing.

Fig.5.3.2(a) and (c) show the lower band and upper band error signals respectively. Fig.5.3.2(b) and (d) show the lower band and upper band learning curves of the fully modulated subbanded ANC. Based on these results, the primary signal variance $\bar{d}_k^2$=0.4512, and the variance of the steady-state system output is $\bar{e}_k^2$ =0.00695, providing an adaptivity of -14.6dB. This is basically the same as was obtained in section 5.2 indicating that implementing the filter bank in sigma-delta modulated format did not result in any obvious deterioration in the performance.

Table 5.3 Complexity for fully modulated subbanded ANC per band (R1=R2=64).

		# of M (B3R0)	# of A (B4R0)	# of A (B4R2)	# of A (B1R1)
AFB & SFB	x_0	0	0	0	64-1
	d_0	0	0	0	64-1
	e	0	0	0	64-1
	decimator B	100/4	100/4	100/4	0
AF	filtering y_0	0	0	9-1	0
	updating a_0	0	9	0	0
	decimator D	100/2	100/2	100/2	0
total		75	84	83	189

Table 5.3 shows the complexity in terms of the number of adders and multipliers for one band, where decimator B denotes the decimator in synthesis filter bank (SBF) part, decimator D denotes the decimator in adaptive filtering part and M(B3 R0)--- full precision multiplier with B3 bits and R0=1 (at Nyquist rate)

M(B2 R2)--- multibit multiplier with B2=$\log_2$64+1=7bits and R2=64

A(B4 R1)--- full precision adder with B4 bits and R1=64

A(B4 R0)--- full precision adder with B4 bits and R0=1 (at Nyquist rate)

A(B4 R2)--- full precision adder with B4 bits and R2=64

A(B1 R1)--- 1-bit adder with B1=1bit and R1=64

The cost function is

C=P*75*B3*R0+84*B4*R0+83*B4*R2+189*B1*R1

As the fully modulated AIC, the ANC structure proposed here contains modulated filter bank part (both AFB and SBF) and modulated adaptive filtering part. For the adaptive filter part, regular FIR filter is needed as decimator (referred to as decimator D). Filter with the same specifications (referred to as decimator B) is needed for SFB part to fulfill 64:1 decimation. Since the decimation can be performed at the system output as opposed to at the output of each band, in other words, one filter rather than two is needed for SFB, only one half of the filter complexity should be calculated as far as the complexity per band in concerned in Table 5.3.

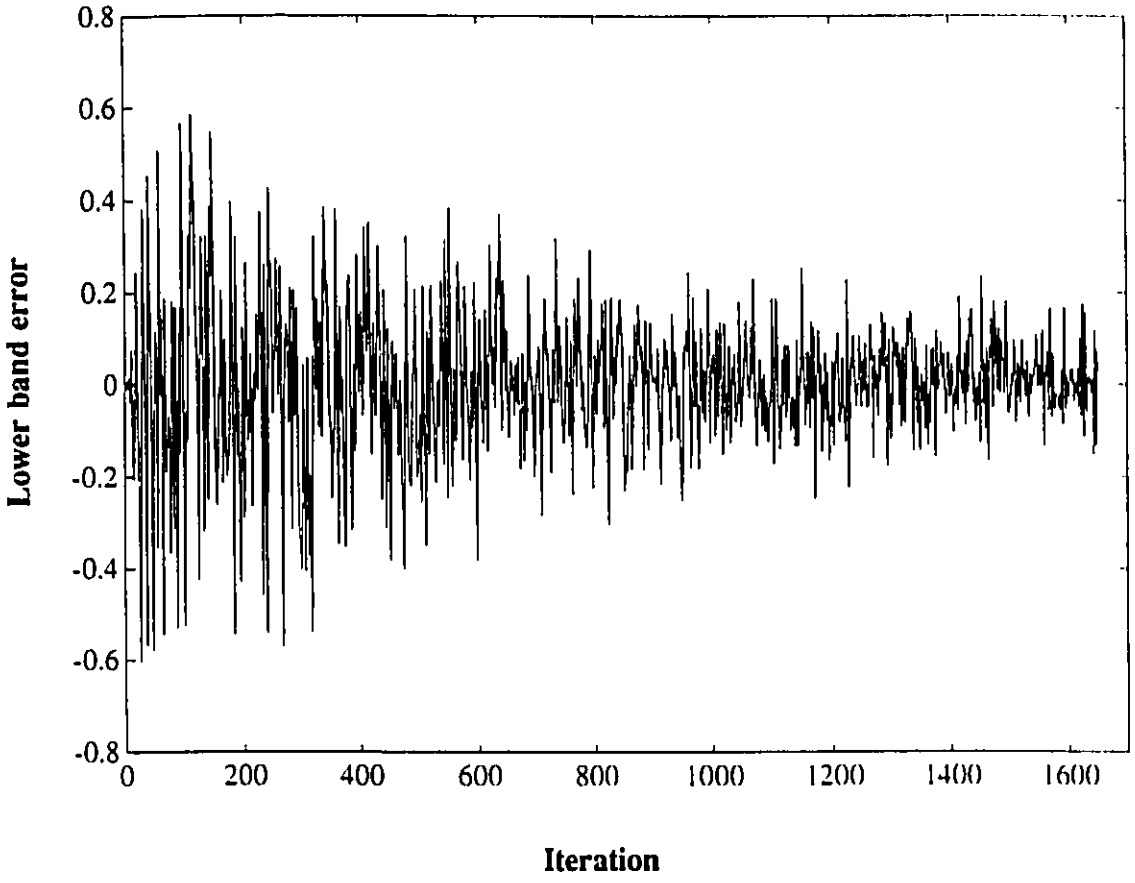

Figure 5.3.2 Subbanded ANC with both filter bank and adaptive part modulated (R1=64, R2=64). (a) time evolution of lower band error signal.

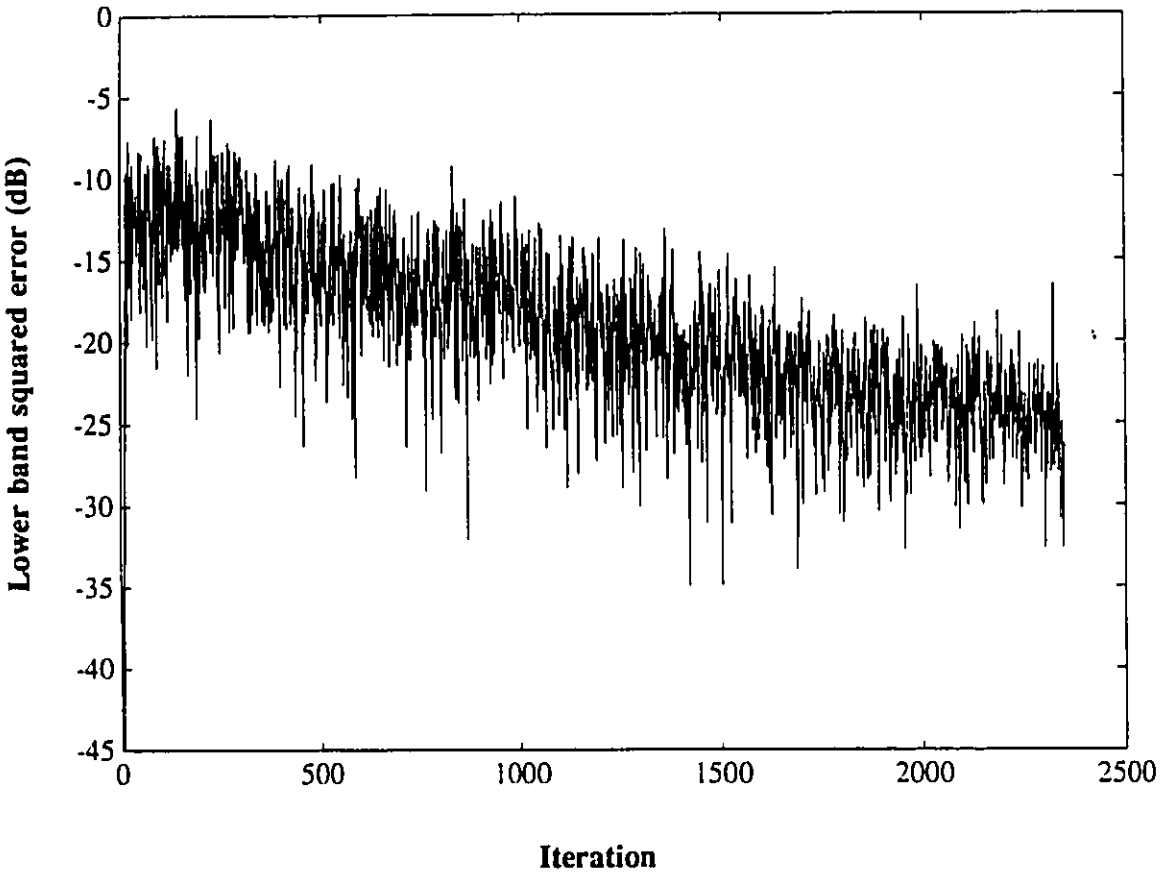

Figure 5.3.2 Subbanded ANC with both filter bank and adaptive part modulated (R1=64, R2=64). (b) time evolution of lower band squared error. Average of 6 simulations.

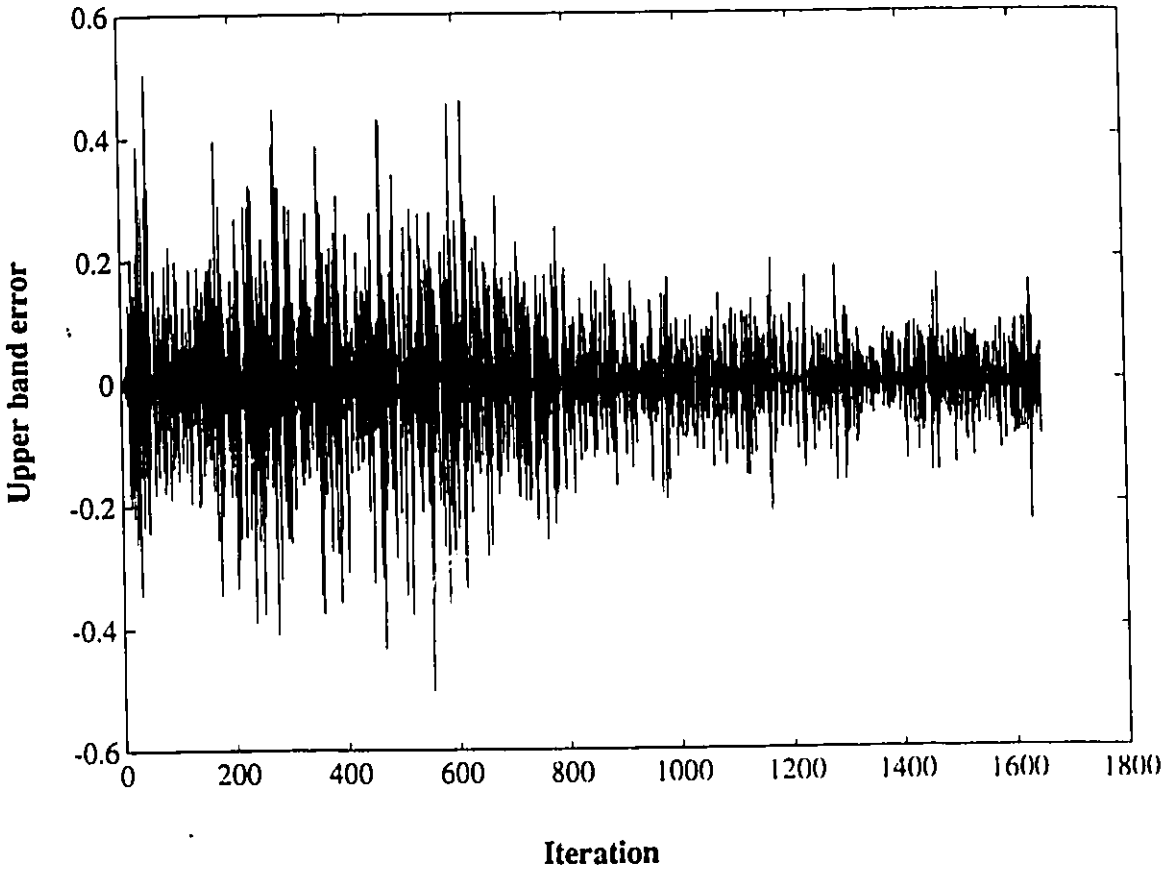

Figure 5.3.2 Subbanded ANC with both filter bank and adaptive part modulated (R1=64, R2=64). (c) time evolution of upper band error signal.

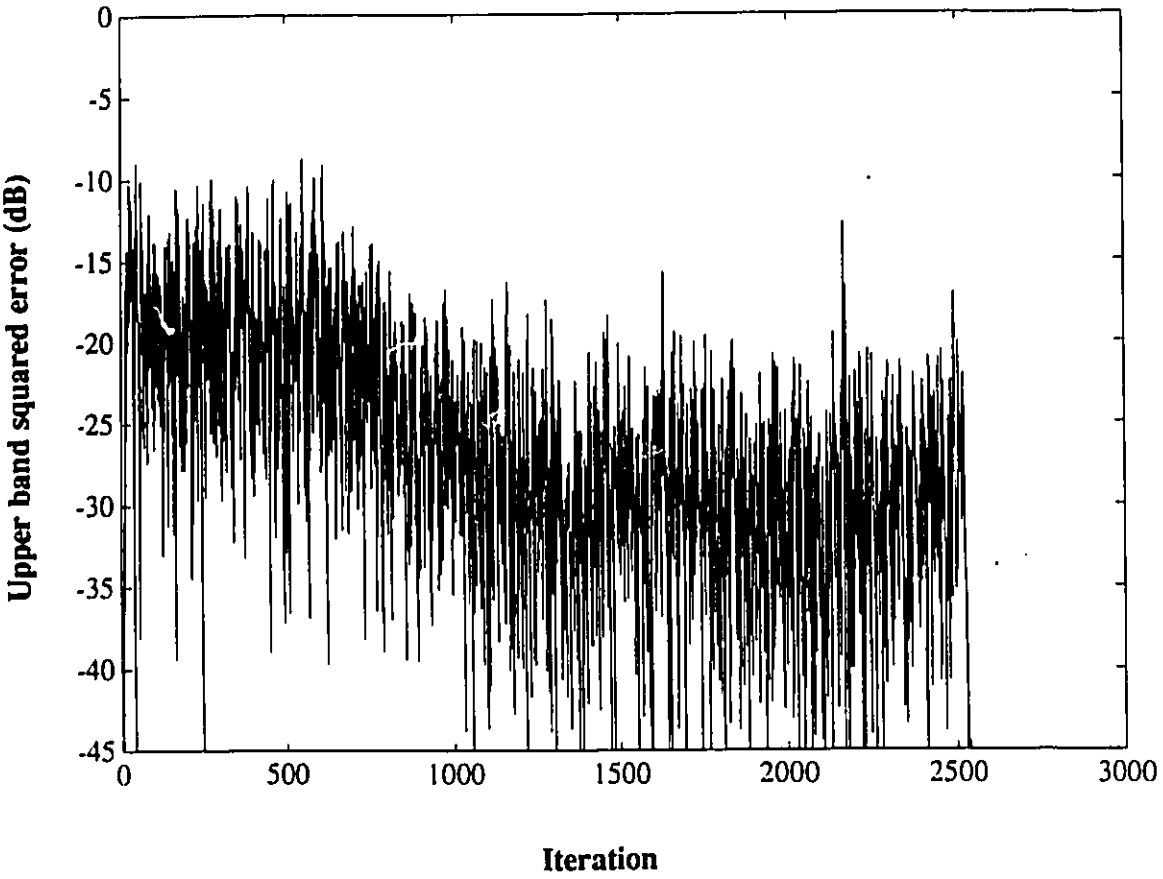

Figure 5.3.2 Subbanded ANC with both filter bank and adaptive part modulated (R1=64, R2=64). (d)Time evolution of upper band squared error. Average of 2 simulations.

5.4 Summary of Observations

The comparison of experimental results shows that fully modulated subbanded adaptive noise canceilers can provide noise power reduction at a generally lower cost. As in the AIC case in chapter 4, this is due to maintaining the signal in 1-bit high-rate sigma-delta modulated representation, thus trading speed for resolution in such a way that the signal can be processed with much less full-precision multiplication operations. As can be seen from the results, while we cannot say that there is more room for complexity reduction in the filter bank implementation than in the adaptive section, but we can argue that it is more desirable to use the fully modulated structure because by keeping the oversampling ratios the same, we do not add any complexity for decimation.

However, in applications where the length of adaptive filters needed is high, the partially sigma-delta modulated structure can provide more savings compared to the conventional structure, since it would require the same decimator.

We also note that for modulated (partially or fully) case, the noise power reduction is lower than that for the conventional structure. The adapitivity of the modulated ANC system is large than the conventional system. One effective way to improve this performance is to increase R1 and R2. From previous simulation results for modulated adaptive filtering using fixed optimal coefficients value, it is known that higher oversampling ratio will offer higher signal-to-noise ratio. This is generally true for both fixed and adaptive FIR filtering.

The quality of the overall performance also depends on the decimator used. For AIC, comb filter was found to be sufficient as decimator for the adaptive filtering part. As we can see from the results here, a comb-filter-based decimator is not functional for such applications as noise cancellation. The input in this case is white noise

covering the whole baseband rather than a "narrowband" sinusoidal interference, which is not very sensitive to the substantial magnitude drooping at the upper region of baseband caused by the frequency response of the comb filter.

We recall from chapter 3 that the performance of noise canceller was limited by the decimator quality. Raising R to 100 could not compensate for the lower quality decimation provided by the comb filter. A good quality decimator is essential for ANC. This obviously limits the potential for savings in the noise cancellation case compared to the interference cancellation, if the decimator is regularly built.

Finally, we note that again, convergence here is slower than for the conventional case, requiring more iterations to reach steady state. However, each iteration would arguably require less time due to the reduced complexity of the required multipliers.

6 Conclusion and Areas of Further Research

In this thesis, we have presented a performance analysis of sigma-delta modulated implementation of subbanded adaptive interference/noise cancellation system. Based on this study, we can conclude that there is significant potential for complexity reduction resulting from maintaining the low-precision high-speed format of the signal. These savings, associated cost and parameters affecting the system performance are summarized as follows.

1. Cost reduction

Generally speaking, sigma-delta modulation technique can bring savings in hardware complexity for the subbanded AIC and ANC. The performance of the several modulated structures is illustrated and analyzed in this thesis. The cost reduction for AIC is more significant compared to the ANC, because of the advantage of using comb-filter-based decimators. But overall, both structures will show much more achievements in savings when used in real applications as discussed before.

2. Convergence speed

Generally, sigma-delta modulated implementation of AIC/ANC requires more iterations to reach steady state. However, this does not necessarily imply longer time to converge, since each iteration for conventional, partially and fully modulated structures involves totally different number of multiplication and addition operations of very different complexity. For the modulated implementation, very few time-consuming full-precision multipliers are needed. Thus, its actual convergence speed is much faster than indicated by the number of iterations. On the other hand,

conventional implementations require fewer iterations, with every iteration requiring full-precision multiplications, i.e. more time per iteration.

3. Decimator quality

The requirements for the quality of the decimator are quite different for the modulated AIC and ANC. While a very economical comb filter is sufficient for AIC, a much better quality FIR decimator is essential for ANC. The cost for decimator is the predominate factor for the proposed modulated structure, assuming all decimators are implemented in direct form. In fact, the cost function we derived in chapter 4 and 5 is based on this direct form implementation of linear phase FIR filter as decimator in our simulation, which is the most costly implementation.

However, all these filters can be built in multiplier-free multistage system as suggested in [T. Saramaki 1988 1990]. In this case, the proposed structure will show greater superiority compared to the conventional structure.

4. Oversampling ratio

For ANC case, the oversampling ratios used are R1=64, R2=64. These are the lower bounds of the typical 64-1024 range suggested in [J. C. Candy 1976]. The performance for modulated ANC will be definitely improved if we bring R1 and R2 higher. [P. W. Wong 1990-1] gave several examples of the sigma-delta modulated system and concluded that the signal-to-noise ratio of such a system is proportional to the logarithm of the oversampling ratio.

Since the implementation with very high oversampling ratio might be unrealizable for high frequency applications, the multistage or multiloop sigma-delta modulator could present an interesting alternative to raising the oversampling ratio [W. Chou 1989][J. C. Candy 1985][N. He 1988]. For a given signal-to-noise ratio, filters implemented using multistage or multiloop sigma-delta modulation can be realized with a significantly smaller oversampling ratio and thus further reduce the overall complexity.

For further research, the following points are suggested:

1. Efficient implementation of decimation filter

As we have mentioned previously, more cost reduction can be achieved by efficiently implementing the decimation filter. [T. Saramaki 1988 1990] are valuable references for the research area covered in this thesis. They provide implementations using a series of coefficients represented by combinations of powers of two, resulting in the decimation filter requiring no general multipliers. We could expect a significantly lower overall cost once the complexity of the decimator is reduced.

2. Multistage or multiloop sigma-delta modulation

Multistage or multiloop sigma-delta modulator has gained more and more attention recently, since better performance can be achieved while keeping the oversampling ratio low, thus the system can operate in a relatively low speed environment. This method has the great potential to implement the proposed AIC/ANC system in a cost efficient way.

3. Multiband filter bank realization

In this thesis, extensive discussions focus on the most basic QMF filter bank structure. To broaden the scope of this thesis, investigations can be conducted on multiband system or even on other filter bank system prototypes if necessary.

References

[Adams 86] R. W. Adams, "Design and Implementation of an Audio 18-Bit Analog-to-Digital Converter Using Oversampling Techniques," *Journal of the Audio Engineering Society*, vol. 34, pp. 153-166, 1986.

[Ardalan 87] S. H. Ardalan and J. J. Paulos, "An Analysis of Nonlinear Behavior in Delta- Sigma Modulator," *IEEE Transaction on Circuits and Systems*, vol. CAS-34, pp. 593-603, 1987.

[Barnwell 81] T. P. Barnwell, "An Experimental Study of Sub-band Codec Design Incorporating Recursive Quadrature Filters and Optimum APDCM," *International. Conference on Acoustics, Speech and Signal Processing*, pp. 808-811, 1981.

[Candy 76] J. C. Candy, Y. Ching and D. S. Alexander, "Using Triangularly Weighted Interpolation to get 13-bit PCM from a Sigma-Delta Modulator," *IEEE Transaction on Communications*, vol. COM-24, pp. 1268-1275, 1976.

[Candy 85] J. C. Candy, "A Use of Double Integration in Sigma-Dleta Modulation," *IEEE Transaction on Communications*, vol. COM-33, pp. 249-258, 1985.

[Candy 86] J. C. Candy, "Decimation for Sigma Delta Modulation," *IEEE Transaction on Communications*, vol. COM-34, pp. 72-76, 1986.

[Candy 91] J. C. Candy and G. C. Temes, *Oversampling Delta-Sigma Data Converters*, IEEE Press, Piscataway, New Jersey, 1991.

[Chou 89] W. Chou, P. W. Wong and R. M. Gray,"Multi-stage Sigma-Delta Modulation," *IEEE Transaction on Information Theory*, vol. IT-35, pp. 784-796, 1989.

[Chu 84] S. Chu and C. S. Burrus, "Multirate Filter Design Using Comb Filters," *IEEE Transaction on Circuits and Systems*, vol. CAS-31, pp. 913-924, 1984.

[Crochiere 83] R. E. Crochiere and L. R. Rabiner, Multirate Digital Processing, Prentice-Hall, Englewood Cliffs, New Jersey, 1983.

[Croisier 76] A. Crosier, D. Esteban and C. Galand, "Perfect Channel Splitting by Use of Interpolation/ Decimation/ Tree Decomposition Technique," *IEEE International Symposium on Information, Circuits and Systems*, 1976.

[Defraeye 85] P. Defraeye, D. Rabaey, W. Roggeman, J. Yde and L. Kiss, "A 3-μm CMOS Digital Codec with Programmable Echo Cancellation and Gain Setting," *IEEE Journal on Solid-State Circuits*, vol. SC-20, pp. 679-687, 1985.

[Dijkstra 87] E. Dijkstra, M. Degrauwe, J. Rijmenants and O. Nys, "A Design Mothodology for Decimation Filters in Sigma Delta A/D Converters," *IEEE Proceeding of the International Symposium on Circuits and Systems*, 1987.

[Dijkstra 88] E. Dijkstra, L. Cardoletti, O. Nys, C. Piguet, and M. Degrauwe, "Wave Digital Decimation Filters in Oversample A/D Converters," *IEEE Proceeding of the International Symposium on Circuits and Systems*, 1988.

[Esteban 81] D. Esteban and C. Galand, "HQMF: Halfband Qudrature Mirror Filters," *International. Conference on Acoustics, Speech and Signal Processing*, pp. 220-223, 1981.

[Friedman 89] V. Friedman, D. M. Brinthaupt, D. P. Chen, T. W. Deppa, J. P. Elward, Jr., E. M. Fields, J. W. Scott and T. R. Wiswanathan, "A Dual-Channel Voise-Band PCM Codec using Sigma-Delta Modulation Technique," *IEEE Journal of Solid-State Circuits*, vol. SC-24, pp. 274-280, 1989.

[Goodman 77] D. J. Goodman and M. J. Carey, "Nine Digital Filters for Decimation and Interpolation," *IEEE Transaction on Acoustics, Speech and Signal Processing*, vol. ASSP-25, pp. 121-126, 1977.

[Goubran 86] R. A. Goubran, R. Hebert and H. M. Hafey, "Background Acoustic Noise Reduction in Mobile Telephony," *IEEE 36th Vehicular Technology Conference*, pp. 72-76, 1986.

[Goulding 90] M. M. Goulding and J. S. Bird, "Speech Enhancement for Mobile Telephone," *IEEE Transactions on Vehicular Technology*, vol. 39, pp. 316-326, 1990.

[Gray 87] R. M. Gray, "Oversampled Sigma-Delta Modulation," *IEEE Transaction on Communications*, vol. COM-35, pp. 481-489, 1987.

[Gray 89-1] R. M. Gray, "Spectral Analysis of Quantization Noise in a Single-Loop Sigma-Delta Modulator with DC Input," *IEEE Transaction on Communications*, vol. 37, pp. 588-599, 1989.

[Gray 89-2] R. M. Gray, W. Chou and P. W. Wong, "Quantization Noise in Single-Loop Sigma-Delta Modulation with Sinusoidal Inputs," *IEEE Transaction on Communications*, vol. 37, pp. 956-968, 1989.

[Haykin 91] S. Haykin, *Adaptive Filter Theory*, Prentice-Hall, Englewood Cliffs, New Jersey, 1991.

[He 88] N. He, F. Kuhlmann and A. Buzo, "Double-Loop Sigma-Delta Modulation with DC Input," *IEEE Transaction on Communications*, vol. COM-38, pp. 487-495, 1990.

[Hebert 90] R. Hebert, R. A. Goubran and H. M. Hafey, "Analysis of Background Noise in Cars," *Canadian Conference on Electrical and Computer Engineering*, pp. 21.4.1-21.4.5, 1990.

[Jain 83] V. K. Jain and R. E. Crochiere, "A Novel Approach to the Design of Analysis/ Synthesis Filter Banks," *International. Conference on Acoustics, Speech and Signal Processing*, pp. 228, 1983.

[Johnston 80] T. D. Johnston, "A Filter Family Designed for Use in Quadrature Mirror Filter Banks," *International. Conference on Acoustics, Speech and Signal Processing*, pp. 291-294, 1980.

[Kellerman 85] W. Kellerman, "Kompensation Akustischer Echos in Frequenz-teilbandern," *Frequenz*, vol. 39, pp. 209-215, 1985.

[Kellerman 88] W. Kellerman, "Analysis and Design of Multirate Systems for Cancellation of Acoustical Echoes," *International. Conference on Acoustics, Speech and Signal Processing*, pp. 2570-2573, 1988.

[Leung 88] B. H. Leung, R. Neff, P. R. Gray and R. W. Brodersen, "Area-Efficient Multichannel Oversampled PCM Voise-Band Coder," *IEEE Journal of Solid-State Circuits*, vol. SC-23, pp. 1351-1357, 1988.

[Matsumoto 88] K. Matsumoto, E. Ishii, L. Yoshitate, K. Amano and R. W. Adams, "An 18-Bit Oversampling A/D Converters for Digital Audio," *ISSCC Digital Technical Papers*, pp. 202-203, 1988.

[Misawa 81] T. Misawa, J. E. Iwersen, L. J. Loporcaro and J. G. Ruth, "Single-Chip per Channel Codec with Filters Utilizing Δ-Σ Modulation,", *IEEE Journal on Solid-State Circuits*, vol. SC-16, pp. 333-341, 1981.

[Motorola] Motorola, "Principles of Sigma-Delta Modulation for A/D Converters", *Application Note.*

[Oppenheim 89] A. V. Oppenheim and R. W. Schafer, *Discrete-time Signal Processing*, Prentice-Hall, Englewood Cliffs, New Jersey, 1989.

[Riegler 73] R. Riegler and R. Compton, "An Adaptive Array for interference rejection," *Proceeding IEEE*, vol. 66, pp. 748-758, 1973.

[Saramaki 88] T. Saramaki and H. Tenhunen, "Efficient VLSI-Realizable Decimators for Sigma-Delta Analog-to-Digital Converters," *IEEE International Symposium on Circuits and Systems*, pp. 1525-1528, 1988.

[Saramaki 90] T. Saramaki, T. Karema, T. Ritoniemi and H. Tenhunen, "Multiplier-Free Decimator Algorithms for Superresolution Oversampled Converters," *IEEE International Symposium on Circuits and Systems*, pp. 3275-3278, 1990.

[Scott 86] J. W. Scott, W. Lee, C. Giancario and C. G. Sodini, "A CMOS Slope Adaptive Delta Modulator, *ISSCC Digital Technical Papers*, pp. 130-131, 1986.

[Tjahjadi 85] T. Tjahjadi and W. J. Steenaart, "Adaptive Filter Realization with a Minimum Number of Multipliers," *IEEE Transaction on Circuits and Systems*, vol. CAS-32, no. 3, 1985.

[Vaidyanathan 93] P. P. Vaidyanathan, *Multirate Systems and Filter Banks*, Prentice-Hall, Englewood Cliffs, New Jersey, 1993.

[Wallace 92] R. B. Wallace and R. Goubran, "Noise Cancelling using Parallel Adaptive Filter Structures," *IEEE Transactions on Circuits and Sytems*, vol. 39, 1992.

[Wei 88] C. H. Wei and N. C. Chen, "Sigma-Delta Modulation Adaptive Digital Filter," *IEEE International Symposium on Circuits and Systems*, pp. 523-526, 1988.

[Welland 89] D. R. Welland, B. P. Del Signore, E. J. Swanson, T. Tanaka, K. Hamashita, S. Hara and K. Takasuka, "Stereo 16-Bit Delta-Sigma A/D Converter for Digital Audio," *Journal of the Audio Engineering Society*, vol. 37, pp. 476-486, 1989.

[Wong 90-1] P. W. Wong and R. M. Gray, "FIR Filters with Sigma-Delta Modulation Encoding," *IEEE Transaction on Acoustics, Speech and Signal Processing*, vol. 38, no. 6, pp. 979-990, 1990.

[Wong 90-2] P. W. Wong and R. M. Gray, "Sigma-Delta Modulation with I.I.D. Gaussian Inputs," *IEEE Transaction on Information Theory*, vol. 36, pp. 784-798, 1990.

[Wong 92] P. W. Wong, "Fully Sigma-Delta Modulation Encoded FIR Filters," *IEEE Transaction on Acoustics, Speech and Signal Processing*, vol. 40, no. 6, pp. 1605-1610, 1992.

Appendix A Frequency Response of Decimation Filters

There are two main regular FIR decimation filters involved in the proposed structures in chapter 4 and 5. Decimator A in chapter 4 and decimator B in chapter 5 denote the lowpass filters used in the SFB to bring the sampling frequency from $64f_N$ down to f_N. Decimator in Fig.3.2.9 in chapter 3 for the same frequency changing has the same specification as decimator B.

Decimator A is a 60 tap Hanning-window-based FIR filter with 64Hz sampling frequency, 0-1Hz passband and 4-32Hz stopband. Decimator B is a 100 tap Hanning-window-based FIR filter with 64Hz sampling frequency, 0-1Hz passband and 2.6-32Hz stopband. Their frequency responses are shown in Fig.A.1 and Fig.A.2 respectively.

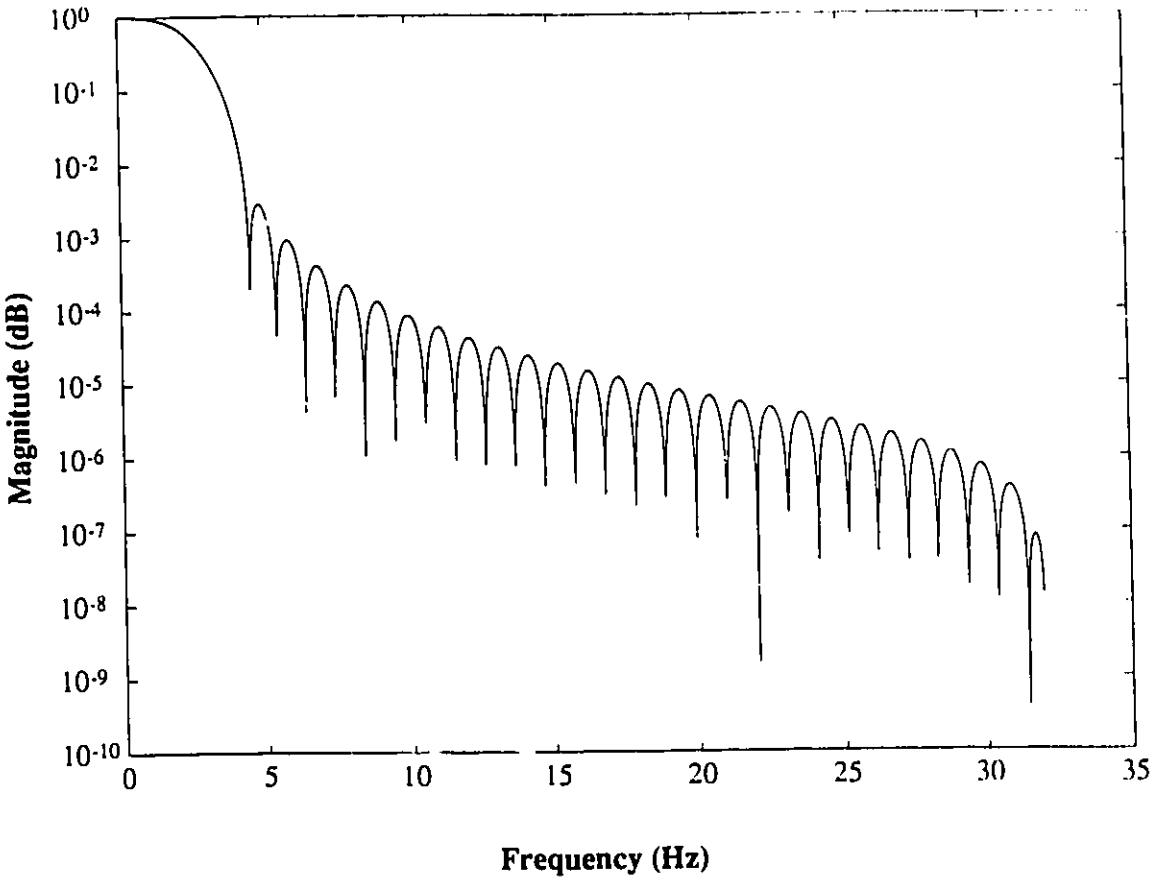

Figure A.1 Frequency response of decimator A with 60 taps.

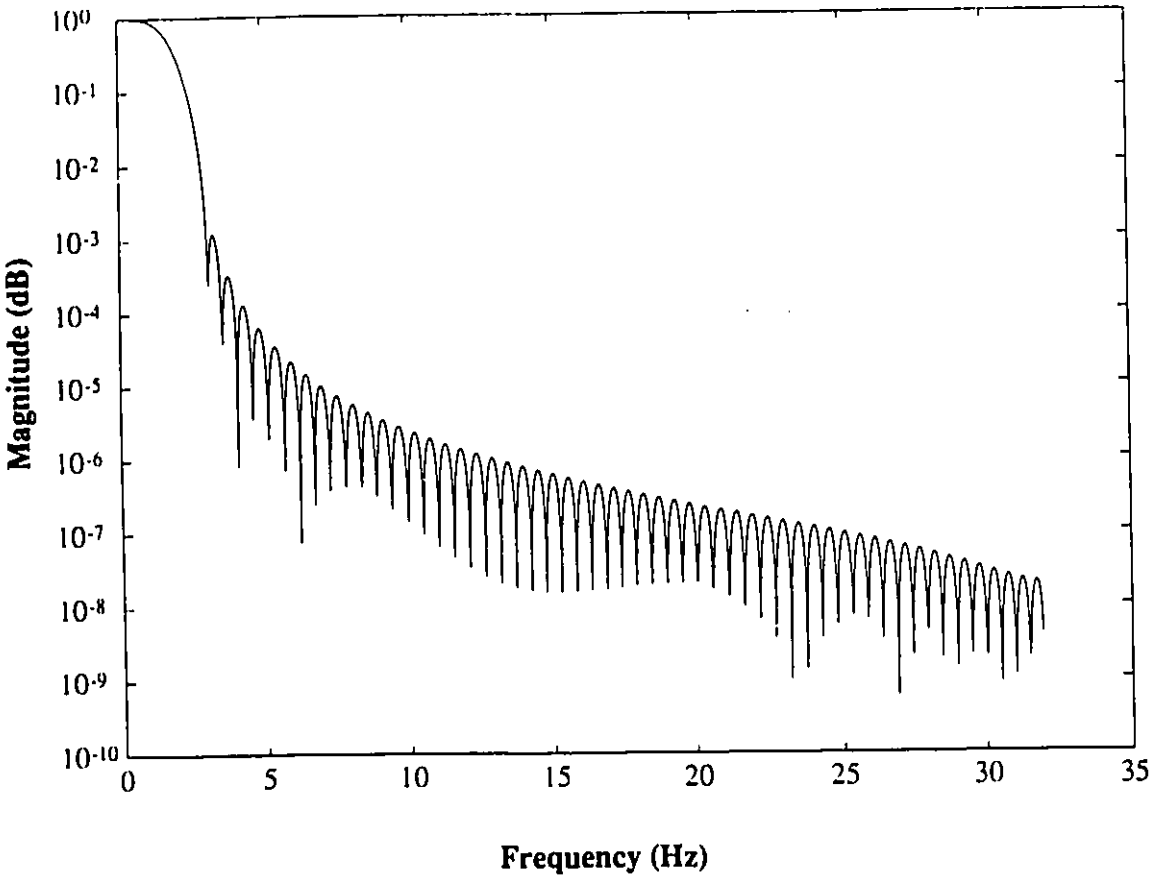

Figure A.2 Frequency response of decimator B with 100 taps.

Appendix B Simulation Program Examples

In this thesis, a Matlab software package on PC is used to simulate various systems and to verify their performances. Computer programs for several typical cases are attached in this appendix.

```
%       Program 0
%       The reproduction of the example in [C. Wei 1988]

        clear;
        N1=1500;

%       The length of the adaptive filter is 32.
        Lx=32+N1-1;
        SQER=zeros(N1,1);

%       The average of the learning curve is taken 10 times.
        nruns=10;
        for times=1:nruns

%       The Nyquist frequency is 8KHz.
        t=0:1/8000:(Lx-1)/8000;

%       The phase shift can be arbitrary.
        phi=5;

%       The 1KHz reference input has an arbitrary phase shift
%       with respect to the primary interference.
        x=7.054*sin(2*pi*1000*t+phi);

        rand('normal');
        t=0:1/8000:(N1+5)/8000;

%       Primary white noise input with zero mean
        and standard deviation 0.25
        ds1=0.25*rand(t);

%       Bandlimiting filter
        lp(1)=0.00856;
        lp(2)=-0.0121;
        lp(3)= 0.0135;
        lp(4)=-0.0113;
        lp(5)=0.00485;
        lp(6)=0.00577;
        lp(7)=-0.0191;
        lp(8)= 0.0326;
        lp(9)=-0.0425;
        lp(10)=0 04475;
        lp(11)=-0.0346;
        lp(12)=0.00686;
        lp(13)=0.04776;
        lp(14)=-0.1602;
        lp(15)=0.61854;
        for n=16:30
        lp(n)=lp(31-n);
        end

%       The white noise is bandlimited up to 3.2KHz.
        ds=conv(ds1,lp);
        t=33/8000:1/8000:(Lx+1)/8000;
        dn=7.054*sin(2*pi*1000*t);

%       The primary input is a combination of a 1KHz sinusoidal
%       interference and a bandlimited white noise.
        for i=1:N1
        d(i)=dn(i)+ds(i+32);
        end

%       Oversampling ratio
        R=4;

%       Initialing the adaptive filter
```

```
        a=[zeros(32,1)]';

%       Step size
        u=2^(-12);
        delta=2/R;

        for n=1:N1
        for k=1:32
        xc(k)=x(k+(n-1));
        end

%       Primary input is oversampled by 4.
        xx=zeros(32*R,1);
        for i=1:32,
        xx(R*(i-1)+1)=xc(i);
        end

%       The modulator is simply a sign identifier.
        ww1=sign(xx);
        ww(1)=ww1(1);
        for k=2:32*R
        ww(k)=ww1(k-1);
        end

        y(n)=0;
        for i=1:R
        yy(i)=0;
        for k=1:32
        yy(i)=yy(i)+a(k)*ww(R*(k-1)+i);
        end

%       The high rate sequence is decoded using a comb filter
%       to produce adaptive filter output.
        y(n)=y(n)+yy(i);
        end

%       The error
        e(n)=d(n)-y(n);
        z=e(n);

%       The adaptive filter update
        a=a+2*delta*u*z*sign(xc);

%       Calculating the squared error
        SQER(n)=SQER(n)+abs(z)^2;
        disp(n)
        disp(times)
        end
        end
        SQER=SQER/nruns;

%       Squared error in dB
        SQER=10*log10(SQER);
```

```
%       Program 1
%       Two-band filter bank overall frequency response

        clear;

%       Filter length
        Lh=64;

%       Filter generator using Hanning window
        wind=hanning(Lh);

%       Lowpass filter with 0.5127 normalized cutoff frequency
        lp=firl((Lh-1),.5127,wind);

%       The highpass filter is a shift-versoin of the lowpass filter.
        for i=1:Lh,
        hp(i)=(-1)^(i-1)*lp(i);
        end

%       Normalized frequency
        Fs=1;
        n=1024;
        t=1;
        b=lp;
        L=Lh;
        for i=1:2,
        a=[1 zeros(1,L-1)];

%       calculating the frequency response
        [h,w]=freqz(b,a,n);
        mag=abs(h);
        f=Fs*w/(2*pi);
        if t==2,

%       Magnitude of the lowpass fitler
                mag2=mag;
        else

%       Magnitude of the highpass filter
                mag1=mag;
                t=2;
                b=hp;
        end
        end
        for i=1:length(mag1),
        m1(i)=mag1(i)^2;
        m2(i)=mag2(i)^2;
        end

%       Overall frequency response of the filter bank
        m=20*log10(m1+m2);
        low=10*log10(m1);
        upper=10*log10(m2);
        plot(f,m)
```

```
%       Program 2
%       Conventional subbanded adaptive interference canceller

        clear;
        N1=1000;

%       Adaptive filter length is 32.
        Lh1=32;
        Lx=Lh1+N1-1;
        SQER1=zeros(N1,1);
        SQER2=zeros(N1,1);

%       Normalized sampling frequency
        t=0:1:(Lx-1);

%       Arbitrary phase shift
        phi=9;

%       Reference input
        x=0.8*sin(2*pi*0.125*(t+phi))+0.8*sin(2*pi*3/9*(t+phi));

%       Primary interference input
        t=0:1:(N1-1);
        dn=0.8*sin(2*pi*0.125*t)+0.8*sin(2*pi*3/9*t);

%       Filter length for filter bank
        Lh=64;

%       Lowpass filter generator using Hanning window
        wind=hanning(Lh);
        lp=fir1((Lh-1),.5127,wind);

%       Shift version of the lowpass filter
        for n=1:Lh
        hp(n)=(-1)^(n-1)*lp(n);
        end


%       Convolution operation and transition effect elimination
        x1=conv(x,lp);
        L1=length(x1);
        x1(L1-Lh/2+2:L1)=[];
        x1(1:Lh/2)=[];
        x2=conv(x,hp);
        x2(L1-Lh/2+2:L1)=[];
        x2(1:Lh/2)=[];

%       Step size for adaptive filters in two bands
        u1=2^(-9);
        u2=2^(-9);

%       Averaging time
        nruns=5;
        for times=1:nruns
        rand('normal');

%       Primary signal input
        t=0:1:(N1-1);
        ds=0.05*rand(t);
        d=ds+dn;

%       Signal splitting using filter bank
        d1=conv(d,lp);
        d2=conv(d,hp);
        L2=length(d1);
        d1(L2-Lh/2+2:L2)=[];
```

```
        d1(1:Lh/2)=[];
        d2(L2-Lh/2+2:L2)=[];
        d2(1:Lh/2)=[];

%       Run function program and calculate error sequence
        [e1,y1,a1]=adic1(x1,d1,Lh1,u1,times);
        [e2,y2,a2]=adic1(x2,d2,Lh1,u2,times+nruns);

%       Squared error
        for n=1:N1
        SQER1(n)=SQER1(n)+abs(e1(n))^2;
        SQER2(n)=SQER2(n)+abs(e2(n))^2;
        end
        end

%       Squared error in dB
        SQER1=10*log10(SQER1/nruns);
        SQER2=10*log10(SQER2/nruns);

%       Signal combining using filter bank
        out1=conv(e1,lp);
        out2=conv(e2,hp);
        out=out1-out2;
```

```
%       Program 3
%       Fully modulated subbanded adaptive interference canceller

        clear;
        N1=1500;
        Lh1=32;
        Lx=Lh1+N1-1;

        t=0:1:(Lx-1);
        phi=5;
        x=0.8*sin(2*pi*0.125*(t+phi))+0.8*sin(2*pi*3/9*(t+phi));

        t=0:1:(N1-1);
        dn=0.8*sin(2*pi*0.125*t)+0.8*sin(2*pi*3/9*t);

        Lh=64;
        wind=hanning(Lh);
        lp=fir1((Lh-1),.5127,wind);
        for n=1:Lh
        hp(n)=(-1)^(n-1)*lp(n);
        end

%       Oversampling ratios for filter bank and adaptive filters
        R1=64;
        R2=4;

%       Both coefficients and input are modulated for filter bank.
        lpp=interp(lp,R1);
        hpp=interp(hp,R1);
        xaa=interp(x,R1,1,0.5);
        for i=1:10,
        end

%       Run function program
        wwn1=omit12(xaa,lpp,Lx,Lh,R1,R2);
        wwn2=omit12(xaa,hpp,Lx,Lh,R1,R2);

%       Step size
        u1=2^(-12);
        u2=2^(-11);

        nruns=5;
        for times=1:nruns
        rand('normal');
        t=0:1:(N1-1);
        ds=0.05*rand(t);
        d=ds+dn;

        d1=fil(d,lp,N1,Lh,R1);
        d2=fil(d,hp,N1,Lh,R1);
        %       d1=conv(d,lp);
        %       d2=conv(d,hp);
        L1=length(d2);
        d1(L1-Lh/2+2:L1)=[];
        d2(L1-Lh/2+2:L1)=[];
        d1(1:Lh/2)=[];
        d2(1:Lh/2)=[];
        N=length(d2);

%       Adaptive filtering with only input modulated
        [e1,y1,a1]=adic3(wwn1,d1,Lh1,u1,R2;times);
        [e2,y2,a2]=adic3(wwn2,d2,Lh1,u2,R2,times+nruns);

        if times==1,
        SQER1=zeros(N,1);
        SQER2=zeros(N,1);
```

```
else
end

for n=1:N
SQER1(n)=SQER1(n)+abs(e1(n))^2;
SQER2(n)=SQER2(n)+abs(e2(n))^2;
end
end

SQER1=10*log10(SQER1/nruns);
SQER2=10*log10(SQER2/nruns);
```

```
%       Program 4
%       Function program used for program 2

        function [e,y,a]=adicl(x,d,Lhl,u,times);
        N=length(d);
        a=[zeros(Lhl,1)]';
        for n=1:N
        for k=1:Lhl
        xc(k)=x(k+(n-1));
        end
        y(n)=0;
        for k=1:Lhl
        y(n)=y(n)+xc(k)*a(k);
        end
        e(n)=d(n)-y(n);
        z=e(n);
        a=a+u*z*xc;
        disp(n)
        disp(times)
        end
```

```
%       Program 5
%       Function program for program 3

        function [e,y,a]=adic3(wwn,d,Lh1,u,R2,times);
        N=length(d);
        a=[zeros(Lh1,1)]';
        delta=2/R2;

        for n=1:N,
        for k=1:Lh1*R2,
        xx(k)=wwn(k+(n-1)*R2);
        end
        ww1=sign(xx);
        ww(1)=ww1(1);
        for k=2:Lh1*R2;
        ww(k)=ww1(k-1);
        end

        y(n)=0;
        for i=1:R2,
        yy(i)=0;
        for k=1:Lh1,
        yy(i)=yy(i)+a(k)*ww(R2*(k-1)+i);
        end
        y(n)=y(n)+1/R2*yy(i);
        end

        e(n)=d(n)-y(n);
        z=e(n);
        for k=1:Lh1,
        a(k)=a(k)+2*u*delta*z*ww(R2*(k-1)+1);
        end
        end
```

```
%       Program 6
%       Function program used for program 3

        function wn=fil(xn,hn,Lx,Lh,R1);
        alpha=0;
        vn=mod(xn,R1,Lx);
        un=mod(hn,R1,Lh);
        wwn=conv(un,vn);
        L1=length(wwn);
        wwn(L1-Lh*R1/2+2:L1)=[];
        wwn(1:Lh*R1/2)=[];
        wn=1/R1*decimate(wwn,R1,50,'fir');
```

```
%       Program 7
%       Function program for sigma-delta modulation

        function vn=mod1(xn,R,L);
        LL=L*R;
        alpha=0;
        xxn=interp(xn,R);

        rn(1)=0;
        for i=1:LL-1,
        rn(i+1)=rn(i)+xxn(i)-quant(rn(i),alpha,1);
        end
        vn=quant(rn,alpha,LL);
```

```
%       Program 8
%       Function program for quantization

        function q=quant(x,alpha,l)
        for i=1:l,
        q(i)=0;
                if x(i)>=alpha,
                        q(i)=1;
                elseif x(i)<-1*alpha,
                        q(i)=-1;
                end
        end
```

```
%       Program 9
%       Function program for signal power spectrum

        function Pyy=power(yn,fs,L2);
        Yn=fft(yn,L2);
        n=length(Yn);
        Pyy=Yn.*conj(Yn)/n;
        f=fs/2*(0:(L2/2))/(L2/2);
        Pyy((L2/2+2):L2)=[];
        Pyy(2:(L2/2))=2*Pyy(2:(L2/2));
        semilogy(f,Pyy)
```

```
%       Program 10
%       Calculation for frequency response

        function Fyy=freq(b,Fs,n);
        L=length(b);
        a=[1 zeros(1,L-1)];
        [h,w]=freqz(b,a,n);
        %       mag=20*log10(abs(h));
        mag=abs(h);
        f=Fs*w/(2*pi);
        plot(f,mag)
        %       semilogy(f,mag,'--')
```

```
%       Program 11
%       Function program for convolution operation
%       in absence of multipiers

        function w=convol(v,u);
        Lv=length(v);
        Lu=length(u);
        for i=1:(Lv+Lu-1),
        w(i)=0;
        if i<=Lu,
              for k=1:i,
                        if v(i-k+1)==1,
                        w(i)=w(i)+u(k);
                        else
                        w(i)=w(i)-u(k);
                        end
                 end
        elseif i>=Lv,
                 for k=i-Lv+1:Lu,
                        if v(i-k+1)==1,
                        w(i)=w(i)+u(k);
                        else
                        w(i)=w(i)-u(k);
                        end
                 end
        else
                 for k=1:Lu,
                        if v(i-k+1)==1,
                        w(i)=w(i)+u(k);
                        else
                        w(i)=w(i)-u(k);
                        end
                 end
        end
        end
```